Numerical Study on

Some Stochastic Models in Biology

Submitted to

Graduate School of Information Science and Technology

Osaka University

January 2014

Thi Hoai Linh NGUYEN

Contents

List of Figures

List of Notations

Ω	sample space
$\mathcal{A}$	collection of events
$\mathbb{P}$	probability measure
$(\Omega, \mathcal{A}, \mathbb{P})$	probability space
$\mathcal{A}_t$	σ-algebra
$P(X)$	probability of event X
$P(X\|Y)$	conditional probability of Xgiven Y has occurred
w.p.1	with probability one
a.s	almost surely
$F_X(x)$	distribution function of X at x
$\mathbb{E}(X)$	expectation of random variable X
$\mathbb{E}(X\|Y)$	conditional expectation of random variable X given Y has occurred
$\mathrm{Var}(X)$	Variance of random variable X
$N(0,1)$	normal distribution with mean 0 and variance 1
$\mathbb{R}^d$	d-dimensional Euclidean space
$(x_1; x_2; \ldots; x_d)$	point in $\mathbb{R}^d$ space
$\|x\|$	norm of vector $x \in \mathbb{R}^d$
$\|x\|$	absolute value of $x \in \mathbb{R}^1$
$< x, y >$	scalar product of vectors x, y
$\mathcal{C}$	space of continuous functions
$\mathcal{B}$	$\sigma -$ algebra of Borel subsets of $\mathbb{R}^1$
$\mathcal{L}$	σ-algebra of Lebesgue subsets of $\mathbb{R}^1$
$\forall$	for all
$\exists$	there exists
$\in$	in or belongs to
(a, b)	set $\{x \in \mathbb{R} \| a < x < b\}$
$[a, b]$	set $\{x \in \mathbb{R} \| a \leqslant x \leqslant b\}$
$(a, b]$	set $\{x \in \mathbb{R} \| a < x \leqslant b\}$

$[a, b)$	set $\{x \in \mathbb{R} \vert a \leqslant x < b\}$
$A \cup B$	union of sets A and B
$A \cap B$	intersection of sets A and B
$A \backslash B$	set of elements of set A that are not in set B
max	maximum value
min	minimum value
sup	supremum
inf	infimum
lim	limitation
lim sup	limit superior
lim inf	limit inferior
$a \wedge b$	the minimum of a and b
$:=$	defined as or denoted by
e^x	exponential function
$\ln x$	natural logarithm
$w.r.t$	with respect to

List of Tables

Chapter 1

Introduction

1.1 Motivation

Knowing the mechanisms of various biological systems is one of vital problems. Direct researches on these systems often take a lot of time and experiments cost immensely. Sometimes they are even unfeasible. Other way in getting desired information about biological systems is constructing mathematical models which describe the systems and then studying the models by using mathematical tools. In the study of some biological systems, numerical simulations on the basis of mathematical models are indispensable. This approach has several advantages: Mathematical modelling is a simple means of doing hypothetical experiments which are not easily done with real phenomena. Numerical simulations are useful in suggesting the relative importance of different features of the models and the effect of varying the magnitude of different parameters. They also have the power of performing simultaneous calculations of many interacting terms. Their outputs can be checked again with the actual observations.

Many systems have been modelled in view of deterministic mechanisms. However, we know that real biological systems are always subject to environmental noises and incompletely understood information. These factors need to be carefully considered so that the model predictions are meaningful and parameter values are possible to interpret. To be realistic, models of biological systems should include these factors. They will be well-modelled by stochastic models which embrace complex variations in their dynamics. Stochastic differential equation is a natural extension of a deterministic differential equation where we model relevant parameters as suitable stochastic processes or add stochastic processes to the driving system equations. This assumes that the dynamics are partly driven by noise.

This dissertation is devoted to a numerical study on stochastic models for some biological systems. More precisely, we study two problems as follows.

The first one is a Stochastic Forest Model. There is no doubt that conservation of forest resources is one of the main subjects in environmental issues.

In order to preserve our forest resources, we must first understand the principles of growth of trees in the forest. Then we can take positive actions to protect our forest from vanishing. In [3, 4], Antonovsky et al. introduced a deterministic, mono-species ecosystem model with two age classes of trees: the young and the old ones. In our study, we are interested in another aspect of the forest model, that is the effects of random factors on the forest model, since a real forest is often subject to environmental noises. It is seen that the asymptotic behavior of the solutions depends strongly on the magnitude of the mortality rate of old age trees. So, on the basis of that age-structured model, we incorporate a noise factor to the mortality rate of old age class. That results in a stochastic forest model.

$$\begin{cases} du &= \{\rho v - [\gamma(v) + f]u\}dt, \\ dv &= (fu - hv)dt + \sigma v dw_t. \end{cases}$$

Here, $u(t)$ and $v(t)$ denote tree densities of young and old age classes, respectively. The parameters ρ, h and f are coefficients of reproduction and mortality of old age trees, and aging of young age trees, respectively; while, $\gamma(v)$ is a mortality of young age trees which is allowed to depend on the old tree density v. The process $\{w_t, t \geqslant 0\}$ is a one-dimensional Brownian motion with coefficient $\sigma > 0$. We are concerned with the long time behavior of solutions which characterizes the stable existence or decline of the forest. Our aim is to consider the existence and uniqueness of global positive solutions and conditions for sustainability of the forest. Our obtained results may provide us some information on the nature of real forest systems.

The second problem concerns with biological swarming. For this problem, we study four models which describe swarming behaviors.

The first one is a stochastic Cucker-Smale model which is stated below

$$\begin{cases} dx_i &= v_i dt, \\ dv_i &= \sum\limits_{j=1}^{N} \psi(\|x_j - x_i\|)(v_j - v_i)dt + \sigma \sum\limits_{j=1}^{N} (v_j - v_i) \circ dw_t, \end{cases} 1 \leqslant i \leqslant N.$$

Here x_i, v_i are respectively the position and velocity of the i-th particle in the system consisting of N particles. All particles interacts with each other through velocity matching rule represented by communication rate ψ. Parameter $\sigma > 0$ is the strength of white noise and $\{w_t,\ t \geqslant 0\}$ is a one-dimensional Brownian motion, and $\circ$ denotes the operation for Stratonovich stochastic differential equations. This model describes flocking behavior of particles. We want to find out conditions for flocking and non-flocking behaviors in the system.

The second one is called the Basic Fish Schooling Model

$$\begin{cases} dx_i(t) = & v_i dt + \sigma_i dw_i(t), \qquad i = 1, 2, \ldots, N, \\ dv_i(t) = & \Big[-\alpha \sum\limits_{j=1,\, j\neq i}^{N} \left(\dfrac{r^p}{\|x_i - x_j\|^p} - \dfrac{r^q}{\|x_i - x_j\|^q} \right) (x_i - x_j) \\ & \quad -\beta \sum\limits_{j=1,\, j\neq i}^{N} \left(\dfrac{r^p}{\|x_i - x_j\|^p} + \dfrac{r^q}{\|x_i - x_j\|^q} \right) (v_i - v_j) \\ & \quad + F_i(t, x_i, v_i) \Big] dt, \qquad i = 1, 2, \ldots, N, \end{cases}$$

which describes the process of schooling of N-fish system. The unknown stochastic processes $x_i(t)$, $v_i(t)$ with values in $\mathbb{R}^d$ denote a position and a velocity of the i-th fish of system at time t; The fish are allowed to swim in the unbounded, continuous and homogeneous space $\mathbb{R}^d$. $\sigma_i dw_i$ denote noise resulting from the imperfectness of information-gathering and action of the i-th fish, where $\{w_i(t),\, t \geqslant 0\}$ $(i = 1, 2, ..., N)$ are independent d-dimensional Brownian motions. Powers p, q satisfying $1 < p < q < \infty$ are fixed exponents, $r > 0$ is a fixed distance and α, β are positive coefficients for interaction between fish and velocity matching, respectively. Finally, the functions $F_i(t, x_i, v_i)$ denote external forces at time t which are given functions defined for (x_i, v_i) with values in $\mathbb{R}^d$. With this model, we would like to survey the model quantitatively and see how some parameters, e.g., population size, critical distance between individuals, contribute to the geometrical structure of created school. Then we study a stochastic dynamical system incorporating white noises which represent various perturbations from the environment to the above model equations. Information about how forming a school is robust with respect to noises is studied by means of computer simulations.

In the other two models which is derived from the basic fish schooling model by incorporating additional components, we are interested in problems of avoiding obstacles and finding food resources. We expect to find out behavioral patterns of the school in the environment with presence of obstacles which can give some information about the cohesiveness of fish schools. We would also like to check the hypothesis that fish benefit better foraging success by forming school. Here we have just introduced briefly the model equations of three over five models under consideration in this dissertation. More descriptive explanations of all five models will be given in concerning chapters.

Studying biological swarming is important because besides more understanding about our world it brings, information acquired from the study of swarming behaviors can be applied to many important problems. Knowledge gained from studying interaction rules between agents in some biological systems may be used to build blocks for the design of artificial systems, such as reactive robotic systems [18], cellular network [47] or to construct information systems [27, 45]. The self-organizing feature of school can provide a deeper insight in design of sensor networks, self-assembly of connected mobile networks, automated parallel delivery of payloads [22, 55].

The information obtained can be seen as guidelines for constructing new information system like ambient system. It seems that we have to consider complex systems whose constituents react each other with certain rules. Such systems may not have a beforehand goal or the goal can even depend on the process. In one hand such systems have robustness, but in the other hand, they also have fragility. We would like to apply our research results on robustness and fragility of self-organizing biological systems for information systems.

1.2 Outline

This dissertation is organized as follows.

Chapter 2 reviews roughly some basic notions in probability theory, several known results for stochastic differential equations and some numerical methods for solving stochastic differential equations. In this chapter, we represent in detail two schemes which will be used to numerically solve the two problems mentioned above. They are the explicit Euler scheme and the order 1.5 strong Taylor scheme.

Chapter 3 is devoted to investigating a Stochastic Forest Model. We first introduce the model equations for the problem. We are concerned with the asymptotic behavior of solutions which characterizes stable existence or decline of the forest. After proving the existence and uniqueness of global positive solutions, we show some sufficient conditions for sustainability of the forest by means of numerical solutions.

Chapter 4 considers conditions for flocking and non-flocking behaviors in Cucker-Smale model. We then surveys the basic fish schooling model describing the process of fish's school formation. After introducing the model equations, we make some quantitative investigations. We study how some parameters, e.g., population size, critical distance between individuals, contribute to the geometrical structure of the school. A stochastic dynamical systems incorporating white noises which represent various perturbations from the environment is constructed. Numerical simulations are performed to show how the school formation is robust with respect to noises.

Chapter 5 is concerned with the problems of avoiding obstacles and finding food resources. We are interested in behavioral patterns of the school in the environment with the presence of obstacles. We find four patterns of school while avoiding obstacles. The relationships between parameters contained in the model and school behaviors are studied. This result shows that the fish school has its cohesiveness. We also find that the fish acquire foraging advantages by forming school.

Chapter 6 contains conclusions and some future researches.

Chapter 7 is Appendix in which we show detailed data of simulation results.

Chapter 2

Preliminaries

This chapter contains some concepts on probability theory, several basic results on stochastic differential equations and two numerical methods for solving these equations. Materials in this chapter are viewed in [7, 23, 28, 37].

2.1 Convergence of random sequences

Many problems deal with approximations to random variables. There are various possible ways of defining limit of a sequence of random variables. We recall here some of them.

We first introduce some notions which will be used in this section. Let $X_n, n = 1, 2, \ldots$ be a sequence of random variables defined on a given probability space $(\Omega, \mathcal{A}, \mathbb{P})$ consisting of the sample space Ω, the collection of events $\mathcal{A}$, and the probability measure $\mathbb{P}$.

Definition 2.1.1 (Almost sure convergence (a.s))**.** A sequence of random variables $\{X_n\}$ converges *almost surely* to random variable X if, for all $\omega \in \Omega$ except a set of probability zero,

$$\lim_{n\to\infty} X_n(\omega) = X(\omega).$$

Or equivalently

$$P\left(\{\omega \in \Omega : \lim_{n\to\infty} |X_n(\omega) - X(\omega)| = 0\right) = 1.$$

So this is also called the convergence with probability one (w.p.1).

Definition 2.1.2 (Mean-square limit (or limit in the mean))**.** We say that the sequence $\{X_n\}$ converges to random variable X in the *mean square* if

$$\lim_{n\to\infty} \mathbb{E}(|X_n - X|^2) = 0.$$

Mean square limit is well known in Hilbert space theory.

Definition 2.1.3 (Limit in probability (or stochastic limit))**.** We can consider the possibility that X_n approaches X in such a way that the probability of deviation from X approaches zero: precisely, this means that if for any $\varepsilon > 0$

$$\lim_{n\to\infty} P(|X_n - X| \geqslant \varepsilon) = 0$$

then the *stochastic limit* of X_n is X.

Definition 2.1.4 (Limit in distribution)**.** An even weaker form of convergence occurs if

$$\lim_{n\to\infty} F_{X_n}(x) = F_X(x) \text{ at all continuous points of } F_X,$$

where $F_Y(y) := P(\{\omega \in \Omega : Y(\omega) < y\})$ is the distribution function of Y at y. In this case the convergence of the limit is said to be *in distribution*. This is also known as convergence in law.

Definition 2.1.5 (Weak convergence)**.**

$$\lim_{n\to\infty} \int_{-\infty}^{\infty} f(x) dF_{X_n}(x) = \int_{-\infty}^{\infty} f(x) dF(x)$$

for all test function $f : \mathbb{R} \to \mathbb{R}$.

Now we show some relationships between the above notions
Almost sure convergence $\Longrightarrow$ stochastic convergence $\Longrightarrow$ convergence in distribution,
Convergence in mean square $\Longrightarrow$ stochastic convergence.

2.2 Stochastic differential equations

2.2.1 Wiener Processes

Definition 2.2.1 (Standard Wiener process)**.** [28, 37] A standard Wiener process is a family of random variables $W = \{W(t), t \geqslant 0\}$ such that $W(t)$ depends continuously on t and satisfies the following conditions.

- $W(0) = 0$ w.p.1,
- For $0 \leqslant s \leqslant t$, the random variable given by the increment $W(t) - W(s)$ is normally distributed with mean zero and variance $t - s$.
- For $0 \leqslant s < t < u < v$, the increments $W(t) - W(s)$ and $W(v) - W(u)$ are independent.

The Wiener process is a mathematical description of Brownian motion.

Remark 2.2.2. A standard Wiener process can be approximated in distribution on any finite time interval by a scaled random walk.

For example, we divide the interval [0, 1] into N subintervals of equal length $\Delta t = \frac{1}{N}$ by partition:

$$0 = t_0 < t_1 < \ldots < t_N = 1$$

and construct a stepwise continuous random walk $S_N(t)$ by taking independent, equally probable steps of length $\pm\sqrt{\Delta t}$ at the endpoint of each subinterval. Starting with independent two-point random variables X_n, $n = 1, 2, \ldots, N$, taking values ± 1 with equal probability, we define

$$\begin{aligned} S_N(t_n) &= (X_1 + X_2 + \ldots + X_n)\sqrt{\Delta t}, \\ S_N(t) &= S_N(t_n), \qquad t_n \leqslant t < t_{n+1},\ n = 0, 1, \ldots, N-1, \\ S_N(0) &= 0. \end{aligned}$$

This random walk has independent increments $X_1\sqrt{\Delta t}$, $X_2\sqrt{\Delta t}$, $X_3\sqrt{\Delta t}$, ... for the given subintervals, but is not a process with independent increments.

$$\begin{aligned} \mathbb{E}(S_N(t)) &= 0, \\ \mathrm{Var}(S_N(t)) &= \Delta t \left[\frac{t}{\Delta t}\right], \text{where } \left[\frac{t}{\Delta t}\right] \text{is the integer part of } \frac{t}{\Delta t}, \\ \mathrm{Var}(S_N(t)) &\to t \quad \text{as } N = \frac{1}{\Delta t} \to \infty \quad \text{for all } \ t \in [0, 1], \\ \mathrm{Var}(S_N(t) - S_N(s)) &\to t - s \quad \text{as } N \to \infty \quad \text{for all } 0 \leqslant s < t \leqslant 1. \end{aligned}$$

By the Central Limit Theorem (stated below), it follows that $S_N(t)$ converges in distribution as $N \to \infty$ to a standard Wiener process.

Theorem 2.2.3 (Classical Central Limit Theorem)**.** *Let $\{X_1, X_2, \ldots, X_n\}$ be a random sample of size n, that is, a sequence of independent and identically distributed random variable with expected values μ and variances σ^2. Let $S_n = \frac{1}{n}(X_1 + X_2 + \ldots + X_n)$. For large n's, the distribution of S_n is approximately normal with mean μ and variance $\frac{\sigma^2}{n}$ (regardless of the shapes of the distribution of individual X_i's).*

2.2.2 White noise

In many time-invariant engineering systems the (time-independent) variance of a stochastic process $X(t)$ can be interpreted as an average power (or energy) and is written as

$$\mathrm{Var}(X(t)) = c(0) = \int_{-\infty}^{\infty} S(\nu) d\nu,$$

where $c(0)$ is the value of the covariance $c(t-s)$ at $s=t$ and $S(\nu)$ denotes the spectral density measuring the average power per unit frequency at frequency ν. Function $S(\nu)$ is real-valued and nonnegative with $S(-\nu) = S(\nu)$ for all ν, and can be extracted from the above expression by an inverse Fourier transform

$$S(\nu) = \int_{-\infty}^{\infty} c(s)e^{-2\pi i\nu s}ds = \int_{-\infty}^{\infty} c(s)\cos(2\pi\nu s)ds.$$

This brings us to Gaussian white noise, which can be thought of as a zero mean wide-sense stationary process with constant nonzero spectral density $S(\nu) = S_0$.

Its average power is uniformly distributed in frequency. Its covariances $c(s) = S_0\delta(s)$ for all s, where $\delta(s)$ is the Dirac function

$$\delta(s) = 0 \quad \forall s \neq 0 : \int_{-\infty}^{\infty} f(s)\delta(s)ds = f(0)$$

for all f continuous at $s=0$.

This suggests that Gaussian white noise $\dot{W}$ is an unusual stochastic process. Let $W = \{W(t),\, t \geqslant 0\}$ be a standard Wiener process. For fixed $h > 0$, we define a new process $X^h = \{X^h(t), t \geqslant 0\}$ by

$$X^h(t) = \frac{W(t+h) - W(t)}{h}, \qquad \text{for all } t \geqslant 0.$$

$X^h(t)$ is a wide-sense stationary Gaussian process with

$$\mu = 0, \quad c(t-s) = \frac{1}{h}\max\left\{0, 1 - \frac{1}{h}|t-s|\right\}.$$

Thus it has spectral density

$$S_h(\nu) = \frac{1}{h}\int_{-h}^{h}\left(1 - \frac{|s|}{h}\right)\cos(2\pi\nu s)ds = \left(\frac{\sin(2\pi\nu h)}{\pi\nu h}\right)^2.$$

This density is very broad for small h and converges to 1 for all $\nu \neq 0$ as h converges to 0, which suggests that the process X^h converges in some sense to a Gaussian white noise process $\dot{W}$ as h converges to 0. Hence a Gaussian white noise process is the derivative of a Wiener process.

2.2.3 Ito stochastic integral

Suppose that we have a probability space $(\Omega, \mathcal{A}, \mathbb{P})$, a Wiener process $W = \{W_t,\, t \geqslant 0\}$ and an increasing family $\{\mathcal{A}_t,\, t \geqslant 0\}$ of sub-σ-algebras of $\mathcal{A}$ such that W_t is $\mathcal{A}_t$-measurable with

$$\mathbb{E}(W_t|\mathcal{A}_0) = 0 \quad \text{and} \quad \mathbb{E}(W_t - W_s|\mathcal{A}_s) = 0 \quad \text{w.p.1} \quad \text{for all } 0 \leqslant s \leqslant t.$$

For $0 < T < \infty$ we define a class $\mathcal{L}_T^2$ of functions $f : [0,T] \times \Omega \to \mathbb{R}$ satisfying

$$\begin{aligned} f \quad &\text{is jointly } \mathcal{L} \times \mathcal{A} - \text{measurable;} \\ &\int_0^T \mathbb{E}(f(t,.)^2)dt < \infty; \\ \mathbb{E}(f(t,.)^2)dt < \infty \qquad &\text{for each} \quad 0 \leqslant t \leqslant T; \\ f(t,.) \quad &\text{is } \mathcal{A}_t\text{-measurable for each} \quad 0 \leqslant t \leqslant T. \end{aligned}$$

Two functions $f, g \in \mathcal{L}_T^2$ are considered to be identical if $f(t,\omega) = g(t,\omega)$ for all (t,ω) except possibly on a subset of $\mu_L \times \mathbb{P}$-measure zero. On $\mathcal{L}_T^2$ we equip the norm

$$\|f\|_{2,T} = \sqrt{\int_0^T \mathbb{E}(f(t,.)^2)dt}. \tag{2.2.1}$$

Then $\mathcal{L}_T^2$ is a Banach space (that is a complete normed linear space), provided we identify functions which differ only on sets of measure zero.

For any partition $0 = t_1 < t_2 < \ldots < t_{n+1} = T$ and any mean-square integrable $\mathcal{A}_{t_j}$-measurable random variables $f_1, f_2, \ldots, f_n$, we define a step function $f \in \mathcal{L}_T^2$ by $f(t,\omega) = f_j(\omega)$, w.p.1, for $t_j \leqslant t < t_{j+1}$ and $j = 1, 2, \ldots, n$. Hence

$$\int_0^T \mathbb{E}(f(t,.)^2)dt = \sum_{j=1}^n \mathbb{E}(f_j^2)(t_{j+1} - t_j).$$

We denote by $\mathcal{S}_T^2$ the subset of all step functions in $\mathcal{L}_T^2$. Then we can approximate any function in $\mathcal{L}_T^2$ by step functions in $\mathcal{S}_T^2$ to any desired degree of accuracy in the norm (2.2.1). To be specific we have $\mathcal{S}_T^2$ is dense in $(\mathcal{L}_T^2, \|.\|_{2,T})$ [37, Lemma 3.2.1].

Let f be a step function in $\mathcal{S}_T^2$ corresponding to a partition $0 = t_1 < t_2 < \ldots < t_{n+1} = T$ and random variables $f_1, f_2, \ldots, f_n$. We define the Ito stochastic integral for f over the interval $[0,T]$ by

$$I(f)(\omega) = \sum_{j=1}^n f_j(\omega)[W_{t_{j+1}}(\omega) - W_{t_j}(\omega)], \tag{2.2.2}$$

w.p.1. $I(f)$ is $\mathcal{A}_T$-measurable because f_j is $\mathcal{A}_{t_j}$-measurable and $W_{t_{j+1}} - W_{t_j}$ is $\mathcal{A}_{t_{j+1}}$-measurable for $j = 1, 2, \ldots, n$. Moreover, each product is integrable over Ω, which follows from the Cauchy-Schwarz inequality and the fact that each term is mean-square integrable; hence $I(f)$ is $\mathcal{A}_T$ integrable. In addition

$$\mathbb{E}(I(f)) = 0,$$

$$\mathbb{E}(I(f)^2) = \int_0^T \mathbb{E}(f(t,.)^2)dt, \tag{2.2.3}$$

$$I(\alpha f + \beta g) = \alpha I(f) + \beta I(g) \text{ w.p.1}, \tag{2.2.4}$$

for any $f, g \in \mathcal{S}_T^2$ and α, $\beta \in \mathbb{R}$.

Since $\mathcal{S}_T^2$ is dense in $(\mathcal{L}_T^2, \|.\|_{2,T})$, for an arbitrary function $f \in \mathcal{L}_T^2$, there exists a sequence of step functions $f^{(n)} \in \mathcal{S}_T^2$ for which

$$\int_0^T \mathbb{E}\left(\left|f^{(n)}(t,.) - f(t,.)\right|^2\right) dt \to 0 \qquad \text{as} \qquad n \to \infty.$$

The Ito integrals $I(f^{(n)})$ specified by (2.2.2) are well-defined and they satisfy

$$\begin{aligned}
&\mathbb{E}\left(\left|I(f^{(n)}) - I(f^{(n+m)})\right|^2\right) = \mathbb{E}\left(\left|I(f^{(n)} - f^{(n+m)})\right|^2\right) \\
&= \int_0^T \mathbb{E}\left(\left|f^{(n)}(t,.) - f^{(n+m)}(t,.)\right|^2\right) dt \\
&\leqslant 2\int_0^T \mathbb{E}\left(\left|f^{(n)}(t,.) - f(t,.)\right|^2\right) dt + 2\int_0^T \mathbb{E}\left(\left|f(t,.) - f^{(n+m)}(t,.)\right|^2\right) dt.
\end{aligned} \tag{2.2.5}$$

(the last inequality is got due to $(a+b)^2 \leqslant 2(a^2+b^2)$).
This means that $\{I(f^n)\}$ is a Cauchy sequence in the Banach space $L^2(\Omega, \mathcal{A}, \mathbb{P})$, and so there exists a unique, w.p.1, random variable I in $L^2(\Omega, \mathcal{A}, \mathbb{P})$ such that $\mathbb{E}(|I(f^{(n)}) - I|^2) \to 0$ as $n \to \infty$. This I is $\mathcal{A}_T$-measurable since it is the limit of $\mathcal{A}_T$-measurable random variables.

In the following, we prove that the limit I is unique regardless the choice of step functions converging to f in $\mathcal{L}_t^2$. Indeed, let $\hat{f}^{(n)}$ be another sequence of step functions converging to f and suppose that $I(\hat{f}^{(n)})$ converges to $\hat{I}$. Then

$$\mathbb{E}\left(\left|I - \hat{I}\right|^2\right) \leqslant 2\mathbb{E}\left(\left|I - I(f^{(n)})\right|^2\right) + 2\mathbb{E}\left(\left|\hat{I} - I(\hat{f}^{(n)})\right|^2\right)$$

Applying (2.2.5) with $f^{(n+m)}$ replaced by $\hat{f}^{(n)}$, then taking limits as $n \to \infty$, we obtain $\mathbb{E}(|I - \hat{I}|^2) = 0$, and hence $I = \hat{I}$, w.p.1.

The Ito stochastic integral $I(f)$ of a function $f \in \mathcal{L}_T^2$ is defined to be the common mean-square limit of sequences of the sums (2.2.2) for any sequence of step functions in $\mathcal{S}_T^2$ converging to f in the norm (2.2.1).

So far we have only considered the Ito integral $I(f)$ of a function $f \in \mathcal{L}_T^2$ over a fixed time interval $[0, T]$. Let B be a Borel subset of $[0, T]$. Then the Ito integral of f over the subset B is the Ito integral $I(fI_B)$ of fI_B over $[0, T]$,

where I_B is the indicator function of B; clearly $fI_B \in \mathcal{L}_T^2$. We denote the Ito integral of f over interval $[t_0, t_1]$ by $\int_{t_0}^{t_1} f dW_s$. For $0 \leqslant t_0 < t_1 < t_2 \leqslant T$, we have

$$fI_{[t_0,t_2]} = fI_{[t_0,t_1]} + fI_{[t_1,t_2]},$$

except at the instant $t = t_1$. So by (2.2.4) we obtain, w.p.1,

$$\int_{t_0}^{t_2} f(s,\omega)dW_s(\omega) = \int_{t_0}^{t_1} f(s,\omega)dW_s(\omega) + \int_{t_1}^{t_2} f(s,\omega)dW_s(\omega).$$

For a variable subinterval $[t_0, t] \subseteq [0, T]$, we form a stochastic process $Z = \{Z_t, t_0 \leqslant t \leqslant T\}$, defined by

$$Z_t(\omega) = \int_{t_0}^{t} f(s,\omega)dW_s(\omega),$$

w.p.1, for $t_0 \leqslant t \leqslant T$. We have Z_t is $\mathcal{A}_t$-measurable with

$$\mathbb{E}(Z_t) = 0 \qquad \text{and} \qquad \mathbb{E}(Z_t^2) = \int_{t_0}^{t} \mathbb{E}(f(s,.)^2)ds.$$

Finally, we extend the Ito integral to a wider class of integrands than those in the space $\mathcal{L}_T^2$. We say that f belongs to $\mathcal{L}_T^\omega$ if f is jointly $\mathcal{L}\times\mathcal{A}$-measurable, $f(t,.)$ is $\mathcal{A}_t$-measurable for each $t \in [0, T]$ and

$$\int_0^T f(s,\omega)^2 ds < \infty,$$

w.p.1; hence $\mathcal{L}_T^2 \subset \mathcal{L}_T^\omega$. We then define $f_n \in \mathcal{L}_T^\omega$ by

$$f_n(t,\omega) = \begin{cases} f(t,\omega) & : \int_0^t f(s,\omega)^2 ds \leqslant n, \\ 0 & : \text{otherwise.} \end{cases}$$

The Ito stochastic integrals $I(f_n)$ of the f_n over $0 \leqslant t \leqslant T$ are thus well-defined. It can then be shown that they converge in probability to a unique, w.p.1, random variable, which we denote by $I(f)$ and call the Ito stochastic integral of $f \in \mathcal{L}_T^\omega$ over the interval $[0, T]$.

2.2.4 Ito formula

Firstly we recall the Ito formulae which is a scalar transformation of a single stochastic differential, by which we mean an expression

$$dX_t(\omega) = e(t,\omega)dt + f(t,\omega)dW_t(\omega). \tag{2.2.6}$$

Here $e(t,\omega)$, $f(t,\omega)$ are two functions with $\sqrt{|e|}$, $f \in \mathcal{L}_T^\omega$.

We need the following lemma

Lemma 2.2.4. [37, Lemma 3.3.1] *Let $U : [0,T] \times \mathbb{R} \to \mathbb{R}$ have continuous partial derivatives $\frac{\partial U}{\partial t}$, $\frac{\partial U}{\partial x}$, and $\frac{\partial^2 U}{\partial x^2}$. Then for any t, $t + \Delta t \in [0,T]$ and x, $x + \Delta x \in \mathbb{R}$, there exist constants $0 \leqslant \alpha$, $\beta \leqslant 1$ such that*

$$U(t+\Delta t, x+\Delta x) - U(t,x) = \frac{\partial U}{\partial t}(t+\alpha\Delta t, x)\Delta t + \frac{\partial U}{\partial x}(t,x)\Delta x + \frac{1}{2}\frac{\partial^2 U}{\partial x^2}(t, x+\beta\Delta x)(\Delta x)^2.$$

Theorem 2.2.5 (The Ito Formula)**.** [37, Theorem 3.3.2] *Let $Y_t = U(t, X_t)$ for $0 \leqslant t \leqslant T$, where U is as in Lemma 2.2.4 and X_t satisfies* (2.2.6)*. Then*

$$Y_t - Y_s = \int_s^t \left[\frac{\partial U}{\partial t}(u, X_u) + e(u,\omega)\frac{\partial U}{\partial x}(u, X_u) + \frac{1}{2}f(u,\omega)^2\frac{\partial^2 U}{\partial x^2}(u, X_u)\right] du + \int_s^t f(u,\omega)\frac{\partial U}{\partial x}(u, X_u) dW_u,$$

w.p.1, for any $0 \leqslant s \leqslant t \leqslant T$.

Now we state the vector form of the Ito formula. Let $U : [0,T] \times \mathbb{R}^d \to \mathbb{R}$ have continuous partial derivatives $\frac{\partial U}{\partial t}$, $\frac{\partial U}{\partial x_k}$, $\frac{\partial^2 U}{\partial x_k \partial x_i}$ for $k, i = 1, 2, \ldots, d$, and define a scalar process $\{Y_t,\ 0 \leqslant t \leqslant T\}$ by

$$Y_t = U(t, X_t) = U(t, X_t^1, X_t^2, \ldots, X_t^d),$$

w.p.1, where X_t satisfies

$$dX_t = e(t,\omega)dt + F(t,\omega)dW_t.$$

Here $e : [0,T] \times \Omega \to \mathbb{R}^d$ with components e^k satisfying $\sqrt{|e^k|} \in \mathcal{L}_T^\omega$ (or $\mathcal{L}_T^2$) for $k = 1, 2, \ldots, d$, and $F : [0,T] \times \mathbb{R}^{d\times m}$ with components $F^{i,j} \in \mathcal{L}_T^\omega$ (or $\mathcal{L}_T^2$) for $k = 1, 2, \ldots, d$ and $j = 1, 2, \ldots, m$.
Then the stochastic differential for Y_t is given by

$$dY_t = \left[\frac{\partial U}{\partial t} + \sum_{k=1}^d e^k(t,\omega)\frac{\partial U}{\partial x_k} + \frac{1}{2}\sum_{j=1}^m\sum_{k=1}^d F^{i,j}(t,\omega)F^{k,j}(t,\omega)\frac{\partial^2 U}{\partial x_i \partial x_k}\right] dt + \sum_{j=1}^m\sum_{i=1}^d F^{i,j}(t,\omega)\frac{\partial U}{\partial x_i} dW_t^j,$$

where the partial derivatives are evaluated at (t, X_t)

2.2.5 Ito stochastic differential equations

For a deterministic ordinary differential equation, under certain conditions, we know how the system behaves at all time t, even if we cannot find a solution analytically. We can always solve it numerically up to any desired precision. However, many biological systems can not be modeled by deterministic ordinary differential equations because they are often subject to environmental noises and incompletely understood information. These systems will be more realistically modeled if we allow some randomness in the description. A stochastic differential equation is a natural extension of a deterministic ordinary differential equation by including some relevant randomized parameters or some suitable form of random processes, or adding a noise term to the driving equations of the system. This approach assumes that some degree of noise is present in the dynamics of the process, for instance, we can use the Wiener process. It leads to a mixed system with both a deterministic and a stochastic part in the following way

$$dX_t = a(t, X_t)dt + b(t, X_t)dW_t \tag{2.2.7}$$

where $X_t = X(t)$ is a stochastic process, not a deterministic function. $W_t = W(t)$ is a Wiener process. It is useful to write $dW_t = \xi_t dt$, where ξ_t is a white noise process which is the derivative of a Wiener process.

We call a process given by an equation of the form (2.2.7) an Ito process. The functions $a(.)$ and $b(.)$ can be nonlinear, where $a(.)$ is the drift part or the deterministic component, and $b(.)$ is the diffusion part or the stochastic component (system noise). Equation (2.2.7) can be interpreted in the integral form

$$X_t = X_{t_0} + \int_{t_0}^{t} a(s, X_s)ds + \int_{t_0}^{t} b(s, X_s)dW_s \tag{2.2.8}$$

where X_{t_0} is a random variable independent of the Wiener process. It is a diffusion process, called an Ito diffusion. The first integral on the right hand side can be interpreted as an ordinary integral, the second integral is an Ito stochastic integral with respect to the Wiener process W_t.

We classify two kinds of solutions for stochastic differential equations: strong solution and weak solution, as defined below.

Definition 2.2.6 (Strong solution)**.** When we change the Wiener process in (2.2.8), we again obtain a unique solution with the new Wiener process in it. Then we call such a solution a strong solution of the stochastic differential equations.

Definition 2.2.7 (Weak solution)**.** When we are free to select a Wiener process and then find a solution corresponding to this particular Wiener process, we call such a solution a weak solution.

Note that some stochastic differential equations only have weak solutions and no strong solutions.

Theorem 2.2.8 (The existence and uniqueness for strong solutions)**.** [37, Theorem 4.5.3] *Given an arbitrary, but fixed instant $0 \leqslant t_0 < T$, and coefficient functions $a, b : [t_0, T] \times \mathbb{R} \to \mathbb{R}$. Fixed a Wiener process $W = \{W_t, t \geqslant 0\}$ with independent components associated with an increasing family of σ-algebras $\{\mathcal{A}_t, t \geqslant 0\}$. That is $W_t = (W_t^1, W_t^2, \ldots, W_t^m)$, where the W^j for $j = 1, 2, \ldots, m$ are scalar Wiener process with respect to $\{\mathcal{A}_t, t \geqslant 0\}$, which are pairwise independent.*

Under the following assumptions:
A_1 (*Measurability*)*: $a = a(t, x)$, $b = b(t, x)$ are jointly $\mathcal{L}^2$-measurable in $(t, x) \in [t_0, T] \times \mathbb{R}$;*
A_2 (*Lipschitz condition*)*: There exists a constant $K > 0$ such that*

$$|a(t, x) - a(t, y)| \leqslant K|x - y|,$$
$$|b(t, x) - b(t, y)| \leqslant K|x - y|,$$

for all $t \in [t_0, T]$, $x, y \in \mathbb{R}$.
A_3 (*Linear growth bound*)*: There exists a constant $L > 0$ such that*

$$|a(t, x)|^2 \leqslant L^2(1 + |x|^2),$$
$$|a(t, x)|^2 \leqslant L^2(1 + |x|^2),$$

for all $t \in [t_0, T]$, $x, y \in \mathbb{R}$.

A_4 (*Initial value*)*: X_{t_0} is $\mathcal{A}_{t_0}$-measurable with $\mathbb{E}(|X_{t_0}|^2) < \infty$,*
the stochastic differential equation

$$dX_t = a(t, X_t)dt + b(t, X_t)dW_t$$

has a pathwise unique strong solution X_t on $[t_0, T]$ with

$$\sup_{t_0 \leqslant t \leqslant T} \mathbb{E}(|X_t|^2) < \infty.$$

We need the following lemmas for proving the above theorem.

Lemma 2.2.9 (The Gronwall inequality)**.** *Let $\alpha, \beta : [t_0, T] \to \mathbb{R}$ be integrable with*

$$0 \leqslant \alpha(t) \leqslant \beta(t) + L \int_{t_0}^{t} \alpha(s)ds$$

for $t \in [t_0, T]$ where $L > 0$. Then

$$\alpha(t) \leqslant \beta(t) + L \int_{t_0}^{t} e^{L(t-s)} \beta(s)ds$$

for $t \in [t_0, T]$.

Lemma 2.2.10. [37, Lemma 4.5.2] *If A_1 and A_2 hold, then the solutions of* (2.2.8) *corresponding to the same initial value and the same Wiener process are pathwise unique.*

Proof. Let X_t and $\hat{X}_t$ be two solutions corresponding to the same initial value and the same Wiener process of (2.2.8) on $[t_0, T]$ with, almost surely, continuous sample paths. Since they may not have finite second moments, we use the following truncation procedure: for $N > 0$ and $t \in [t_0, T]$ we define

$$I_t^{(N)}(\omega) = \begin{cases} 1 & : |X_u(\omega)|,\ |\hat{X}_u(\omega)| \leqslant N \quad \text{for} \quad t_0 \leqslant u \leqslant t, \\ 0 & : \text{otherwise.} \end{cases}$$

We have $I_t^{(N)}$ is $\mathcal{A}_t$-measurable and $I_t^{(N)} = I_t^{(N)} I_s^{(N)}$ for $t_0 \leqslant s \leqslant t$. Consequently, the integrals in the following expression are meaningful:

$$\begin{aligned} Z_t^{(N)} = I_t^{(N)} \int_{t_0}^{t} I_s^{(N)} \Big(a(s, X_s) - a(s, \hat{X}_s) \Big)\, ds \\ + I_t^{(N)} \int_{t_0}^{t} I_s^{(N)} \Big(b(s, X_s) - b(s, \hat{X}_s) \Big)\, dW_s, \end{aligned} \tag{2.2.9}$$

where $Z_t^{(N)} = I_t^{(N)}(X_t - \hat{X}_t)$. From the Lipschitz condition A_2 we have

$$\begin{aligned} &\max\left\{ \left| I_s^{(N)} \Big(a(s, X_s) - a(s, \hat{X}_s) \Big) \right|, \left| I_s^{(N)} \Big(b(s, X_s) - b(s, \hat{X}_s) \Big) \right| \right\} \\ &\leqslant K I_s^{(N)} |X_s - \hat{X}_s| \leqslant 2KN \end{aligned} \tag{2.2.10}$$

for $t_0 \leqslant s \leqslant t$. Thus the second order moments exist for $Z_t^{(N)}$ and so do the two integrals in (2.2.9). Using the inequality $(a+b)^2 \leqslant 2(a^2 + b^2)$, the Cauchy-Schwarz inequality and the property (2.2.3) of the Ito integral we obtain from (2.2.9)

$$\begin{aligned} \mathbb{E}\left(\left| Z_t^{(N)} \right|^2 \right) &\leqslant 2\mathbb{E}\left(\left| \int_{t_0}^{t} I_s^{(N)} \Big(a(s, X_s) - a(s, \hat{X}_s) \Big)\, ds \right|^2 \right) \\ &\quad + 2\mathbb{E}\left(\left| \int_{t_0}^{t} I_s^{(N)} \Big(b(s, X_s) - b(s, \hat{X}_s) \Big)\, dW_s \right|^2 \right) \\ &\leqslant 2(T - t_0) \int_{t_0}^{t} \mathbb{E}\left(\left| I_s^{(N)} \Big(a(s, X_s) - a(s, \hat{X}_s) \Big) \right|^2 \right) ds \\ &\quad + 2 \int_{t_0}^{t} \mathbb{E}\left(\left| I_s^{(N)} \Big(b(s, X_s) - b(s, \hat{X}_s) \Big) \right|^2 \right) ds, \end{aligned}$$

which we combine with (2.2.10) to get

$$\mathbb{E}\left(\left|Z_t^{(N)}\right|^2\right) \leqslant L\int_{t_0}^{t} \mathbb{E}\left(\left|Z_s^{(N)}\right|^2\right) ds$$

for $t \in [t_0, T]$ where $L = 2(t - t_0 + 1)K^2$. Applying the Gronwall inequality with $\alpha(t) = \mathbb{E}(|Z_t^{(N)}|^2)$ and $\beta \equiv 0$, we conclude that

$$\mathbb{E}\left(\left|Z_t^{(N)}\right|^2\right) = \mathbb{E}\left(\left|I_t^{(N)}\left(X_t - \hat{X}_t\right)\right|^2\right) = 0,$$

and hence $I_t^{(N)} X_t = I_t^{(N)} \hat{X}_t$, w.p.1, for each $t \in [t_0, T]$. Since the sample paths are continuous almost surely, they are bounded almost surely. Thus we can make the probability

$$P\left(I_t^{(N)} \neq 1\, \forall t \in [t_0, T]\right) \leqslant P\left(\sup_{t_0 \leqslant t \leqslant T} |X_t| > N\right) + P\left(\sup_{t_0 \leqslant t \leqslant T} \left|\hat{X}_t\right| > N\right)$$

arbitrarily small by taking N sufficiently large. This means that $P(X_t \neq \hat{X}_t) = 0$ for each $t \in [t_0, T]$, and hence that $P(X_t \neq \hat{X}_t : t \in D) = 0$ for any countably dense subset D of $[t_0, T]$. As the solutions are continuous and coincide on a countably dense subset of $[t_0, T]$, they must coincide, almost surely, on the entire interval $[t_0, T]$. Thus the solutions of (2.2.8) are pathwise unique. □

Proof of Theorem 2.2.8. In view of Lemma 2.2.10 we have only to establish the existence of a continuous solution X_t on $[t_0, T]$ for the given Wiener process $W = \{W_t, t \geqslant 0\}$. For doing this, we use the successive approximation method. We define

$$\begin{aligned} X_t^{(0)} &\equiv X_{t_0} \\ X_t^{(n+1)} &= X_{t_0} + \int_{t_0}^{t} a(s, X_s^{(n)})ds + \int_{t_0}^{t} b(s, X_s^{(n)})dW_s \end{aligned} \tag{2.2.11}$$

for $n = 0, 1, 2, \ldots$. If for a fixed $n \geqslant 0$ the approximation $X_t^{(n)}$ is $\mathcal{A}_t$-measurable and continuous on $[t_0, T]$, then it follows from assumptions A_1, A_2 and A_3 that the integrals in (2.2.11) are meaningful and that the resulting process $X_t^{(n+1)}$ is also $\mathcal{A}_t$-measurable and continuous on $[t_0, T]$. As $X_t^{(0)}$ is $\mathcal{A}_t$-measurable and continuous on $[t_0, T]$, it follows by induction that so is each $X_t^{(n)}$ for $n = 1, 2, 3, \ldots$.

From assumption A_4 and the definition of $X_t^{(0)}$, it is clear that

$$\sup_{t_0 \leqslant t \leqslant T} \mathbb{E}\left(\left|X_t^{(0)}\right|^2\right) < \infty.$$

Applying the inequality $(a+b+c)^2 \leqslant 3(a^2+b^2+c^2)$, the Cauchy-Schwarz inequality $|(x,y)| \leqslant |x|\,|y|$, the identity (2.2.3) and the linear growth bound A_3 to (2.2.11) we obtain

$$\begin{aligned}
&\mathbb{E}\left(\left|X_t^{(n+1)}\right|^2\right) \\
&\leqslant 3\mathbb{E}(|X_{t_0}|^2) + 3\mathbb{E}\left(\left|\int_{t_0}^t a(s,X_s^{(n)})ds\right|^2\right) + 3\mathbb{E}\left(\left|\int_{t_0}^t b(s,X_s^{(n)})dW_s\right|^2\right) \\
&\leqslant 2\mathbb{E}(|X_{t_0}|^2) + 3(T-t_0)\mathbb{E}\left(\int_{t_0}^t \left|a(s,X_s^{(n)})\right|^2 ds\right) + 3\mathbb{E}\left(\int_{t_0}^t \left|b(s,X_s^{(n)})\right|^2 ds\right) \\
&\leqslant 3\mathbb{E}(|X_{t_0}|^2) + 3(T-t_0+1)K^2\mathbb{E}\left(\int_{t_0}^t \left(1+|X_s^{(n)}|^2\right) ds\right)
\end{aligned}$$

for $n = 0, 1, 2, \ldots$. By induction we thus have

$$\sup_{t_0 \leqslant t \leqslant T} \mathbb{E}\left(\left|X_t^{(n)}\right|^2\right) \leqslant C_0 < \infty \tag{2.2.12}$$

for $n = 1, 2, 3, \ldots$.

Similarly to the derivation of the inequality (2.2.9), except now factors like $I_t^{(N)}$ are not required because of (2.2.12), we can show that

$$\mathbb{E}\left(\left|X_t^{(n+1)} - X_t^{(n)}\right|^2\right) \leqslant L\int_{t_0}^t \mathbb{E}\left(\left|X_s^{(n+1)} - X_s^{(n)}\right|^2\right) ds \tag{2.2.13}$$

for $t \in [t_0, T]$ and $n = 1, 2, 3, \ldots$ where $L = 2(T - t_0 + 1)K^2$. Then using the Cauchy formula

$$\int_{t_0}^t \int_{t_0}^{t_{n-1}} \cdots \int_{t_0}^{t_1} f(s)ds dt_1 \ldots dt_{n-1} = \frac{1}{(n-1)!}\int_{t_0}^t (t-s)^{n-1} f(s)ds$$

in repeated iterations of (2.2.13), we obtain

$$\mathbb{E}\left(\left|X_t^{(n+1)} - X_t^{(n)}\right|^2\right) \leqslant \frac{L^n}{(n-1)!}\int_{t_0}^t (t-s)^{n-1}\mathbb{E}\left(\left|X_s^{(1)} - X_s^{(0)}\right|^2\right) ds \tag{2.2.14}$$

for $t \in [t_0, T]$ and $n = 1, 2, 3, \ldots$. Also, using the growth bound A_3 instead of the Lipschitz condition A_2 in the derivation of (2.2.13) for $n = 0$, we find that

$$\mathbb{E}\left(\left|X_t^{(1)} - X_t^{(0)}\right|^2\right) \leqslant L\int_{t_0}^t \left(1 + \mathbb{E}(|X_s^{(0)}|^2)\right) ds$$

$$\leqslant L(T-t_0)\left(1+\mathbb{E}(|X_{t_0}|^2)\right)=C_1.$$

Inserting this into (2.2.14), we get

$$\mathbb{E}\left(\left|X_t^{(n+1)}-X_t^{(n)}\right|^2\right)\leqslant\frac{C_1L^n(t-t_0)^n}{n!}$$

for $t\in[t_0,T]$ and $n=0,1,2,\ldots$, and hence

$$\sup_{t_0\leqslant t\leqslant T}\mathbb{E}\left(\left|X_t^{(n+1)}X_t^{(n)}\right|^2\right)\leqslant\frac{C_1L^n(T-t_0)^n}{n!}\tag{2.2.15}$$

for $n=0,1,2,\ldots$. This implies the mean-square convergence of the successive approximations uniformly on $[t_0,T]$, but we need the almost sure convergence of their sample paths uniformly on $[t_0,T]$. To show this we define

$$Z_n=\sup_{t_0\leqslant t\leqslant T}\left|X_t^{(n+1)}-X_t^{(n)}\right|$$

for $n=0,1,2,\ldots$ and so from (2.2.10), we obtain

$$\begin{aligned}Z_n\leqslant&\int_{t_0}^{T}\left|a(s,X_s^{(n)})-a(s,X_s^{(n-1)})\right|ds\\&+\sup_{t_0\leqslant t\leqslant T}\left|\int_{t_0}^{t}\left(b(s,X_s^{(n)})-b(s,X_s^{(n-1)})\right)dW_s\right|.\end{aligned}$$

Using the Doob inequality

$$\mathbb{E}\left(\sup_{0\leqslant s\leqslant t}|X_t|^p\right)\leqslant\left(\frac{p}{p-1}\right)^p\mathbb{E}(|X_t|^p),$$

the Cauchy-Schwarz inequality and the Lipschitz condition A_2, we determine

$$\begin{aligned}\mathbb{E}\left(|Z_n|^2\right)&\leqslant 2(T-t_0)K^2\int_{t_0}^{T}\mathbb{E}\left(\left|X_s^{(n)}-X_s^{(n-1)}\right|^2\right)ds\\&\quad+8K^2\int_{t_0}^{T}\mathbb{E}\left(\left|X_s^{(n)}-X_s^{(n-1)}\right|^2\right)ds\\&\leqslant 2(T-t_0+4)K^2\int_{t_0}^{T}\mathbb{E}\left(\left|X_s^{(n)}-X_s^{(n-1)}\right|^2\right)ds,\end{aligned}$$

which we combine with (2.2.15) to conclude that

$$\mathbb{E}\left(|Z_n|^2\right)\leqslant\frac{C_2L^{n-1}(T-t_0)^{n-1}}{(n-1)!}$$

for $n = 1, 2, 3, \ldots$, where $C_2 = 2C_1K^2(T-t_0+4)(T-t_0)$. Then, after applying the Markov inequality

$$P(\{\omega \in \Omega : |X(\omega)| \geqslant a\}) \leqslant \frac{1}{a^p}\mathbb{E}(|X|^p)$$

for any $a, p > 0$ to each term and summing, we have

$$\sum_{n=1}^{\infty} P\left(Z_n > \frac{1}{n^2}\right) \leqslant C_2 \sum_{n=1}^{\infty} \frac{n^4}{(n-1)!} L^{n-1}(T-t_0)^{n-1},$$

where the series on the right hand side converges by the ratio test. Hence the series on the left hand side also converges, so by the Borel-Cantelli Lemma [37, Lemma 2.1.4] we conclude that the Z_n converge to 0, almost surely, so that the successive approximations $X_t^{(n)}$ converge, almost surely, uniformly on $[t_0, T]$ to a limit $\hat{X}_t$ defined by

$$\hat{X}_t = X_{t_0} + \sum_{n=0}^{\infty} [X_t^{(n+1)} - X_t^{(n)}].$$

It follows from (2.2.12) that $\hat{X}$ is mean square bounded on $[0, T]$. As the limit of $\mathcal{A}^\star$-adapted processes, $\hat{X}$ is $\mathcal{A}^\star$-adapted and as the uniform limit of continuous processes it is continuous. In view of this and the growth bound A_3, the right hand side of the integral equation (2.2.8) is well defined for process $\hat{X}$. It remains to show that it then equals the left hand side. Taking the limit as $n \to \infty$ in (2.2.11) we see that $\hat{X}$ is a solution of (2.2.8). The left hand side of (2.2.11) converges to $\hat{X}$ uniformly on $[t_0, T]$. Concerning the right hand side, by the Lipschitz condition A_2, we have

$$\left| \int_{t_0}^{t} a(s, X_s^{(n)})ds - \int_{t_0}^{t} a(s, \hat{X}_s^{(n)})ds \right| \leqslant K \int_{t_0}^{t} \left| X_s^{(n)} - \hat{X}_s \right| ds \to 0$$

and

$$\int_{t_0}^{t} \left| b(s, X_s^{(n)}) - b(s, \hat{X}_s) \right|^2 ds \leqslant K^2 \int_{t_0}^{t} \left| X_s^{(n)} - \hat{X}_s \right|^2 ds \to 0,$$

w.p.1, which imply that

$$\int_{t_0}^{t} a(s, X_s^{(n)})ds \to \int_{t_0}^{t} a(s, \hat{X}_s)ds$$

w.p.1, and

$$\int_{t_0}^{t} b(s, X_s^{(n)})dW_s \to \int_{t_0}^{t} b(s, \hat{X}_s)dW_s,$$

in probability, as $n \to \infty$ for each $t \in [t_0, T]$. Hence the right hand side of (2.2.11) converges to the right hand side of (2.2.8), and so the limit process $\hat{X}$ satisfies the stochastic integral equation (2.2.8).

This completes the proof of the existence and uniqueness of a strong solution of the stochastic differential equation (2.2.7) for an initial value X_{t_0} with $\mathbb{E}(|X_{t_0}|^2) < \infty$. □

2.2.6 Stratonovich stochastic differential equations

Ito stochastic differential equation is only one kind of stochastic differential equations in which we use Ito integral. Another one that is frequently used is the Stratonovich integral, in which the integrand is evaluated at the midpoint $\frac{1}{2}\left(f_j^{(n)} + f_{j+1}^{(n)}\right)$ of each partition subinterval of a given partition. This integral is very convenient for use because it satisfies the usual transformation rule of classical calculus, such as the chain rule. Therefore, methods that have been developed to solve ordinary differential equations can sometimes be used successfully to solve Stratonovich stochastic differential equations. Stratonovich stochastic differential equations are defined similarly to those of Ito.

We denote a Stratonovich differential equation by

$$dX_t = \underline{a}(t, X_t)dt + b(t, X_t) \circ dW_t \tag{2.2.16}$$

or in integral form

$$X_t = X_{t_0} + \int_{t_0}^{t} \underline{a}(s, X_s)ds + \int_{t_0}^{t} b(s, X_s) \circ dW_s,$$

where the Stratonovich integral of $h(t, X_t(\omega))$ for a function $h = h(t, x)$ and a diffusion process X_t

$$\int_0^T h(s, X_s(\omega)) \circ dW_s \tag{2.2.17}$$

to be the mean-square limit of the sums

$$S_n(\omega) = \sum_{j=1}^{n} h\left(t_j^{(n)}, \frac{1}{2}\left(X_{t_j^n} + X_{t_{j+1}^n}\right)\right)(W_{t_j^n} - W_{t_{j+1}^n})$$

for partitions $0 = t_1^{(n)} < t_2^{(n)} < \ldots < t_{n+1}^{(n)} = T$ with

$$\delta^{(n)} = \max_{1 \leqslant j \leqslant n} \left|t_{j+1}^{(n)} - t_j^{(n)}\right| \to 0 \quad \text{as} \quad n \to \infty.$$

The integral (2.2.17) is meaningful if the above limits exist and are unique, w.p.1. To ensure that we need to impose some restrictions on h and X_t. Let $W = \{W_t,\, t \geqslant 0\}$ be a Wiener process with an associated family $\{\mathcal{A}_t,\ t \geqslant 0\}$ of increasing σ-algebras. Moreover, suppose that

- X_t is a diffusion process in $\mathbb{R}$ for $0 \leqslant t \leqslant T$ with continuous drift $a = a(t, x)$ and diffusion coefficient $b = b(t, x)$.
- $h : [0, T] \times \mathbb{R} \to \mathbb{R}$ is continuous in t with the partial derivative $\frac{\partial h}{\partial x}$ continuous in both t and x.
- The function f defined by $f(t, \omega) := h(t, X_t(\omega))$ belongs to the function space $\mathcal{L}_T^2$ which requires X_t to be $\mathcal{A}_t$-measurable for each $0 \leqslant t \leqslant T$ and
$$\int_0^T \mathbb{E}\left(|h(t, X_t)|^2\right) dt < \infty.$$

If we start with the Stratonovich differential equation (2.2.16), then the corresponding Ito stochastic differential equation (that is they have common solutions) is
$$dX_t = a(t, X_t)dt + b(t, X_t)dW_t$$
with the drift modified to an a defined by
$$a(t, x) = \underline{a}(t, x) + \frac{1}{2}b(t, x)\frac{\partial b}{\partial x}(t, x).$$

For vector stochastic differential equation we have similar relationships between these as stated below: Let X_t be a solution of the vector Ito stochastic differential equation
$$dX_t = a(t, X_t)dt + b(t, X_t)dW_t$$
where $a, X \in \mathbb{R}^d$, $b \in \mathbb{R}^{d\times m}$, $W \in \mathbb{R}^m$.
Then its corresponding Stratonovich SDEs is
$$dX_t = \underline{a}(t, X_t) + b(t, X_t) \circ dW_t,$$
where the modified drift is defined component wise by
$$\underline{a}^i(t, X) = a^i(t, X) - \frac{1}{2}\sum_{j=1}^{d}\sum_{k=1}^{m} b^{j,k}(t, X)\frac{\partial b^{i,k}}{\partial x_j}(t, X).$$

Remark 2.2.11. Note that we can always switch a stochastic differential equation from Ito SDEs to Stratonovich SDEs and vice verse. This is very useful because depending on the certain situation we will choose the one which is easier to interpret. For example, as the systems containing many equations we should use the Stratonovich form because we can apply usual transformation rules of classical calculus; Using the existence and uniqueness results for Ito SDEs (Theorem 2.2.8), we can obtain the analogous results for the corresponding Stratonovich SDEs; From a Stratonovich SDE, we can use the corresponding Ito SDE to determine the appropriate coefficients of the Fokker-Planck equation for a diffusion process as arising as the solution of original equations.

2.3 Some numerical methods for solving SDEs

For numerical method for solving stochastic differential equations, we refer the reader to some literatures [7, 23, 28, 37, 38, 39, 40]

2.3.1 Multiple Ito integrals

Definition 2.3.1 (Multi-index)**.** A row vector $\alpha = (j_1, j_2, \ldots, j_l)$ with $j_i \in \{0, 1, \ldots, m\}$ for $i \in \{1, 2, \ldots, l\}$ and $m = 1, 2, 3, \ldots$, is called a multi-index of length $l := l(\alpha) \in \{1, 2, \ldots\}$. Here m denotes the number of components of the Wiener process under consideration. We denote by v the multi-index of length zero.

We write $n(\alpha)$ for the number of components of a multi-index α which are equal to 0.

Denote by $\mathcal{M}$ the set of all multi-indeces

$$\mathcal{M} = \{(j_1, j_2, \ldots, j_l) : j_i \in \{0, 1, \ldots, m\}, i \in \{1, \ldots, l\}, \text{for } l = 1, 2, 3, \ldots\} \cup \{v\}.$$

Given $\alpha \in \mathcal{M}$ with $l(\alpha) \geqslant 1$, we write $-\alpha$ and $\alpha-$ for the multi-index in $\mathcal{M}$ obtained by deleting the first and the last component, respectively, of α.

We define below some sets of adapted right continuous stochastic processes $f = \{f(t), t \geqslant 0\}$ with left hand limits:

$$\mathcal{H}_v = \{f : |f(t,\omega)| < \infty, \text{ w.p.1, for each } t \geqslant 0\},$$

$$\mathcal{H}_{(0)} = \left\{ f : \int_0^t |f(s,\omega)| ds < \infty, \text{ w.p.1, for each } t \geqslant 0 \right\},$$

$$\mathcal{H}_{(1)} = \left\{ f : \int_0^t |f(s,\omega)|^2 ds < \infty, \text{ w.p.1, for each } t \geqslant 0 \right\}.$$

We write $\mathcal{H}_{(j)} = \mathcal{H}_{(1)}$ for each $j \in \{2, \ldots, m\}$ if $m \geqslant 2$.

Let ρ and τ be two stopping times with $0 \leqslant \rho(\omega) \leqslant \tau(\omega) \leqslant T$, w.p.1. Then, for a mutli-index $\alpha = (j_1, j_2, \ldots, j_l) \in \mathcal{M}$ with $l := l(\alpha)$ and a process $f \in \mathcal{H}_\alpha$ (H_α will be defined latter), we define the multiple Ito integral $I_\alpha[f(.)]_{\rho,\tau}$ recursively by

$$I_\alpha[f(.)]_{\rho,\tau} := \begin{cases} f(\tau) & : l = 0 \\ \int_\rho^\tau I_{\alpha-}[f(.)]_{\rho,s} ds & : l \geqslant 1 \text{ and } j_l = 0 \\ \int_\rho^\tau I_{\alpha-}[f(.)]_{\rho,s} dW_s^{j_l} & : l \geqslant 1 \text{ and } j_l \geqslant 1. \end{cases}$$

For multi-indices $\alpha = (j_1, j_2, \ldots, j_l) \in \mathcal{M}$ with length $l(\alpha) > 1$, we define recursively the set

$$\mathcal{H}_\alpha = \{f : \{I_{\alpha-}[f(.)]_{\rho,t} \in \mathcal{H}_{(j_l)}, \, t \geqslant 0\}.$$

2.3.2 Ito-Taylor expansions

This subsection states the Ito-Taylor expansion for a d-dimensional Ito process

$$X_t = X_{t_0} + \int_{t_0}^{t} a(s, X_s)ds + \sum_{j=1}^{m} \int_{t_0}^{t} b^j(s, X_s)dW_s^j,$$

where $t \in [t_0, T]$.

Definition 2.3.2 (Hierarchical set)**.** A nonempty subset $\mathcal{A} \subset \mathcal{M}$ is an hierarchical set if the multi-indeces in $\mathcal{A}$ are uniformly bounded in length, i.e., $\sup_{\alpha\in\mathcal{A}} l(\alpha) < \infty$ and $-\alpha \in \mathcal{A}$ for each $\alpha \in \mathcal{A}\backslash\{v\}$, where v is the multi-index of length zero.

Definition 2.3.3 (Remainder set)**.** For any given hierarchical set $\mathcal{A}$, we define the remainder set $\mathcal{B}(\mathcal{A})$ of $\mathcal{A}$ by

$$\mathcal{B}(\mathcal{A}) = \{\alpha \in \mathcal{M}\backslash\mathcal{A} : -\alpha \in \mathcal{A}\}.$$

Theorem 2.3.4. [37, Theorem 5.5.1] *Let ρ and τ be two stopping times with*

$$t_0 \leqslant \rho(\omega) \leqslant \tau(\omega) \leqslant T,$$

w.p.1; let $\mathcal{A} \subset \mathcal{M}$ be an hierarchical set; and let $f : \mathbb{R}^+ \times \mathbb{R}^d \to \mathbb{R}$. Then the Ito-Taylor expansion

$$f(\tau, X_\tau) = \sum_{\alpha\in\mathcal{A}} I_\alpha[f_\alpha(\rho, X_\rho)]_{\rho,\tau} + \sum_{\alpha\in\mathcal{B}(\mathcal{A})} I_\alpha[f_\alpha(., X.)]_{\rho,\tau}, \tag{2.3.1}$$

holds, provided all of the derivatives of f, a and b and all of the multiple Ito integrals appearing in (2.3.1) *exist.*

2.3.3 Stochastic approximation

In order to evaluate the convergence for stochastic process, there are two criteria of optimality: the strong and the weak orders of convergence. But in the scope of this dissertation, we consider only the strong one. Strong approximation is used when we want to find a good pathwise approximation.

We consider a d-dimensional Ito process $X = \{X_t,\ t \geqslant 0\}$ satisfying the stochastic differential equation

$$dX_t = a(t, X_t)dt + b(t, X_t)dW_t$$

or in integral form

$$X_t = X_{t_0} + \int_{t_0}^{t} a(s, X_s)ds + \int_{t_0}^{t} b(s, X_s)dW_s,$$

where $a : \mathbb{R}_+ \times \mathbb{R}^d \to \mathbb{R}^d$, $b : \mathbb{R}_+ \times \mathbb{R}^d \to \mathbb{R}^{d\times m}$, $W = \{W_t, |, t \geqslant 0\}$: m-dimensional Wiener process.

Definition 2.3.5 (Stochastic time discrete approximation)**.** Let $t_0 = \tau_0 < \tau_1 < \ldots < \tau_N = T$ be a time discretization. A stochastic time discrete approximation of X_t is a sequence $\{Y_n,\ n = 0, 1, \ldots, N\}$ approximating X_t at $\tau_n,\ n = 0, 1, \ldots, N$.

Definition 2.3.6 (Stochastic continuous time approximation)**.** A stochastic continuous time approximation of X_t is a continuous time stochastic process $Y = \{Y(t),\ t_0 \leqslant t \leqslant T\}$ satisfying $Y(\tau_n) = Y_n$.

We can obtain stochastic continuous time approximations from stochastic time discrete approximations by using interpolation methods. The following example introduces two interpolations commonly used.

Example 2.3.7. 1) **Piecewise constant interpolation**

$$Y(t) = Y_{n_t}, \quad n_t = \max\{n = 0, 1, \ldots, N :\ \tau_n \leqslant t\}.$$

2) **Linear interpolation**

$$Y(t) = Y_{n_t} + \frac{t - \tau_n}{\tau_{n_t+1} - \tau_{n_t}}(Y_{n_t+1} - Y_{n_t}).$$

Definition 2.3.8 (Approximation criterion)**.** To evaluate a strong approximation we use the absolute error criterion

$$\varepsilon := \mathbb{E}(|X_T - Y(T)|),$$

where $\mathbb{E}(Z)$ is the expectation of random variable Z.

Definition 2.3.9 (Strong approximation or pathwise approximation)**.** A time discrete approximation Y^δ with maximum step size δ *converges strongly* to X_t at time T if

$$\lim_{\delta \to 0} \mathbb{E}(|X_T - Y^\delta(T)|) = 0.$$

A time discrete approximation Y^δ *converges strongly with order* $\gamma > 0$ at time T if there exist constants $C > 0$, $\delta_0 > 0$ such that

$$\varepsilon(\delta) = \mathbb{E}(|X_T - Y^\delta(T)|) \leqslant C\delta^\gamma$$

for any $\delta \in (0, \delta_0)$.

The order of convergence shows us the rate of strong convergence.

Definition 2.3.10 (Strong consistence)**.** A time discrete approximation Y^δ with maximum step size δ corresponding to a time discretization $(\tau)_\sigma = \{\tau_n : n = 0, 1, \ldots\}$ with increment $\Delta_n = \tau_{n+1} - \tau_n$ is *strongly consistent* if there exists a nonnegative function $c = c(\delta)$ with

$$\lim_{\delta \downarrow 0} c(\delta) = 0$$

such that

$$\mathbb{E}\left(\left|\mathbb{E}\left(\frac{Y_{n+1}^{\delta}-Y_n^{\delta}}{\Delta_n}|\mathcal{A}_{\tau_n}\right)-a(\tau_n,Y_n^{\delta})\right|^2\right)\leq c(\delta)$$

and

$$\mathbb{E}\left(\frac{1}{\Delta_n}|Y_{n+1}^{\delta}-Y_n^{\delta}-\mathbb{E}(Y_{n+1}^{\delta}-Y_n^{\delta}|\mathcal{A}_{\tau_n})-b(\tau_n,Y_n^{\delta})\Delta W_n|^2\right)\leq c(\delta)$$

for all fixed values $Y_n^{\delta}=y$ and $n=0,1,\ldots$. Here $\Delta W_n=W_{\tau_{n+1}}-W_{\tau_n}$.

2.3.4 Some strong schemes for SDEs

The Ito-Taylor expansions are used to derive time discrete strong approximations which are called strong Taylor approximations. This subsection introduces two of them: the explicit Euler scheme and the order 1.5 strong Taylor scheme which we shall apply to study our problems numerically.

The explicit Euler scheme

In the general multi-dimensional case with $d,m=1,2,\ldots$, the k-th component of the explicit Euler scheme has the form

$$Y_{n+1}^k=Y_n^k+a^k\Delta+\sum_{j=1}^{m}b^{k,j}\Delta W^j,$$

where $\Delta W^j=W_{\tau_n+1}^j-W_{\tau_n}^j=I_{(j)}$ is the $N(0;\Delta)$ distributed increment of the j-th component of the m-dimensional standard Wiener process W on $[\tau_n,\tau_{n+1}]$ and $\Delta W^{j_1},\Delta W^{j_2}$ are independent for $j_1\neq j_2$; $b=[b^{k,j}]$ is a $d\times m$-matrix.

In the following, we prove that the explicit Euler scheme

$$Y_{n+1}=Y_n+a(\tau_{n+1}-\tau_n)+b(W_{\tau_{n+1}}-W_{\tau_n})$$

is strongly consistent with $c(\delta)\equiv 0$. Indeed,

$$\begin{aligned}
&\mathbb{E}\left(\left|\mathbb{E}\left(\frac{Y_{n+1}^{\delta}-Y_n^{\delta}}{\Delta_n}\Big|\mathcal{A}_{\tau_n}\right)-a(\tau_n,Y_n^{\delta})\right|^2\right)\\
&=\mathbb{E}\left(\left|\mathbb{E}\left(a(\tau_n,Y_n^{\delta})+\frac{b(\tau_n,Y_n^{\delta})}{\Delta_n}\Delta W_n\Big|\mathcal{A}_{\tau_n}\right)-a(\tau_n,Y_n^{\delta})\right|^2\right)\\
&=\mathbb{E}\left(\left|a(\tau_n,Y_n^{\delta})+\mathbb{E}\left(\frac{b(\tau_n,Y_n^{\delta})}{\Delta_n}\Delta W_n\Big|\mathcal{A}_{\tau_n}\right)-a(\tau_n,Y_n^{\delta})\right|^2\right)\\
&=\mathbb{E}\left(\left|\frac{b(\tau_n,Y_n^{\delta})}{\Delta_n}[\mathbb{E}(W_{n+1}|\mathcal{A}_{\tau_n})-W_n]\right|^2\right)\quad\text{(because }\{W_n\}\text{ is a Martingale)}\\
&=0.
\end{aligned}$$

$$
\begin{aligned}
&\mathbb{E}\left(\frac{1}{\Delta_n}\left|Y^\delta_{n+1}-Y^\delta_n-\mathbb{E}(Y^\delta_{n+1}-Y^\delta_n|\mathcal{A}_{\tau_n})-b(\tau_n,Y^\delta_n)\Delta W_n\right|^2\right)\\
&=\mathbb{E}\left(\frac{1}{\Delta_n}\left|a\Delta_n+b\Delta W_n-\mathbb{E}(a\Delta_n+b\Delta W_n|\mathcal{A}_{\tau_n})-b\Delta W_n\right|^2\right)\\
&=\mathbb{E}\left(\frac{1}{\Delta_n}|a\Delta_n-\mathbb{E}(a\Delta_n+b\Delta W_n|\mathcal{A}_{\tau_n})|^2\right)\\
&=\mathbb{E}\left(\frac{1}{\Delta_n}|a\Delta_n-a\Delta_n-\mathbb{E}(b\Delta W_n|\mathcal{A}_{\tau_n})|^2\right)\\
&=\mathbb{E}\left(\frac{1}{\Delta_n}|\mathbb{E}(b\Delta W_n)|\mathcal{A}_{\tau_n}\right)\\
&=0.
\end{aligned}
$$

Where $\Delta_n=\tau_{n+1}-\tau_n$ and $\Delta W_n=W_{\tau_{n+1}}-W_{\tau_n}$.

In general, the explicit Euler scheme has strong order of convergence at least $\gamma=0.5$. This scheme is also called the order 0.5 strong Taylor scheme. In special cases, the scheme may actually achieve a higher order of strong convergence. For example, when the noise is additive, that is when the diffusion coefficient has the form

$$b(t,x)\equiv b(t)$$

for all $(t,x)\in\mathbb{R}^+\times\mathbb{R}^d$ and under appropriate smoothness assumptions on a,b it turns out that the Euler scheme has order of strong convergence $\gamma=1.0$.

The order 1.5 strong Taylor scheme

In the general multi-dimensional case with $d,m=1,2,\dots$ the k-th component of the order 1.5 strong Taylor scheme takes the form

$$
\begin{aligned}
Y^k_{n+1}=Y^k_n+a^k\Delta+\frac{1}{2}L^0a^k\Delta^2+\sum_{j=1}^m(b^{k,j}\Delta W^j+L^0b^{k,j}I_{(0,j)}+L^ja^kI_{(j,0)})\\
+\sum_{j_1,j_2=1}^m L^{j_1}b^{k,j_2}I_{(j_1,j_2)}+\sum_{j_1,j_2,j_3=1}^m L^{j_1}L^{j_2}b^{k,j_3}I_{(j_1,j_2,j_3)},
\end{aligned}
$$

where

$$
\begin{aligned}
L^0&=\frac{\partial}{\partial t}+\sum_{k=1}^d a^k\frac{\partial}{\partial x^k}+\frac{1}{2}\sum_{k,l=1}^d\sum_{j=1}^m b^{k,j}b^{l,j}\frac{\partial^2}{\partial x^k\partial x^l},\\
L^j&=\sum_{k=1}^d b^{k,j}\frac{\partial}{\partial x^k},\qquad j=1,2,\dots,m,\\
I_{(j_1,\dots,j_l)}&=\int_{\tau_n}^{\tau_{n+1}}\dots\int_{\tau_n}^{s_2}dW^{j_1}_{s_1}\dots dW^{j_l}_{s_l},\\
&j_1,\dots,j_l\in\{0,1,\dots,m\},\ l=1,2,\dots,\ n=0,1,\dots\text{with } W^0_t=t.
\end{aligned}
$$

Remark 2.3.11. The order 1.5 strong Taylor scheme can be derived from the Ito-Taylor expansion with the hierarchical set

$$\mathcal{A} = \{v, (0), (1), (0,1), (1,0), (0,0), (1,1,1)\}.$$

We can obtain more accurate strong Taylor schemes by including further multiple stochastic integrals from the stochastic Taylor expansion in the scheme. These multiple stochastic integrals contain additional information about the sample path of the Wiener process.

Theorem 2.3.12. [37, Theorem 10.6.3] *Let $Y^\delta = \{Y^\delta(t),\, t \in [0,T]\}$ be the order γ strong Ito-Taylor approximation, for a given $\gamma = 0.5,\, 1.0,\, 1.5,\, 2.0, ...$, corresponding to a time discretization $(\tau)_\delta$, where $\delta \in (0,1)$. Suppose that the coefficient functions f_α satisfy*

$$|f_\alpha(t,x) - f_\alpha(t,y)| \leqslant K_1|x-y| \tag{2.3.2}$$

for all $\alpha \in \mathcal{A}_\gamma$, $t \in [0,T]$ and $x, y \in \mathbb{R}^d$;

$$f_{-\alpha} \in C^{1,2} \qquad \text{and} \qquad f_\alpha \in \mathcal{H}_\alpha$$

for all $\alpha \in \mathcal{A}_\gamma \cup \mathcal{B}(\mathcal{A}_\gamma)$; and

$$|f_\alpha(t,x)| \leqslant K_2(1+|x|) \tag{2.3.3}$$

for all $\alpha \in \mathcal{A}_\gamma \cup \mathcal{B}(\mathcal{A}_\gamma)$, $t \in [0,T]$ and $x \in \mathbb{R}^d$. Then

$$\mathbb{E}\left(\sup_{0\leqslant t\leqslant T} |X_t - Y^\gamma(t)|^2 \big| \mathcal{A}_0\right) \leqslant K_3(1+|X_0|^2)\delta^{2\gamma} + K_4|X_0 - Y^\gamma(0)|^2.$$

The constants K_1, K_2, K_3, K_4 do not depend on δ.

In order to prove the above theorem we need the following lemma.

Lemma 2.3.13. [37, Lemma 10.8.1] *Suppose for a multi-index $\alpha \in \mathcal{M}\backslash\{v\}$, time discretization $(\tau)_\delta$ with $\delta \in (0,1)$ and a right continuous adapted process $g \in H_\alpha$ that*

$$R_{t_0,u} := \mathbb{E}\left(\sup_{t_0\leqslant s\leqslant u} |g(s)|^2 \big| \mathcal{A}_{t_0}\right) < \infty,$$

and let

$$F_t^\alpha := \mathbb{E}\left(\sup_{t_0\leqslant z\leqslant t} \left| \sum_{n=0}^{n_s-1} I_\alpha[g(.)]_{\tau_n,\tau_{n+1}} + I_\alpha[g(.)]_{\tau_{n_s},z} \right|^2 \big| \mathcal{A}_{t_0}\right).$$

Then

$$F_t^\alpha \leqslant \begin{cases} (T-t_0)\delta^{2(l(\alpha)-1)} \int_{t_0}^{t} R_{t_0,u}\, du & : l(\alpha) = n(\alpha) \\ 4^{l(\alpha)-n(\alpha)+2}\delta^{l(\alpha)+n(\alpha)-1} \int_{t_0}^{t} R_{t_0,u} & : l(\alpha) \neq n(\alpha), \end{cases}$$

w.p.1, for each $t \in [t_0, T]$.

Proof of Theorem 2.3.12. From the uniform moment estimates [37, Exercise 4.5.5] we have

$$\mathbb{E}\left(\sup_{0\leqslant s\leqslant T}|X_s|^2\big|\mathcal{A}_0\right)\leqslant C_1(1+|X_0|^2). \tag{2.3.4}$$

We can show that

$$\mathbb{E}\left(\sup_{0\leqslant s\leqslant T}|Y^\delta(s)|^2\big|\mathcal{A}_0\right)\leqslant C_2(1+|Y^\delta(0)|^2), \tag{2.3.5}$$

where the constant C_2 does not depend on the maximum step size δ. In addition, from the Ito-Taylor expansion (2.3.1) we can represent the Ito process X as

$$X_\tau=\sum_{\alpha\in\mathcal{A}_\gamma}I_\alpha[f_\alpha(\rho,X_\rho)]_{\rho,\tau}+\sum_{\alpha\in\mathcal{B}(\mathcal{A}_\gamma)}I_\alpha[f_\alpha(.,X.)]_{\rho,\tau}$$

for any two stopping times ρ and τ with $0\leqslant\rho\leqslant\tau\leqslant T$, w.p.1. Thus, we can write

$$\begin{aligned}X_t=X_0&+\sum_{\alpha\in\mathcal{A}_\gamma\setminus\{v\}}\left\{\sum_{n=0}^{n_t-1}I_\alpha[f_\alpha(\tau_n,X_{\tau_n})]_{\tau_n,\tau_{n+1}}+I_\alpha[f_\alpha(\tau_{n_t},X_{\tau_{n_t}})]\right\}\\&+\sum_{\alpha\in\mathcal{B}(\mathcal{A}_\gamma)}\left\{\sum_{n=0}^{n_t-1}I_\alpha[f_\alpha(.,X.)]_{\tau_n,\tau_{n+1}}+I_\alpha[f_\alpha(.,X.)]_{\tau_{n_t},t}\right\}.\end{aligned} \tag{2.3.6}$$

Otherwise, let $\gamma=0.5,\ 1.0,\ 1.5,\ 2.0,...$ and $d,m=1,2,\ldots$. Then, for a given time discretization $(\tau)_\delta$ we define the general multi-dimensional order γ strong Ito-Taylor approximation $Y=\{Y(t),\,t\geqslant 0\}$ by the vector equation [37, (10.6.4)]

$$\begin{aligned}Y(t)&=Y_{n_t}+\sum_{\alpha\in\mathcal{A}_\gamma\setminus\{v\}}I_\alpha[f_\alpha(\tau_{n_t},Y_{N_t})]_{\tau_{n_t},t}\\&=\sum_{\alpha\in\mathcal{A}_\gamma}I_\alpha[f_\alpha(\tau_{n_t},Y_{n_t})]_{\tau_{n_t},t},\end{aligned} \tag{2.3.7}$$

From (2.3.6) and (2.3.7) we obtain

$$\begin{aligned}Z(t)&=\mathbb{E}\left(\sup_{0\leqslant s\leqslant t}|X_s-Y^{\delta(s)}|^2\big|\mathcal{A}_0\right)\\&\leqslant C_3\left(|X_0-Y^\delta(0)|^2+\sum_{\alpha\in\mathcal{A}_\gamma\setminus\{v\}}R_t^\alpha+\sum_{\alpha\in\mathcal{B}(\mathcal{A}_\gamma)}U_t^\alpha\right)\end{aligned} \tag{2.3.8}$$

for all $t\in[0,T]$, where R_t^α and u_t^α will be defined below when they are estimated. In particular, from Lemma 2.3.13 and the Lipschitz condition (2.3.2) we have

$$R_t^\alpha:=\mathbb{E}(\sup_{0\leqslant s\leqslant t}|\sum_{n=0}^{n_s-1}I_\alpha[f_\alpha(\tau_n,X_{\tau_n})-f_\alpha(\tau_n,Y_n^\delta)]_{\tau_n,\tau_{n+1}}$$

$$I_\alpha[f_\alpha(\tau_{n_t}, X_{\tau_{n_t}}) - f_\alpha(\tau_{n_s}, Y^\delta_{n_t})]_{\tau_{n_s},s}|\Big|\mathcal{A}_0)$$

$$\leqslant C_4 \int_0^t \mathbb{E}\left(\sup_{0\leqslant s\leqslant u} \left|f_\alpha(\tau_{n_t}, X_{\tau_{n_t}}) - f\alpha(\tau_{n_s}, Y^\delta_{n_t})\right|^2 \Big|\mathcal{A}_0\right) du$$

$$\leqslant C_4 K_1^2 \int_0^t Z(u)du \tag{2.3.9}$$

for all $\alpha \in \mathcal{A}_\gamma$.

In addition, for all $\alpha \in \mathcal{B}(\mathcal{A}_\gamma)$ from Lemma 2.3.13, (2.3.3) and (2.3.5) we have

$$U_t^\alpha := \mathbb{E}\left(\sup_{0\leqslant s\leqslant t} |\sum_{n=0}^{n_s-1} I_\alpha[f_\alpha(., X.)]_{\tau_n,\tau_{n+1}} + I_\alpha[f_\alpha(., X.)]_{\tau_{n_s},s}|^2\Big|\mathcal{A}_0\right)$$
$$\leqslant C_5\left(1 + |X_0|^2\right)\delta^{\phi(\alpha)}, \tag{2.3.10}$$

where

$$\phi(\alpha) = \begin{cases} 2(l(\alpha)-1) & : l(\alpha) = n(\alpha) \\ l(\alpha) + n(\alpha) - 1 & : l(\alpha) \neq n(\alpha) \end{cases}.$$

For all such α we have $l(\alpha) \geqslant \gamma+1$ when $l(\alpha) = n(\alpha)$ and $l(\alpha)+n(\alpha) \geqslant 2\gamma+1$ when $l(\alpha) \neq n(\alpha)$. Thus, for all $\alpha \in \mathcal{B}(\mathcal{A}_\gamma)$, (2.3.10) gives

$$U_t^\alpha \leqslant C_5\left(1 + |X_0|^2\right)\delta^{2\gamma}. \tag{2.3.11}$$

Combining (2.3.8), (2.3.9) and (2.3.11) we obtain

$$Z(t) \leqslant C_7|X_0 - Y^\delta(0)|^2 + C_8\left(1 + |X_0|^2\right)\delta^{2\gamma} + C_9\int_0^t Z(u)du$$

for all $t \in [0, T]$. By the assumed bounds (2.3.4) and (2.3.5), $Z(t)$ is bounded, so by the Gronwall inequality (Lemma 2.2.9) we obtain

$$Z(T) \leqslant K_3\left(1 + |X_0|^2\right)\delta^{2\gamma} + K_4|X_0 - Y^\delta(0)|^2,$$

which is the assertion of the theorem. □

Chapter 3

Forest Model

This chapter is devoted to investigating long-time behavior of solutions to a stochastic forest model. First, we review the existence and uniqueness results for global positive solutions. Then, we will study long-time behavior of solutions numerically.

3.1 Model equations

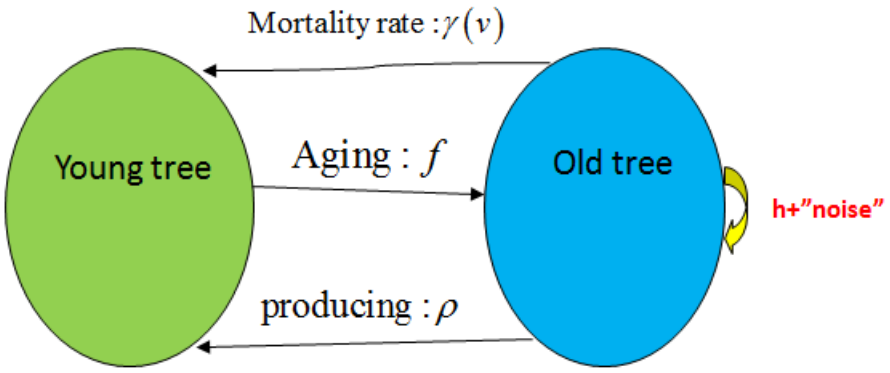

Figure 3.1: Forest model diagram

In [3, 4], Antonovsky et al. have presented a deterministic, mono-species ecosystem model with two age classes of trees: the young age class and the old age class:

$$\begin{cases} du &= \{\rho v - [\gamma(v) + f]u\}dt, \\ dv &= (fu - hv)dt. \end{cases} \tag{3.1.1}$$

Here, $u(t)$ and $v(t)$ denote tree densities of young and old age classes, respectively. The parameter f is the aging coefficient of young tree. It stands for proportion of young trees growing into old trees as time goes by. ρ is the reproduction rate of young trees from seeds of old trees. h is the mortality

rate of old age trees. While, $\gamma(v)$ is a mortality of young age trees which is allowed to depend on the old-tree density v.

We assume that there exists some optimal value of v under which the recruitment of young age trees is maximal. Considering qualitative nature of the forest system, it is usually taken as $\gamma(v) = a(v-b)^2 + c$, here a, b, c are positive constants (See Figure 3.2). It deduces that at $v = b$ the function $\gamma(v)$ attains its minimal value c. This is reasonable because when the density of old trees is too large then they will cover almost the area, so the young tree may not get enough light from the sun and nutrient from soil. Conversely, if v is too small then they can not protect young trees from negative effect from the environment, for example heavy rain, soil erosion. That makes the mortality rate of young age trees to increase. For ecological reason, initial values are always taken nonnegative, i.e., $u(0), v(0) \geqslant 0$.

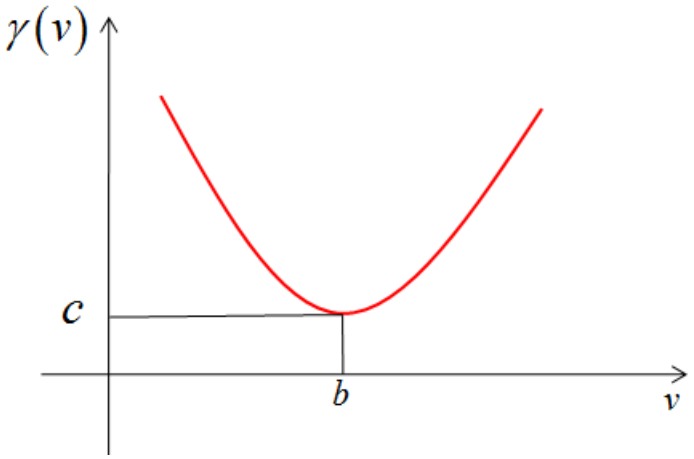

Figure 3.2: Mortality of old tree function

Remark 3.1.1. With non-negative initial value $u(0) \geqslant 0$ and $v(0) \geqslant 0$, solutions of (3.1.1) is non-negative and global. The non-negative stationary solutions are:

$$P_1 = (0,0),$$

$$P_2 = \left(\frac{h}{f}\left(b + \sqrt{\frac{\rho f - h(c+f)}{ah}}\right), b + \sqrt{\frac{\rho f - h(c+f)}{ah}}\right) \text{ if } h \leqslant \frac{\rho f}{c+f},$$

$$P_3 = \left(\frac{h}{f}\left(b - \sqrt{\frac{\rho f - h(c+f)}{ah}}\right), b - \sqrt{\frac{\rho f - h(c+f)}{ah}}\right)$$

$$\text{if } \frac{\rho f}{ab^2 + c + f} \leqslant h \leqslant \frac{\rho f}{c+f}.$$

Furthermore, if $h \in \left(\frac{\rho f}{c+f}, \infty\right)$ then P_1 is globally asymptotically stable, that is $\lim_{t\to\infty} u(t) = \lim_{t\to\infty} v(t) = 0$ for any initial value $u(0) \geqslant 0$ and $v(0) \geqslant 0$. In the

other words, the forest falls into decline; if $h \in \left(\frac{\rho f}{ab^2+c+f}, \frac{\rho f}{c+f}\right)$ then P_1 and P_2 are stable and P_3 is unstable; if $h \in \left(0, \frac{\rho f}{ab^2+c+f}\right)$ then P_1 is unstable, and P_2 is stable.

Now we will show some numerical results illustrating those results.

Example 3.1.2. In Figure 3.3, we illustrate that when $h \in \left(\frac{\rho f}{ab^2+c+f}, \frac{\rho f}{c+f}\right)$ then among 10 trajectories which start from $u(0) = v(0) = k$, $k = 1, 2, \ldots, 10$, some tend to P_1 and the others tend to P_2.

Example 3.1.3. Figure 3.4 shows that if $h \in \left(0, \frac{\rho f}{ab^2+c+f}\right)$ then P_1 is unstable, and P_2 is stable. In this figure, we draw 13 trajectories starting from $(u(0), v(0))$, where $u(0) = 10$ and $v(0) = 0, 0.5, 1, \ldots, 6$, in phase space (u, v). We can see that all these tend to P_2.

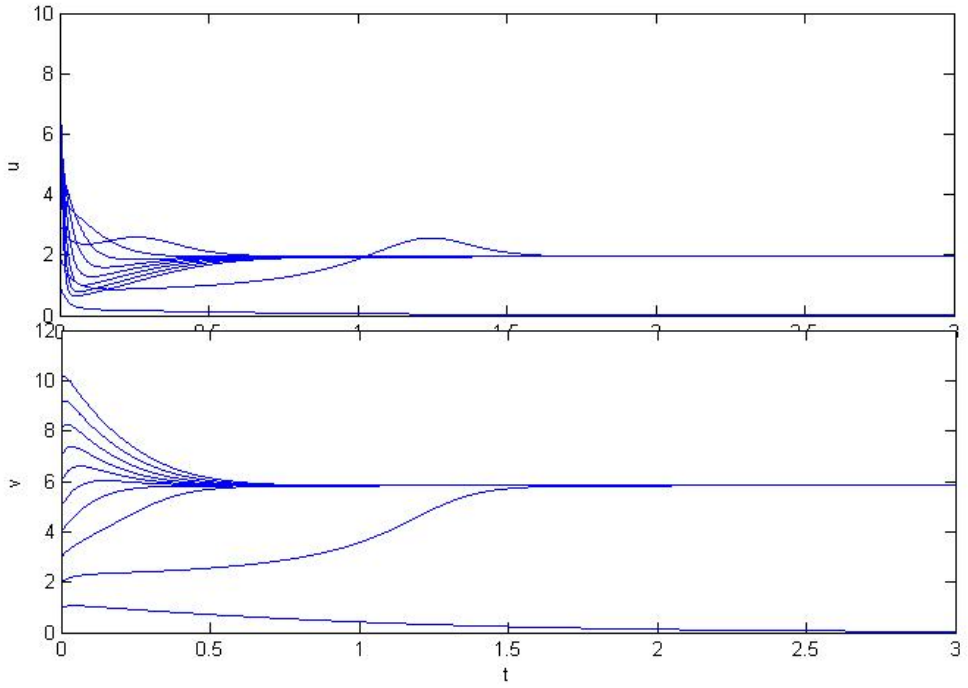

Figure 3.3: $h \in \left(\frac{\rho f}{ab^2+c+f}, \frac{\rho f}{c+f}\right)$ then P_1 and P_2 are stable

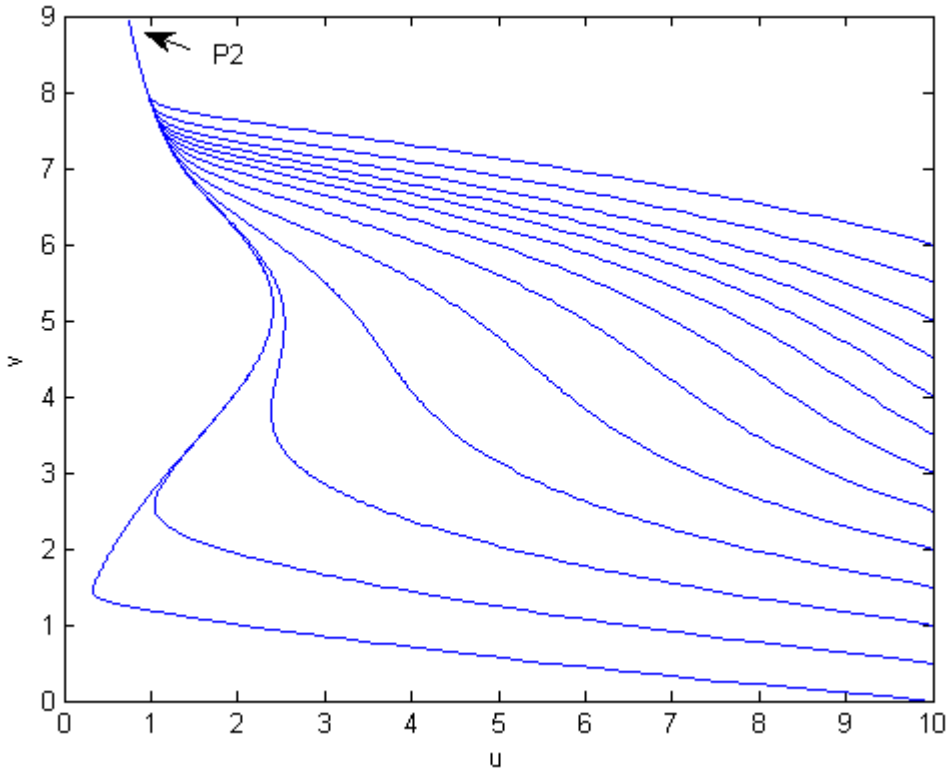

Figure 3.4: $h \in \left(0, \frac{\rho f}{ab^2+c+f}\right)$ then P_1 is unstable, and P_2 is stable

From the above results we see that the asymptotic behavior of solutions of (3.1.1) depends strongly on the magnitude of mortality of old age trees h. On the other hand, we know that real forest systems are always subject to environmental noises such as temperature, humidity, amount of sunlight, etc. However, it is very difficult to survey a mathematical model that includes noise factor to many elements. So, it is meaningful to begin with a simple model focusing on a central element. It is interesting to consider the above model with effect of noise on h, i.e., $h \rightsquigarrow h+$noise (See Figure 3.1). This is the motivation to study the following stochastic forest model which is performed by Ito stochastic differential equations in $\mathbb{R}^2$:

$$\begin{cases} du &= \{\rho v - [\gamma(v) + f]u\}dt, \\ dv &= (fu - hv)dt + \sigma v dw_t. \end{cases} \tag{3.1.2}$$

Here the process $\{w_t, t \geqslant 0\}$ is a one-dimensional Brownian motion defined on a complete probability space $(\Omega, \mathcal{F}, \{\mathcal{F}_t\}_{t\geqslant 0}, \mathbb{P})$ with filtration satisfying the usual conditions [35] with coefficient $\sigma > 0$.

Remark 3.1.4. In our model, we consider the mortality rate of old age trees $h + \sigma$ which contains two components: h is a well-understood component

and σ is a random or noise component. The component h can be considered as a controllable parameter as it includes the number of old tree human cut down for their need. So that the study of sustainability of forest gives us information for effectively exploiting our food resource without destroying it.

3.2 Numerical scheme for forest model

We apply the 1.5 order strong Taylor scheme to the above system, we get the following iteration scheme:

$$\begin{cases} u_{s+1} &= u_s + \{\rho v_s - [a(v_s-b)^2 + c + f]\, u_s\}\,\Delta + \rho\sigma v_s \Delta Z \\ &\quad + \dfrac{\Delta^2}{2}\Big\{ -\rho v_s\,[a(v_s-b)^2 + c + f] + [a(v_s-b)^2 + c + f]^2\, u_s \\ &\quad + (f u_s - h v_s)\rho\Big\}, \\ v_{s+1} &= v_s\left\{1 + \dfrac{\sigma^2}{2}\left[(\Delta W)^2 - \Delta\right] - h\sigma\Delta Z\right\} + (f u_s - h v_s)\Delta + \sigma v_s \Delta W \\ &\quad + \sigma(f u_s - h v_s)(\Delta W \Delta - \Delta Z) \\ &\quad + \dfrac{\Delta^2}{2}\left\{f\rho v_s - [a(v_s-b)^2 + c + f]\, f u_s - h(f u_s - h v_s)\right\} \\ &\quad + \dfrac{\sigma^3}{2} v_s \left[\dfrac{(\Delta W)^2}{3} - \Delta\right]\Delta W, \\ &\quad s = 0, 1, \ldots, n-1. \end{cases}$$

Here $\Delta = t_{s+1} - t_s$ for all $s = 0, 1, \ldots, n-1$ and $\Delta Z = I_{(1,0)} = \int\limits_{\tau_n}^{\tau_{n-1}} dW_{s_1} ds_2$. The pair $(\Delta W, \Delta Z)$ can be determined from two independent $N(0,1)$ random variables $U_1,\ U_2$ through:

$$\Delta W = U_1\sqrt{\Delta}, \qquad \Delta Z = \frac{1}{2}\Delta^{3/2}\left(U_1 + \frac{1}{\sqrt{3}}U_2\right).$$

Our objective of studying this problem is to study the asymptotic behavior of solutions to the above stochastic model equations. In order to achieve that we will survey:

(a) The existence, uniqueness, and boundedness of global solutions.
(b) Sufficient conditions for the decline of the system.
(c) The support of stationary density.

3.3 Some results

Now we will state briefly some theoretical results and illustrate some of the results by numerical simulations using the order 1.5 strong Taylor scheme. The content of this section mainly lies in the paper [43].

3.3.1 Existence, uniqueness and boundedness of global positive solution

Theorem 3.3.1 (Existence of unique global solution)**.** *For any* $(u_0, v_0) \in \mathbb{R}^2_+$, *there exists a unique solution* (u_t, v_t) *of* (3.1.2) *for* $t \geqslant 0$. *Furthermore, with probability one,* $\mathbb{R}^2_+$ *is positively invariant for* (3.1.2)*, i.e., if* $(u_0, v_0) \in \mathbb{R}^2_+$ *then* $(u_t, v_t) \in \mathbb{R}^2_+$ *for all* $t \geqslant 0$ *with probability one.*

Proof. Since the functions on the right side of (3.1.2) are locally Lipschitz continuous, for any initial value $(u_0, v_0) \in \mathbb{R}^2_+$ there is a unique local solution (u_t, v_t) defined on an interval $[0, \tau)$, where $\tau \leq \infty$. If $\tau < \infty$ it is an explosion time, i.e., $\lim_{t\to\tau}(|u_t| + |v_t|) = \infty$ (see for instance [6, 19]). To show that this solution is global and $\mathbb{R}^2_+$ is positively invariant, we use the technique of localization introduced in [31].

Let $k_0 > 0$ be sufficiently large for u_0 and v_0 to lie within interval $[\frac{1}{k_0}, k_0]$. Denote $H_k = [\frac{1}{k}, k] \times [\frac{1}{k}, k]$ then $\cup_{k=k_0}^{\infty} H_k = \mathbb{R}^2_+$. Let us define a sequence of stopping times for each integer $k \geqslant k_0$ by

$$\tau_k = \inf\{t > 0 : (u_t, v_t) \notin H_k\}.$$

Here we use convention that the infimum of the empty set is ∞. Since τ_k is nondecreasing as $k \to \infty$, there exists a limit $\tau_\infty = \lim_{k\to\infty} \tau_k$. It is clear that $\tau_\infty \leq \tau$ a.s.

Suppose to the contrary that $\mathbb{P}(\Omega^*) > 0$ where $\Omega^* = \{\omega \in \Omega : \tau < \infty\}$. Then, $\tau_\infty < \infty$ on Ω^*. Therefore, there would exist $T > 0$ and $\epsilon \in (0, 1)$ such that $\mathbb{P}\{\tau_\infty < T\} > \epsilon$. Consider a positive function $V(u, v) = u^2 + v^2 - \ln u - \ln v$ on $\mathbb{R}^2_+$. Using the Ito formula, we have

$$dV(u(t), v(t)) = LV(u(t), v(t))dt + (2\sigma^2 v^2 - \sigma v)dw_t, \tag{3.3.1}$$

where infinitesimal operator L is

$$LV(u, v) = \frac{1}{2}\sigma^2 v^2 \frac{\partial^2 V}{\partial v^2} + [\rho v - \{a(v - b)^2 + c + f\}u]\frac{\partial V}{\partial u} + (fu - hv)\frac{\partial V}{\partial v}.$$

It is seen that

$$\begin{aligned} LV(u, v) =& 2(\rho + f)uv - 2[a(v - b)^2 + c + f]u^2 + (\sigma^2 - 2h)u^2 + a(v - b)^2 \\ & - \frac{\rho v}{u} - \frac{fu}{v} + c + f + h + \frac{\sigma^2}{2}. \end{aligned}$$

Therefore, there exist $M_i > 0$ $(i = 1, 2)$ such that $LV(u, v) < M_1 V(u, v) + M_2$ for all $(u, v) \in \mathbb{R}^2_+$. It then follows from (3.3.1) that

$$\int_0^{t\wedge\tau_k} dV(u(s), v(s)) \leq \int_0^{t\wedge\tau_k} [M_1 V(u(s), v(s)) + M_2]ds$$

$$+ \int_0^{t\wedge\tau_k} (2\sigma^2 v(s)^2 - \sigma v(s)) dw_s.$$

Taking expectations of both sides of this inequality, we have for $t \leq T$,

$$\mathbb{E}V((u_{t\wedge\tau_k}, v_{t\wedge\tau_k})) \leq V(u(0), v(0)) + M_2(t\wedge\tau_k) + M_1\mathbb{E}\int_0^{t\wedge\tau_k} V(u(s), v(s))ds$$

$$\leq [V(u(0), v(0)) + M_2 T] + M_1 \int_0^t \mathbb{E}V(u(s\wedge\tau_k), v(s\wedge\tau_k))ds.$$

By the Gronwall inequality (Lemma 2.2.9), for any $0 < t \leq T$ it holds true that

$$\begin{aligned}\mathbb{E}V((u_{t\wedge\tau_k}, v_{t\wedge\tau_k})) &\leq [V(u(0), v(0)) + M_2 T]e^{M_1 t} \\ &\leq [V(u(0), v(0)) + M_2 T]e^{M_1 T}.\end{aligned}$$

Therefore,

$$\begin{aligned}[V(u(0), v(0)) + M_2 T]e^{M_1 T} &\geqslant \mathbb{E}V((u_{T\wedge\tau_k}, v_{T\wedge\tau_k})) \\ &\geqslant \mathbb{E}[1_{\{\tau_\infty < T\}} V((u_{T\wedge\tau_k}, v_{T\wedge\tau_k}))] \\ &= \mathbb{E}[1_{\{\tau_\infty < T\}} V(u(\tau_k), v(\tau_k)].\end{aligned}$$

On the other hand, if $\tau_k < \infty$ then

$$\begin{aligned}V((u_{T\wedge\tau_k}, u_{T\wedge\tau_k})) &\geqslant \min\left\{k^2 - \ln k, \left(\frac{1}{k}\right)^2 - \left(\frac{1}{k}\right)\right\} \\ &= \min\left\{k^2 - \ln k, \ln k + \frac{1}{k^2}\right\}.\end{aligned}$$

Therefore

$$[V(u(0), v(0)) + M_2 T]e^{M_1 T} \geqslant \epsilon \min\left\{k^2 - \ln k, \ln k + \frac{1}{k^2}\right\}.$$

Letting $k \to \infty$ we arrive at a contradiction

$$\infty > [V(u(0), v(0)) + M_2 T]e^{M_1 T} = \infty.$$

This implies that $\mathbb{P}\{\tau = \infty\} = 1$. Consequently, $\mathbb{R}^2_+$ is an invariant set. The proof is complete. □

Theorem 3.3.2 (Boundedness)**.** *For any $(u_0, v_0) \in \mathbb{R}^2_+$, the following statements hold true.*

(i) $\sup_{t\geqslant 0} u(t) \leqslant M^\star := \max\{u_0,\, M_0\}$ *a.s.*

(ii) $\limsup_{t\to\infty} u(t) \leqslant M_0$ *a.s.*

(iii) *For every $\theta \in \left[1,\, 1 + \frac{2h}{\sigma^2}\right)$, there exists $M_\theta > 0$ such that*

$$\limsup_{t\to\infty} \mathbb{E}v^\theta(t) \leqslant M_\theta.$$

(iv) $\liminf_{t\to\infty} v(t) = 0 \qquad a.s.$

Here

$$\begin{aligned} M_0 &= \inf\{u \,|\, \rho v - [a(v-b)^2 + c + f]u < 0 \text{ for every } v > 0\} \\ &= \inf\left\{u \,|\, \frac{\rho v}{a(v-b)^2 + c + f} - u < 0 \text{ for every } v > 0\right\} \\ &= \sup_{v>0} \frac{\rho v}{a(v-b)^2 + c + f} \\ &= \frac{\rho\sqrt{ab^2 + c + f}}{\sqrt{a}\left[(\sqrt{ab^2 + c + f} - \sqrt{a}b)^2 + c + f\right]}. \end{aligned} \tag{3.3.2}$$

For the proof of this theorem, we refer the reader to [60].

In Figure 3.5, we draw the end points $(u(T), v(T))$ at time $T = 50$ of 2601 trajectories starting from different points $(u_0, v_0) \in \{(x, y) : x, y = 0.2n, n = 0, 1, \ldots, 50\}$. This figure illustrates results stated in Theorem 3.3.2. For (iii) statement, here we take $\theta = 1$, then we have $M_1 = \frac{f}{h} M_0$. This figure also suggests the support of the stationary density function of random variable $(u(t), v(t))$ when it exists.

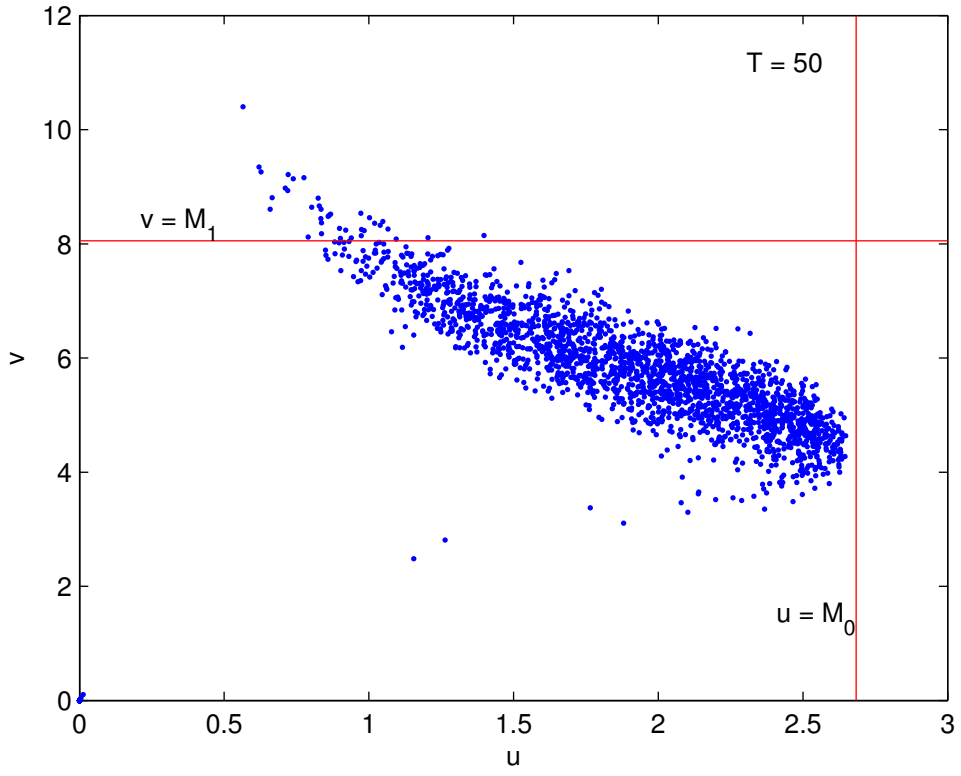

Figure 3.5: States of trajectories at a long-time instant

3.3.2 Stability of forest

Example 3.1.2 and Example 3.1.3 show the stability of solution in deterministic model. We now want to observe the asymptotic behavior of solutions to stochastic system (3.1.2) under relatively small noise. To do that, we repeat simulations similar to those in Example 3.1.2 and Example 3.1.3 with small noises.

Example 3.3.3. In Figure 3.6, we illustrate that when $h \in \left(\frac{\rho f}{ab^2+c+f}, \frac{\rho f}{c+f}\right)$ and $\sigma = 0.5$ which is relatively small, then among 6 trajectories which start from $u(0) = v(0) = k$, $k = 1, 2, \ldots, 6$, some tend to P_1 and the others oscillate around P_2.

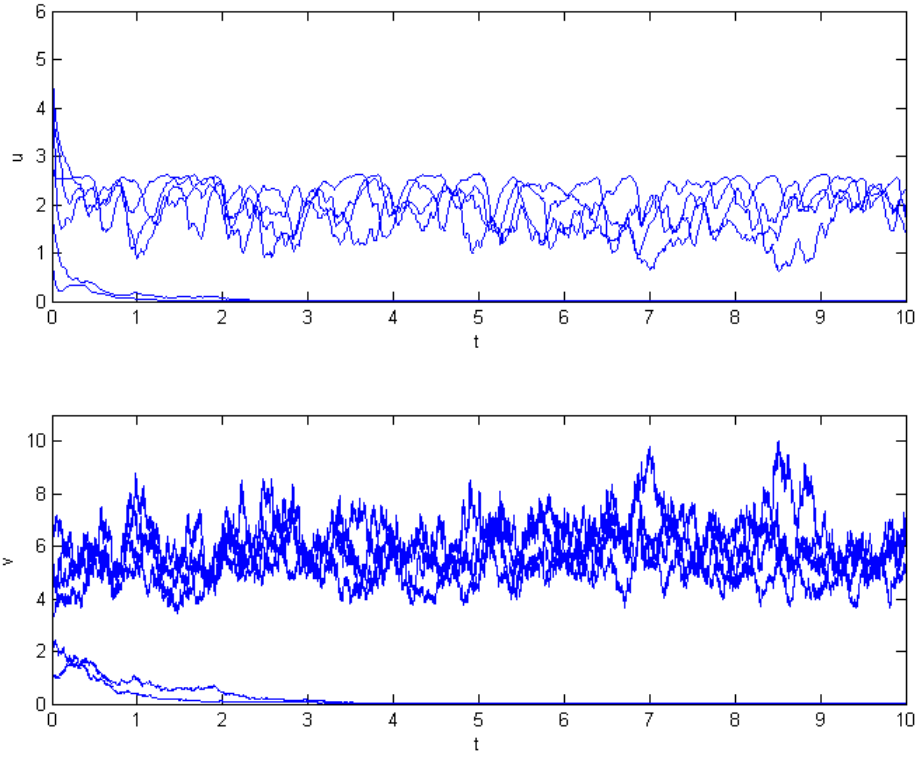

Figure 3.6: Asymptotic behavior of solutions under small noises (a)

Example 3.3.4. In this example we take $h \in \left(0, \frac{\rho f}{ab^2+c+f}\right)$ and small noise (here we set $\sigma = 0.5$). In Figure 3.7, we draw 13 trajectories starting from $(u(0), v(0))$ where $u(0) = 10$ and $v(0) = 0, 0.5, 1, \ldots, 6$ in phase space (u, v). We can see that all these tend to a small neighbour of P_2.

Next, let's observe some more stable examples showing that, if σ and h are sufficiently small, then the forest can survive stably.

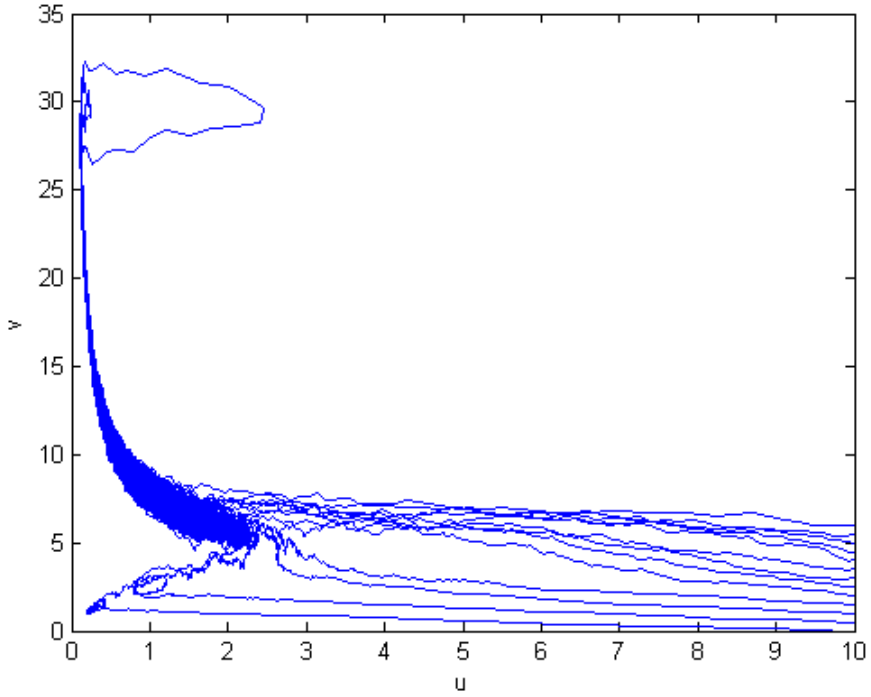

Figure 3.7: Asymptotic behavior of solutions under small noises (b)

Set $a = 2$, $b = 1$, $c = 2.5$, $f = 4$, $\rho = 5$, $h = 1$, $\sigma = 0.5$, and take an initial value $(u(0), v(0)) = (2, 1)$. Figure 3.8 shows a sample trajectory of $(u(t), v(t))$ in the phase space and graphs of $u(t)$ and $v(t)$. Figure 3.9 plots the points $(u(T), v(T))$ at $T = 10^3$ for 10^4 sample trajectories corresponding to different trajectories of Wiener process.

From the above examples we see that with small noises, then the behavior of solutions to stochastic model seems to be predictable from the results for deterministic model. They are only primary observations, we will now state more quantitative results in Subsection 3.3.3.

3.3.3 Decline of forest

In this subsection, we show that if the mortality of old age trees or noise's magnitude are larger than some critical values, then the forest falls into decline. More precisely, if $h \geqslant \min\left\{\frac{\rho f}{c+f}, \frac{f(\rho+2abM^*)}{ab^2+c+f}\right\}$ or $\sigma^2 > \frac{(\rho+c-h)^2}{2c}$, then decline of the forest takes place. In the second case, an almost sure convergence to zero is shown.

Theorem 3.3.5. *Assume that*

$$h \geqslant \min\left\{\frac{\rho f}{c+f}, \frac{f(\rho+2abM^*)}{ab^2+c+f}\right\},$$

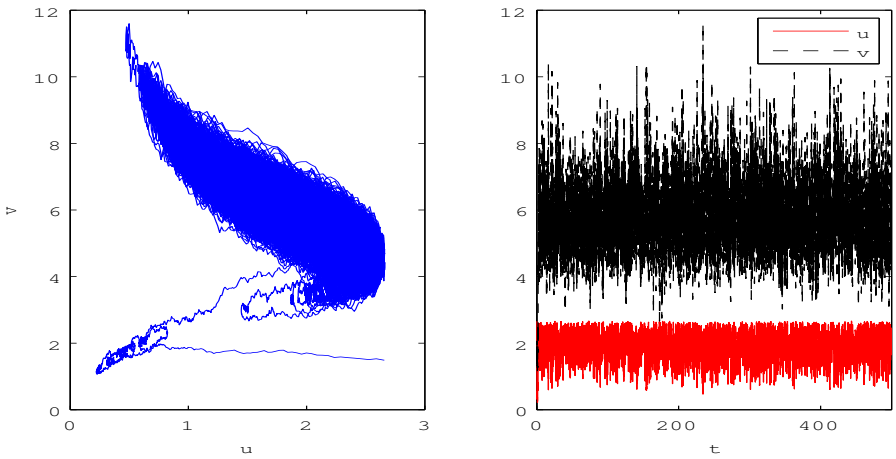

Figure 3.8: Stability of stochastic forest model

where $M^* = \max\{u_0, M_0\}$ *and* M_0 *is defined in* (3.3.2). *Then,* $u(t)$ *and* $v(t)$ *converge to* 0 *in expectation as* t *tends to infinity, that is*

$$\lim_{t\to\infty} \mathbb{E}u(t) = \lim_{t\to\infty} \mathbb{E}v(t) = 0.$$

Consequently, $u(t)$ *and* $v(t)$ *converge to* 0 *in probability as* t *tends to infinity, i.e., for any constant* $c_1 > 0$,

$$\lim_{t\to\infty} \mathbb{P}\{u(t) \geqslant c_1\} = \lim_{t\to\infty} \mathbb{P}\{v(t) \geqslant c_1\} = 0.$$

Furthermore, for any compact set $A \subset \mathbb{R}^2_+$,

$$\lim_{t\to\infty} \mathbb{P}\{(u(t), v(t)) \in A\} = 0.$$

Proof. First, we consider the case $h \geqslant \frac{\rho f}{c+f}$. It follows from (3.1.2) that

$$\begin{cases} \mathbb{E}u(t) \leq u(0) + \int_0^t [\rho \mathbb{E}v(s) - (c+f)\mathbb{E}u(s)]ds, \\ \mathbb{E}v(t) = v(0) + \int_0^t [f\mathbb{E}u(s) - h\mathbb{E}v(s)]ds. \end{cases}$$

Since functions $\varpi_1(X,Y) = \rho Y - (c+f)X$ and $\varpi_2(X,Y) = fX - hY$ are non-decreasing with respect to arguments Y and X respectively, it follows from the comparison theorem that

$$\mathbb{E}u(t) \leq x(t), \quad \mathbb{E}v(t) \leq y(t) \qquad \text{for every } t \geqslant 0,$$

where $(x(t), y(t))$ satisfies the following equations

$$\begin{cases} \frac{dx(t)}{dt} = \rho y(t) - (c+f)x(t), \\ \frac{dy(t)}{dt} = fx(t) - hy(t) \end{cases} \tag{3.3.3}$$

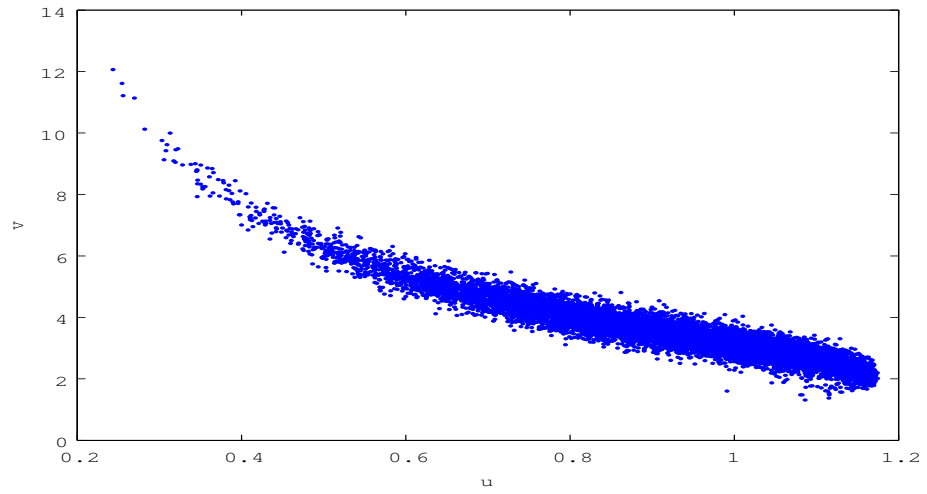

Figure 3.9: Support of invariant measure

with an initial value $(x(0), y(0)) = (u_0, v_0)$. One can show from (3.3.3) that

$$\lim_{t\to\infty} x(t) = \frac{\beta_1(c+f) - \beta_2\rho}{h(c+f) - \rho f}, \qquad \lim_{t\to\infty} y(t) = \frac{\beta_2 h - \beta_1 f}{h(c+f) - \rho f}.$$

Therefore, $(\frac{\beta_1(c+f)-\beta_2\rho}{h(c+f)-\rho f}, \frac{\beta_2 h-\beta_1 f}{h(c+f)-\rho f})$ is a stationary solution of (3.3.3). Consequently,

$$\begin{cases} [\rho f + (c+f)^2]\beta_1 = \rho(c+f+h)\beta_2, \\ [f(c+f) + hf]\beta_1 = (\rho f + h^2)\beta_2. \end{cases}$$

This algebraic equation system has a unique solution $\beta_1 = \beta_2 = 0$. Hence, we obtain

$$\lim_{t\to\infty} \mathbb{E}u(t) = \lim_{t\to\infty} \mathbb{E}v(t) = 0.$$

Second, we consider the case $h \geqslant \frac{f(\rho+2abM^*)}{ab^2+c+f}$. It follows from (3.1.2) and Theorem 3.3.2 that

$$\begin{cases} \mathbb{E}u(t) \leq u(0) + \int_0^t [\rho\mathbb{E}v(s) + 2ab\mathbb{E}(u(s)v(s)) - (ab^2 + c + f)\mathbb{E}u(s)]ds \\ \qquad\qquad \leq u(0) + \int_0^t [(\rho + 2abM^*)\mathbb{E}v(s) - (ab^2 + c + f)\mathbb{E}u(s)]ds, \\ \mathbb{E}v(t) = v(0) + \int_0^t [f\mathbb{E}u(s) - h\mathbb{E}v(s)]ds. \end{cases}$$

By the same arguments as above, we derive that

$$\lim_{t\to\infty} \mathbb{E}u(t) = \lim_{t\to\infty} \mathbb{E}v(t) = 0.$$

Finally, for any constants $0 < c_1 < c_2, 0 < d_1 < d_2$, by using the Chebyshev inequality, we have

$$P\{(u(t), v(t)) \in [c_1, c_2] \times [d_1, d_2]\} \leq P\{\sqrt{u(t)} \geqslant \sqrt{c_1}\} \leq \frac{1}{c_1}\mathbb{E}u(t).$$

By the above result, it is now easy to prove the rest of assertions of theorem. □

Set $a = 3, b = 4, c = 5, f = 6, \rho = 7, \sigma = 0.2$ and take $(u(0), v(0)) = (4, 3)$. By computing 500 sample trajectories of $u(t)$ and $v(t)$, we obtain Figure 3.10 which illustrates the graphs of expectation of young age trees and old age trees with $h = 1.71$ and $h = 2.11$ both of which satisfy the condition in Theorem 3.3.5.

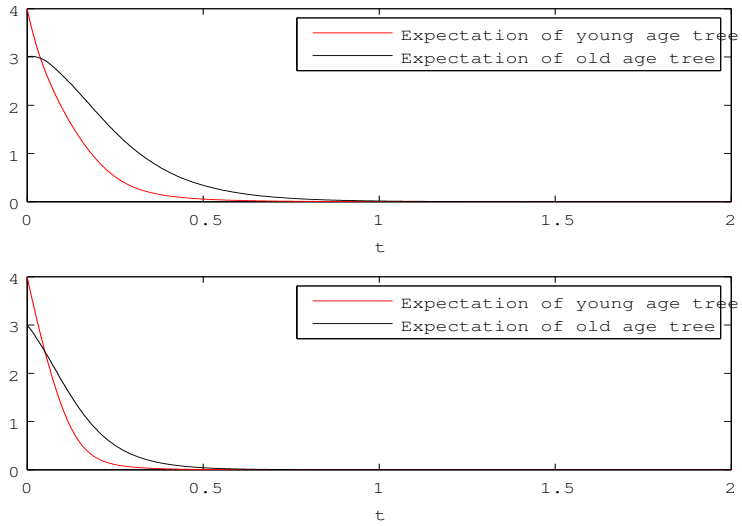

Figure 3.10: Decline of forest under large mortality of old age trees

In the following theorem, we shall show the almost sure convergence of $u(t)$ and $v(t)$ to 0.

Theorem 3.3.6. *If one of the following conditions holds true:*

H1*:* $\inf\limits_{x\in(0,\frac{c+f}{f})} F_1(x) < 0,$

H2*:* $\sup\limits_{x\in(\frac{2\rho}{\sigma^2+2h},\frac{c+f}{f})} F_1(x) > 0$ *and* $\inf\limits_{x\in(\frac{2\rho}{\sigma^2+2h},\frac{c+f}{f})} F_2(x) < 0,$ *where*

$$\begin{aligned} F_1(x) =& f^2x^4 + 2f(\sigma^2 + h - c - f)x^3 + [(c + f - h)^2 \\ & - 2\rho f - 2(c + f)\sigma^2]x^2 + 2\rho(c + f - h)x + \rho^2, \\ F_2(x) =& fx^2 - (c + f + h)x + \rho. \end{aligned} \tag{3.3.4}$$

Then

$$\lim_{t\to\infty} u(t) = \lim_{t\to\infty} v(t) = 0 \qquad \text{a.s.}$$

Proof. Let $Q(u,v) := \ln(u+kv), k>0$. Using the Ito formula, we see that

$$dQ(u(t),v(t)) = K(u(t),v(t))dt + \frac{\sigma kv}{u+kv}dw_t, \tag{3.3.5}$$

where

$$K(u,v) = \frac{(kf-c-f)u+(\rho-kh)v}{u+kv} - \frac{\sigma^2k^2v^2}{2(u+kv)^2} - \frac{au(v-b)^2}{u+kv}.$$

First, we show that under **H1** or **H2** there exists a sufficiently small $\epsilon>0$ such that $K(u,v)\leq -\frac{\epsilon}{2}$ for every $(u,v)\in\mathbb{R}^2_+$. A sufficient condition (in fact, it is also necessary condition) for this is showing existence of $\epsilon>0$ such that for every $u>0, v>0$,

$$\begin{aligned} F(u,v) :=& [2(c+f-kf)-\epsilon]u^2 - 2[k(kf-c-f)+\rho-kh+k\epsilon]vu \\ &+ [\sigma^2k^2+2k(kh-\rho)-k^2\epsilon]v^2 \geqslant 0. \end{aligned} \tag{3.3.6}$$

It is easy to see that under assumption **H1**, there exists sufficiently small $\epsilon_1>0$ such that quadratic equation $F(u,v)=0$ in variable u has non-positive discriminant for every $v>0$. Similarly, under assumption **H2**, there exists $\epsilon_2>0$ such that this quadratic equation has non-positive two solutions for every $v>0$. We set $\epsilon := \max\{\epsilon_1,\epsilon_2\}$. Therefore, (3.3.6) holds true.

Next, from (3.3.5), we have

$$\begin{aligned} \frac{1}{t}Q(u(t),v(t)) &= \frac{1}{t}Q(u(0),v(0)) + \frac{1}{t}\int_0^t K(u(s),v(s))ds + \frac{1}{t}\int_0^t \frac{\sigma v(s)}{u(s)+v(s)}dw_s \\ &\leq \frac{1}{t}Q(u(0),v(0)) - \epsilon + \frac{1}{t}\int_0^t \frac{\sigma v(s)}{u(s)+v(s)}dw_s. \end{aligned} \tag{3.3.7}$$

We set $M_t := \int_0^t \frac{\sigma v(s)}{u(s)+v(s)}dw_s$, then $\{M_t\}_{t\geqslant 0}$ is a real valued continuous martingale vanishing at $t=0$. Furthermore, M_t has quadratic form:

$$< M >_t = \int_0^t \frac{\sigma^2v^2(s)}{[u(s)+v(s)]^2}ds \leq \sigma^2 t.$$

Since a continuous local martingale can be represented as time-change Brownian motion [35, Theorem 4.6], we have

$$\lim_{t\to\infty}\frac{M_t}{t} = 0 \qquad \text{a.s.}$$

Therefore, it follows from (3.3.7) that

$$\limsup_{t\to\infty}\frac{1}{t}Q(u(t),v(t)) \leq -\epsilon \qquad \text{a.s.}$$

Consequently, $\lim_{t\to\infty} Q(u(t), v(t)) = -\infty$ a.s. It induces that

$$\lim_{t\to\infty} u(t) = \lim_{t\to\infty} v(t) = 0 \qquad \text{a.s.}$$

The proof is complete. □

Remark 3.3.7. Consider the case $F_1(1) < 0$ which implies that **H1** takes place. This condition is equivalent to $\sigma^2 > \frac{(\rho+c-h)^2}{2c}$. By Theorem 3.3.6, this means that a large noise cause decline of the forest.

Let us next observe examples suggesting decline of forest when σ is sufficiently large.

We set $a = 3$, $b = 4$, $c = 5$, $f = 6$, $h = 2$, $\rho = 7$, $\sigma = 1$ and take $(u(0), v(0)) = (4, 3)$. Figure 3.11 illustrates a sample trajectory of $(u(t), v(t))$ on phase space on the left and separated graphs for $u(t)$ and $v(t)$ on the right.

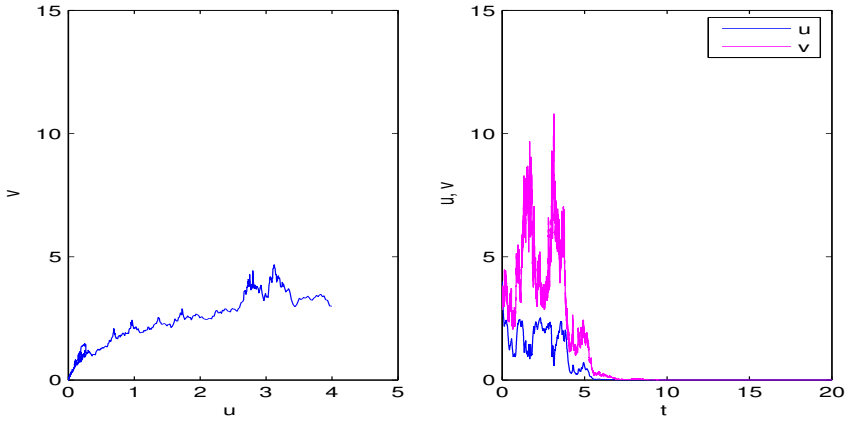

Figure 3.11: Decline of forest under large noise

Figure 3.12 represents 6 trajectories of solution to the system corresponding to 6 initial value $(u(0), v(0)) = (u_0, v_0)$, $u_0 = 10$, $v_0 = 0, 1, \ldots, 5$. The calculations are made with the same parameter as above except for h and σ. We set $h = 0.5$ and $\sigma = 3.7$. We can see that all these trajectories tend to $P_1 = (0, 0)$.

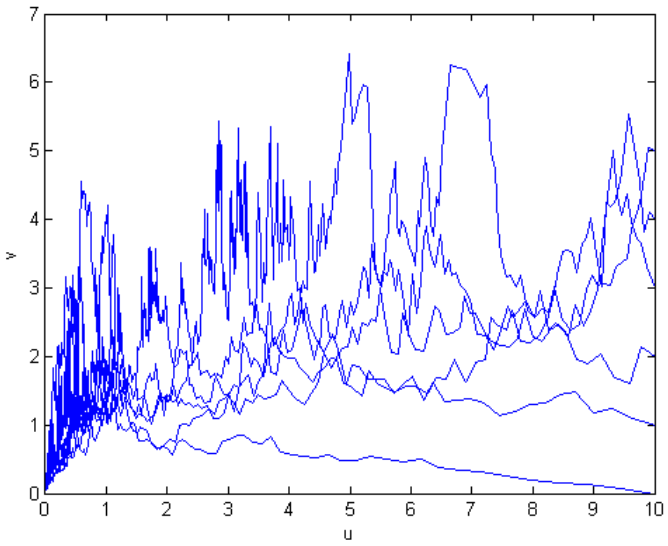

Figure 3.12: Forest decays under large noise

Chapter 4

Swarming Behavior

In this chapter, we study two models concerning with swarming of animals: the stochastic Cucker-Smale model and the basic fish schooling model. For both of them we consider swarming behaviors and influences of noise on swarming behaviors.

4.1 Related works

Swarming behavior is a collective behavior exhibited by animals. Specifically, "flocking" is the term used to refer to swarm behavior in bird, "herding" to refer to swarm behavior in quadrupeds, "shoaling" or "schooling" to refer to swarm behavior in fish. Swarming is one of the most easily observed in the real world but challenging to study phenomena in biology. It has attracted many interests of scientists from diverse fields: biologists, engineers, mathematicians, computer scientists, physicists, etc.

There are many researches dealing with this phenomena which can be classified into two categories: experimental and theoretical studies.

Empirical study on fish schooling has been done in [8, 10, 12, 36, 49, 51, 52]. We could mention here some of them. Keenleyside [36] considered the density of fish in space. His method measures essentially the nonrandom distribution of the individual fish, using a chi-squared statistic - the more closely they are schooling, the more nonrandom the distribution. With different approach comparing to Keenleyside's, Breder [8, 10] measured the fish-to-fish distances using photographs taken from above. He gave some preliminary measurements concerning the relative speed of swimming of the different members of the school. He also pointed out a number of structural characteristic on the basis of quantitative observations.

As for the theoretical approach we want to quote [1, 5, 9, 17, 24, 29, 30, 50, 55, 57, 63, 64, 66, 68]. Vicsek et al. [64] introduced a simple difference model, assuming that each particle is driven with a constant absolute velocity and the average direction of motion of the particles in its neighborhood together with some random perturbation. Oboshi et al. [50] presented another difference

model in which an individual selects one basic behavioral pattern from four based on the distance between it and its nearest neighbor. Olfati-Saber [55] and D´Orsogna et al. [17] constructed deterministic differential models using a generalized Morse and attractive/repulsive potential functions, respectively. In [24], the authors constructed a behavior model in which the influence of neighbors is formulated by the interface between the states of neighbors and a map of changes in these states. The same model show both schooling behavior with a high degree of polarization and territorial behavior due to the influencee neighbors can have on duality. Viscido et al. [66] studied the effect of population size and number of influential neighbors on the emergent properties of fish schools. They are also explored the most social factors, such that the functional form of attraction to - and repulsion from- neighbors, alignment with neighbors, regions of no social force, scaling of neighbor influence, random noise,... that contribute to fish school formation and maintenance using a series of computer simulation experiments in [67]. Our models presented in this dissertation also follow this approach.

4.2 Cucker-Smale model

4.2.1 Introduction to a stochastic Cucker-Smale model

Based on the model presented by Vicsek et al. in [64], Cucker and Smale [14, 15] introduced a model for an N-particle system in the space $\mathbb{R}^d$ $(d = 1, 2, 3, \ldots)$. The position of the i-th particle is denoted by $x_i(t)$ $(i = 1, 2, \ldots, N)$. Its velocity is denoted by $v_i(t)$ $(i = 1, 2, \ldots, N)$. The Cucker-Smale system is as follows

$$\begin{cases} x_i' &= v_i, \\ v_i' &= \dfrac{1}{N}\displaystyle\sum_{j=1}^{N} \psi(\|x_j - x_i\|)(v_j - v_i), \end{cases} \qquad 1 \leqslant i \leqslant N. \qquad (4.2.1)$$

Here, the weights $\psi(\|x_j - x_i\|)$ quantify the influence between the i-th and the j-th particles. The communication rate ψ is a non-increasing function from $[0, \infty)$ to itself of the distances between particles. This function has various forms. In [14, 15], $\psi(s) = \frac{K}{(c+s^2)^\beta}$, while in [25, 26], $\psi(s) = \frac{K}{(c+s^2)^\beta}$, $\psi(s) = \frac{K}{s^{2\beta}}$ or $\psi(s) = \text{const}$. For such functions, it is shown that when $\beta \geqslant \frac{1}{2}$ the convergence is guaranteed under some condition on the initial positions and velocities of particles.

Some authors extend the above deterministic models to ones that embrace more complicated variations. This is necessary because all real systems are subject to environmental noises and include incompletely understood information. One of the ways to do that is including stochastic influences or noise. For example, in [16], Cucker and Mordecki modified the model (4.2.1) in $\mathbb{R}^3$

by adding random noise to it

$$\begin{cases} x_i' &= v_i, \\ v_i' &= \sum\limits_{j=1}^{N} \psi(\|x_j - x_i\|)(v_j - v_i) + H_i \end{cases} \qquad 1 \leqslant i \leqslant N. \quad (4.2.2)$$

Here the communication rate ψ has the same form as that in (4.2.1). External force $H_i(t)$ is a three-dimensional Gaussian centered, stationary stochastic process and satisfies a δ-dependence condition for some $\delta > 0$, that is, two sets $\{H_i(s)|s \leqslant t\}$ and $\{H_i(s)|s \geqslant t + \delta\}$ are independent for each t. Moreover, $H_i(t)$ has $\mathcal{C}^0$ trajectories and independent coordinates. The authors showed that the conditional ν-nearly flocking occurs in finite time with a confidence which is similar to the conditional flocking of the deterministic system (4.2.1). That is, for $\nu > 0$ small enough, there exists a time T_0 depending on ν and initial values $v_i(0)$ $(1 \leqslant i \leqslant N)$ such that for every $t \in [0, T_0)$, $\sum\limits_{i,j} \|v_i(t) - v_j(t)\| \leqslant \nu$ with a positive probability. This probability, however, is not one and the interval time for the occuring is not $[0, \infty)$. In other words, it is just nearly flocking, not flocking. Ha and collaborators [2, 25, 26], in another approach, studied Cucker-Smale systems with presence of white noise. They achieved some remarkable results: In [2], by giving another definition for flocking which is relative to almost surely convergence, the author showed flocking of system under consideration which cover the case of the communication weight in [14, 15]. If the communication rate satisfies a lower bound condition, then the relative fluctuations of velocities around a mean velocity have a uniformly bounded variance in time [25, 26].

We are also interested in the effect of white noise on the system. On the other hand, the flocking behavior strongly depends on the communication rate ψ in (4.2.1). This motivates us to study the following stochastic Cucker-Smale system which incorporates a noise factor to the communication rate:

$$\begin{cases} dx_i &= v_i dt, \\ dv_i &= \sum\limits_{j=1}^{N} \psi(\|x_j - x_i\|)(v_j - v_i)dt + \sigma \sum\limits_{j=1}^{N} (v_j - v_i) \circ dw_t, \end{cases} \quad 1 \leqslant i \leqslant N. \quad (4.2.3)$$

Here $\sigma > 0$ is the strength of white noise and $\{w_t,\, t \geqslant 0\}$ is a one-dimensional Brownian motion defined on a complete probability space with normal filtration $(\Omega, \mathcal{F}, \{\mathcal{F}\}_{t \geqslant 0}, \mathbb{P})$ satisfying the usual conditions [35], and $\circ$ denotes the operation for Stratonovich stochastic differential equations. We assume that the communication rate $\psi : [0, \infty) \to [0, \infty)$ is locally Lipschitz continuous.

4.2.2 Existence of global solution

Before studying some flocking features of (4.2.3), we must prove the existence of global solution to the system. This is stated in the following theorem.

Theorem 4.2.1 (Existence and uniqueness of global solution)**.** *For any given initial values* $(x_i(0), v_i(0)) \in \mathbb{R}^{2d}$ $(1 \leqslant i \leqslant N)$*, system* (4.2.3) *has a unique global solution.*

Proof. Since the functions on the right side of (4.2.3) are locally Lipschitz continuous on $\mathbb{R}^{2d}$, there is a unique solution $(x_i(t), v_i(t))\,(1 \leqslant i \leqslant N)$ defined on an interval $[0, \tau)$, where $\tau \leqslant \infty$ and if $\tau < \infty$ it is an explosion time [6, 19], i.e.,

$$\tau = \sup\{t : \sup_{s\in[0,t),1\leqslant i\leqslant N} [||x_i(s)|| + ||v_i(s)||] < \infty\}.$$

Put

$$||x|| = \sqrt{\sum_{i=1}^{N} ||x_i||^2}, \quad ||v|| = \sqrt{\sum_{i=1}^{N} ||v_i||^2}, \quad \bar{x} = \frac{1}{N}\sum_{i=1}^{N} x_i, \quad \bar{v} = \frac{1}{N}\sum_{i=1}^{N} v_i.$$

It follows from system (4.2.3) that

$$\begin{cases} d\bar{x} = \bar{v}dt, \\ d\bar{v} = \mathbf{0}. \end{cases}$$

Then almost surely $\bar{x}(t) = \bar{x}(0) + \bar{v}(0)t$ and $\bar{v}(t) = \bar{v}(0)$ for every $t \in [0, \tau)$. Without loss of generality, we may assume that $\bar{x}(0) = \bar{v}(0) = \mathbf{0}$. Then,

$$\sum_{i=1}^{N} x_i(t) = \sum_{i=1}^{N} v_i(t) = \mathbf{0} \qquad \text{a.s.}$$

and

$$\sum_{i,j=1}^{N} ||v_i(t) - v_j(t)||^2 = 2N||v(t)||^2. \tag{4.2.4}$$

It follows from the second equation of (4.2.3) and from the chain rule of Stratonovich stochastic differential equation that

$$\begin{aligned} d||v||^2 =& \sum_{i=1}^{N} d||v_i||^2 = 2\sum_{i=1}^{N} < v_i, dv_i > \\ =& 2\sum_{i,j=1}^{N} \psi(||x_j - x_i||) < v_i, v_j - v_i > dt + 2\sigma \sum_{i,j=1}^{N} < v_i, v_j - v_i > \circ dw_t. \end{aligned} \tag{4.2.5}$$

We have

$$\sum_{i,j=1}^{N} < v_i, v_j - v_i > = \sum_{i,j=1}^{N} < v_i - v_j, v_j - v_i > + \sum_{i,j=1}^{N} < v_j, v_j - v_i >$$

$$= -\sum_{i,j=1}^{N} ||v_i - v_j||^2 - \sum_{i,k=1}^{N} < v_k, v_i - v_k >,$$

which induces

$$2\sum_{i,j=1}^{N} < v_i, v_j - v_i > = -\sum_{i,j=1}^{N} ||v_i - v_j||^2$$
$$= -2N||v||^2 \quad (\text{ see (4.2.4)}). \tag{4.2.6}$$

Furthermore, it follows from

$$\sum_{i,j=1}^{N} \psi(||x_j - x_i||) < v_i, v_j - v_i > = -\sum_{i,j=1}^{N} \psi(||x_j - x_i||)||v_i - v_j||^2$$
$$+ \sum_{i,j=1}^{N} \psi(||x_j - x_i||) < v_j, v_j - v_i >$$

that

$$2\sum_{i,j=1}^{N} \psi(||x_j - x_i||) < v_i, v_j - v_i > = -\sum_{i,j=1}^{N} \psi(||x_j - x_i||)||v_i - v_j||^2. \tag{4.2.7}$$

Thus, by (4.2.5)-(4.2.7), we obtain

$$d||v||^2 = -\sum_{i,j=1}^{N} \psi(||x_j - x_i||)||v_i - v_j||^2 dt - 2N\sigma||v||^2 \circ dw_t.$$

Or, equivalently, in the Ito form:

$$d||v||^2 = \left[-\sum_{i,j=1}^{N} \psi(||x_j - x_i||)||v_i - v_j||^2 + 2N^2\sigma^2||v||^2\right] dt - 2N\sigma||v||^2 dw_t. \tag{4.2.8}$$

Hence, by using the comparison theorem in [31], it follows from (4.2.8) that for every $t \geqslant 0$, $||v(t)||^2 \leqslant V(t)$ a.s., where $V(t)$ satisfies the following equation

$$\begin{cases} dV = 2N^2\sigma^2 V dt - 2N\sigma V dw_t, \\ V(0) = ||v(0)||^2. \end{cases}$$

This linear equation has a unique global solution $V(t) = V(0)e^{-2N\sigma w_t}$. Thus for every $t \in [0, \tau)$

$$||v(t)|| \leqslant ||v(0)||e^{-N\sigma w_t} \qquad \text{a.s.} \tag{4.2.9}$$

Then, from the first equation of (4.2.3) we have almost surely

$$\begin{aligned} d||x||^2 &= \sum_{i=1}^{N} d||x_i||^2 = 2\sum_{i=1}^{N} < x_i, v_i > dt \\ &\leqslant 2||x||\,||v||dt \leqslant 2||v(0)||e^{-N\sigma w_t}||x||dt. \end{aligned}$$

By the comparison theorem, we obtain $||x(t)||^2 \leqslant X(t)$ for all $t \geqslant 0$, where $X(t)$ satisfies the following equation

$$\begin{cases} dX = 2||v(0)||e^{-N\sigma w_t}\sqrt{X}dt, \\ X(0) = ||x(0)||^2 > 0. \end{cases}$$

Since $X(t) = [||x(0)|| + ||v(0)|| \int_0^t e^{-N\sigma w_s}ds]^2$, then for every $t \in [0, \tau)$

$$||x(t)|| \leqslant ||x(0)|| + ||v(0)|| \int_0^t e^{-N\sigma w_s}ds \qquad \text{a.s.} \qquad (4.2.10)$$

From (4.2.9), (4.2.10) and the definition of τ, we see that $\tau = \infty$ a.s. It means that the solution to (4.2.3) is unique and global. □

4.2.3 Flocking and non-flocking behaviors

In this subsection, we show some results concerning non-flocking and flocking of the system under noise. For proof of the theoretical results in this part, we refer the reader to [59]. Numerical results are shown by means of simulations based on the explicit Euler scheme which we represented in Chapter 2. Before that, we introduce a new definition of flocking.

Definition 4.2.2 (Time-asymptotic flocking)**.** The state $(x_i(t), v_i(t))$ of particles $(1 \leqslant i \leqslant N)$ in system (4.2.3) has a *time-asymptotic flocking* if, for $1 \leqslant i, j \leqslant N$, the velocity alignment and group forming in the following senses, respectively, are satisfied

b) $\lim\limits_{t\to\infty} \mathbb{E}||v_i - v_j||^2 = 0.$

a) $\sup\limits_{0\leqslant t<\infty} \mathbb{E}||x_i - x_j|| < \infty.$

We assume that the communication rate satisfies an upper bound condition $\alpha := \sup\limits_{s\geqslant 0} \psi(s) > \infty$.

Theorem 4.2.3 (Non-flocking theorem)**.** [59] *If $\sigma > \sqrt{\frac{\alpha}{N}}$ then the particles do not flock.*

Now we show an example of non-flocking. The parameters are set: $\sigma = 0.3$ and $\psi(s) = \frac{1}{(1+s^2)^{0.25}}$ which satisfy the condition in Theorem 4.2.3. We compute 100 trajectories of solution of (4.2.3) in $\mathbb{R}^2$ with $N = 50$ and initial values $(x_i(0), v_i(0))$ are randomly generated in $[0, 0.1]^4$. Figure 4.1 illustrates behavior of function $f(t) = \sum_{i<j} \mathbb{E}\|v_i(t) - v_j(t)\|^2$ up to time $T = 0.2$. We see that values of function $f(t)$ become extremely large even at small time instant t.

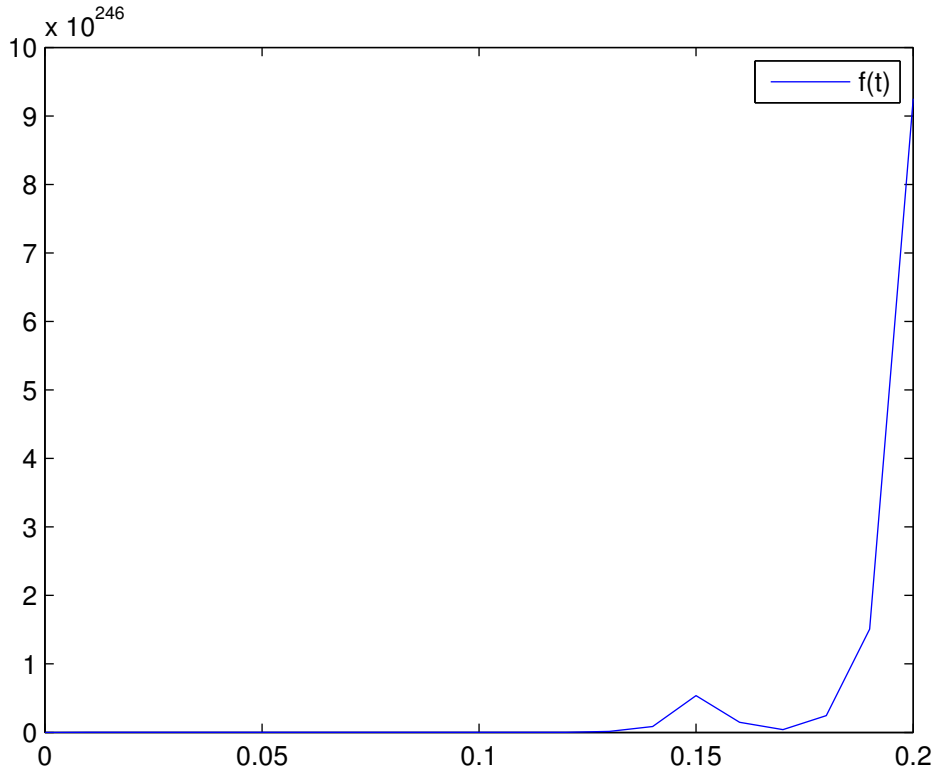

Figure 4.1: Non-flocking in two-dimensional space

Theorem 4.2.4 (Flocking theorem)**.** [59] *Assume that there exists* $\psi^* > 0$ *such that*

$$\inf_{s \geqslant 0} \psi(s) \geqslant \psi^*.$$

If $\sigma < \sqrt{\frac{\psi^*}{N}}$ *then particles flock under any initial values* $(x_i(0), v_i(0)) \in \mathbb{R}^{2d}\, (1 \leqslant i \leqslant N)$.

Let us next observe an example showing flocking. Set $\sigma = 0.05$ and $\psi(s) = 1$, then the condition in Theorem 4.2.4 is satisfied with $\psi^\star = 1$. Initial values $(x_i(0), v_i(0))$ are generated randomly in $[0, 1]^6$. Figure 4.2 shows the

evolution of 50 particle group at four time instants $T = 0, 0.02, 0.5, 1$. Each vector shows position and direction of motion of each particle. The lengths of vectors represent the magnitudes of velocity vectors (or speeds) of particles. In words, the group starts at random positions and velocities at time $t = 0$, by obeying (4.2.3), after a short period of time, it reaches to a flock-state, that is all particles' velocities tend to a common one.

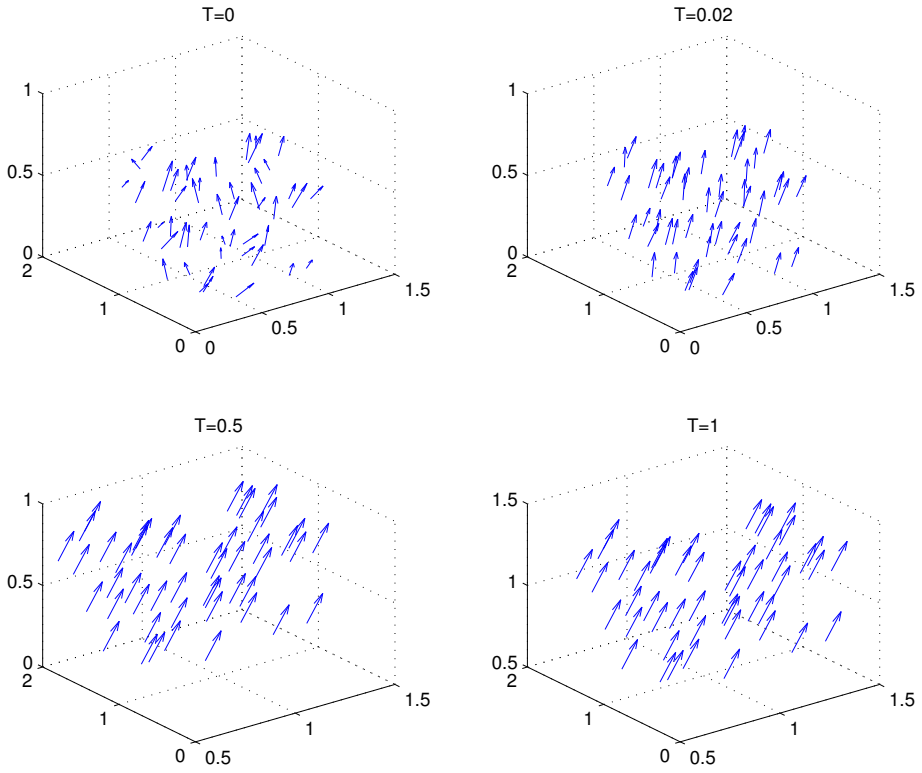

Figure 4.2: Flocking in three-dimensional space

4.3 Basic fish schooling model

As mentioned in Chapter 1, using mathematical models is a powerful method for studying biological systems. The first step of this is to construct the model for the system under consideration. It is a very important problem to build models which are suitable for our objectives from knowledge and information obtained by observations.

In Camazine-Deneubourg-Franks-Sneyd-Theraulaz-Bonabeau [11, Chapter 11], the authors proposed a model of schooling based on self-organization. The model incorporates the known behaviors and sensory capabilities of in-

dividual fish as they move in a school. Three of four main features and assumptions are:

a. The school has no leaders and each fish follows the same behavioral rules.

b. To decide where to move, each fish uses some form of weighted average of the position and orientation of its nearest neighbors.

c. There is a degree of uncertainty in the individual's behavior that reflects both the imperfect information-gathering ability of a fish and the imperfect execution of the fish's actions.

Base on the above fish's behavioral rules, Uchitane and collaborators [61] introduced an ordinary differential equations (ODE)

$$\begin{cases} dx_i(t) = & v_i dt + \sigma_i dw_i(t), \qquad i = 1, 2, \dots, N, \\ dv_i(t) = & \Big[-\alpha \sum\limits_{j=1,\, j\neq i}^{N} \left(\dfrac{r^p}{\|x_i - x_j\|^p} - \dfrac{r^q}{\|x_i - x_j\|^q} \right) (x_i - x_j) \\ & \quad -\beta \sum\limits_{j=1,\, j\neq i}^{N} \left(\dfrac{r^p}{\|x_i - x_j\|^p} + \dfrac{r^q}{\|x_i - x_j\|^q} \right) (v_i - v_j) \\ & \quad + F_i(t, x_i, v_i) \Big] dt, \qquad i = 1, 2, \dots, N, \end{cases} \tag{4.3.1}$$

for describing the process of schooling of N-fish system. Each fish is regarded as a moving particle in the Euclidean space $\mathbb{R}^d$, where $d = 2$ or 3. The unknown $x_i(t)$ is a stochastic process with values in $\mathbb{R}^d$ denoting a position of the i-th fish of system at time t; meanwhile, $v_i(t)$ is a stochastic process with values in $\mathbb{R}^d$ denoting a velocity of the i-th fish at time t. The fish are allowed to swim in the unbounded, continuous and homogeneous space $\mathbb{R}^d$.

The first equations of (4.3.1) are stochastic equations concerning x_i, where $\sigma_i dw_i$ denote noise resulting from the imperfectness of information-gathering and action of the i-th fish. In fact, $\{w_i(t),\, t \geqslant 0\}$ $(i = 1, 2, ..., N)$ are independent d-dimensional Brownian motions defined on a complete probability space with filtration $(\Omega, \mathcal{F}, \{\mathcal{F}_t\}_{t\geqslant 0}, \mathbb{P})$ satisfying the usual conditions [35]. The second equations are deterministic equations on v_i, where $1 < p < q < \infty$ are fixed exponents, $r > 0$ is a fixed distance and α, β are positive coefficients for interaction between fish and velocity matching, respectively. The parameters will differ from species to species. For example, for species having long vision field we should take interaction range, characterised by p, q large; for species which is small, the critical distance is taken shorter than that of bigger ones. Finally, the functions $F_i(t, x_i, v_i)$ denote external forces at time t which are given functions defined for (x_i, v_i) with values in $\mathbb{R}^d$. It is assumed that $F_i(t, x_i, v_i)$ $(i = 1, 2, \dots, N)$ are locally Lipschitz continuous.

Here we model the interaction between fish similar to that between elements in particle systems. We assume that the perception of fish is global, namely each fish have interactions with all other member in the group. This

is different from many other works where each individual only interacts with some others lying in some local neighbors, for example repulsive-reaction field, parallel-orientation field, attractive-reaction field, as in [33, 53, 65]. In future works, we will study the models that take fish's vision into account. The idea of using repulsive force and attractive force comes from physics that in any particle system, every particles interacts with each other with two kinds of forces: the repulsive force and attractive force. In addition, the magnitudes of these forces depend on the distance between two particles. We model separation and alignment mechanisms through pairwise repulsive and attractive forces. More precisely, the interaction between the i-th and the j-th fish can be expressed through

$$-\alpha\left(\frac{r^p}{\|x_i-x_j\|^p}-\frac{r^q}{\|x_i-x_j\|^q}\right)(x_i-x_j).$$

By this, if the distance between x_i and x_j exceeds a given critical distance r, that is $\|x_i-x_j\|>r$ then the attractive force is dominant, or the interaction is attraction. Conversely, if $\|x_i-x_j\|<r$ then the repulsive force is dominant, or the interaction is repulsion. This holds true for any $1<p<q<\infty$.

A similar weight of average is used for velocity matching

$$-\beta\sum_{j=1,\,j\neq i}^{N}\left(\frac{r^p}{\|x_i-x_j\|^p}+\frac{r^q}{\|x_i-x_j\|^q}\right)(v_i-v_j).$$

From now on, we called the above model the basic fish schooling model (or shortly the basic model). Uchitane-Yagi [62] introduce an optimization algorithm which is devised on a basic of the same equation model as above. The main result derived is that if parameters included in the algorithm are suitably set, then their scheme can show very good performance even in higher dimensional problem. But we are interested in another aspect, that is using computer simulations to study fish schooling principles. The reason we use the ODE model is that such a model can describe the fish's behavior precisely. Moreover, an ODE model is tractable for making numerical simulations. In this chapter, we will use the explicit Euler scheme for stochastic differential equations which has been introduced by Kloeden and Platen [37].

4.4 Quantitative investigations for basic model

The objective of this section is to investigate quantitatively the model introduced in the previous section. More detail, we study geometrical structures of the fish school when the fish move by obeying the kinematic equations (4.3.1) and create a swarm. For this purpose, we intend to introduce several quantitative notions: Distance to School Mates, Minimum Distance, Mean Distance to School Mates, Diameter of School, Variance of Velocity, and ε-Graph, to measure the geometrical structure of school. We in addition

introduce a notion of ε, θ-schooling where ε is fixed almost equal to r and θ is a tolerance speed difference. We then perform many numerical computations to clarify effects of each parameter or exponent of the equations in determining geometry of structures of school. These will be presented in Subsection 4.4.1 with absence of noise. Next, in Subsection 4.4.2, we focus on studying effects of the noise which is an indispensable factor in the real world to school forming. In particular, it will be shown that, if the noise's magnitude is larger than a certain threshold, then fish can no longer form a school. Main results in this section is published in [42].

4.4.1 Various measures for geometrical structures of school

In this subsection we want to introduce various measures to study the geometrical structures of school. Using these measures we will also clarify contributions of exponents and parameters included in (4.3.1) to the geometrical structures of school by examining numerical examples.

For simplicity, we consider throughout this section the deterministic case, i.e., $\sigma_i = 0$ for all i. $(x_i(t), v_i(t))$ denotes a trajectory of the i-th fish in the phase space $\mathbb{R}^d \times \mathbb{R}^d$.

Distance to school mates

For each fish i, put

$$\mathrm{DS}_i(t) = \min_{1 \leqslant j \leqslant N,\, j \neq i} \|x_j(t) - x_i(t)\|, \qquad 0 < t < \infty,\ i = 1, 2, \ldots, N.$$

By definition, $\mathrm{DS}_i(t)$ denotes the distance between the i-th individual to its nearest mates at time t. We call $\mathrm{DS}_i(t)$ the distance of i-th fish to the school mates. It is observed that $\mathrm{DS}_i(t)$ depends on the position $x_i(t)$ considerably. If $x_i(t)$ is near the center of school, i.e., $\bar{x}(t) = \frac{1}{N}\sum_{j=1}^{N} x_i(t)$, then $\mathrm{DS}_i(t)$ is much smaller than r; on the contrary, if $x_i(t)$ is in the periphery of school, then $\mathrm{DS}_i(t)$ can be almost equal to the maximum value r.

Minimum distance

We define

$$\mathrm{MiDS}(t) = \min_{1 \leqslant i \leqslant N} \mathrm{DS}_i(t), \qquad 0 < t < \infty,$$

and call this value the minimum distance of school. This is the nearest distance between two fish in a group of N individuals at time t. Basically, $\mathrm{MiDS}(t)$ is dependent on r. But, it is seen that $\mathrm{MiDS}(t)$ depends on the exponents p and q, too. For example, we have

$$\lim_{p \to \infty} \mathrm{MiDS}(T) = r,$$

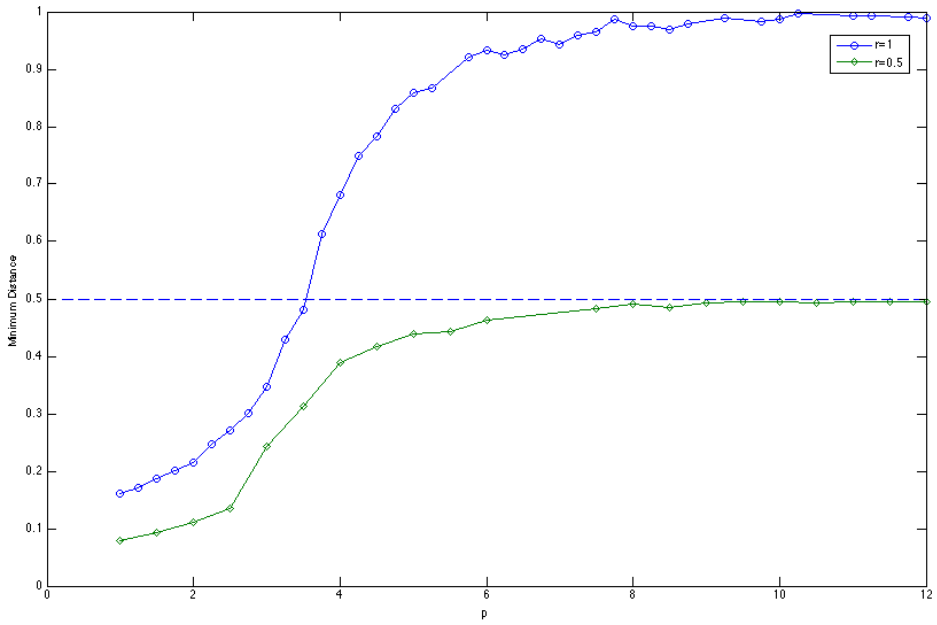

Figure 4.3: Dependence of minimum distance on exponent p

provided that T is a sufficiently large time. That is the nearest distance tends to the critical distance as power p tends to infinity for sufficiently large time T. By simulations, we find such a relationship between r and MiDS(T).

We consider a 100-fish system in the 2-dimensional space with $F_i = -5.0v_i$, which is often used to present the resistance against the moving particles. We fix two initial positions for two examples of 100-individual system (the initial positions $x_i(0),\ 1 \leqslant i \leqslant 100$, are randomly distributed in the square domain $[0, 10]^2 \subset \mathbb{R}^2$) with all null initial velocities $v_i = (0, 0),\ (1 \leqslant i \leqslant 100)$. Taking the critical distance $r = 1$ for the first example and $r = 0.5$ for the second, we tune the exponent p from 1 to 12 and always keep the relation $q = p + 1$. Other parameters are chosen as follows: $\alpha = 1$, $\beta = 0.5$, step size $\delta = 0.001$. The result is got after 30.000 running steps, that is at time $T = 30$. Figure 4.3 illustrates the dependence of MiDS(T) on the exponent p.

Remark 4.4.1. The model we consider contains many parameters, but we can find that the powers p and q are especially meaningful. p and q are concerned with a range of interactions among fish. As p and q increase, the range shortens and approaches sharply to the critical length r, namely, if $\|x_i - x_j\| > r$ the attraction between i and j is dominant and if $\|x_i - x_j\| < r$ the repulsive is very strong. □

In order to simplify our arguments, in what follows of this section, we will always take q so that $q = p + 1$. This assures the condition $q > p$ in modeling

and the difference is similar to that of the Van der Waals and the Newton's law, where $p = 3$ and $q = 4$.

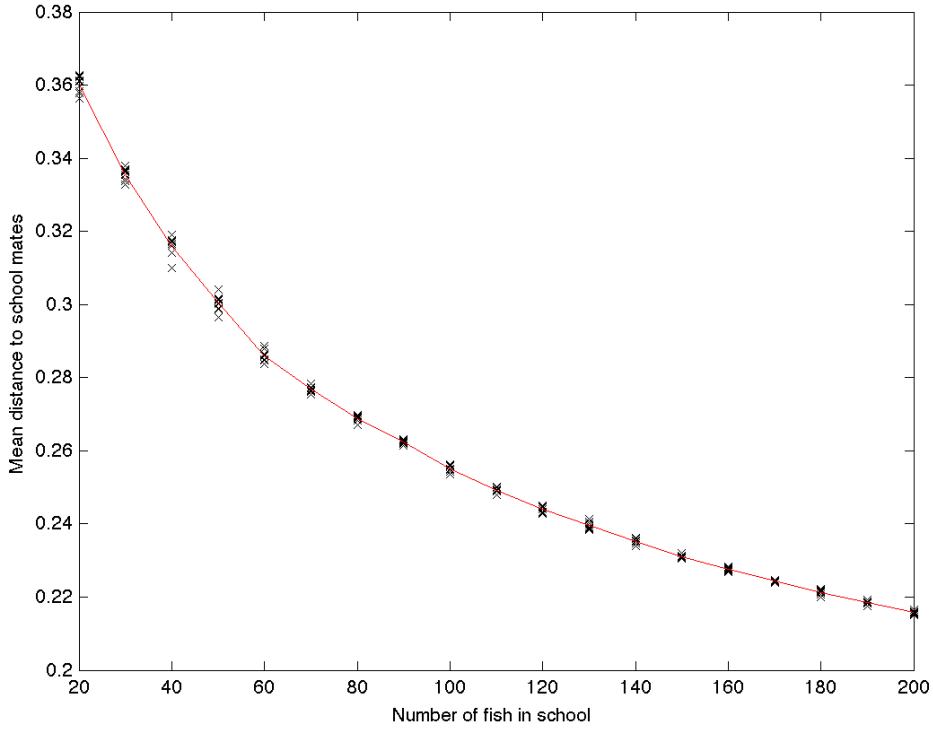

Figure 4.4: Dependence of mean distance on population size

Mean distance to school mates

We consider the mean of $\mathrm{DS}_i(t)$, i.e.,

$$\mathrm{MDS} = \frac{1}{N}\sum_{i=1}^{N} \mathrm{DS}_i(t), \qquad 0 < t < \infty.$$

This quantity is called the mean distance to school mates and is one of quantitative measures which are used to study the internal structure of the fish school.

It may be a very interesting question to know how $\mathrm{MDS}(t)$ depends on the total number of fish. In order to examine this, we consider an N-fish system in the 3-dimensional space with $F_i = -5.0v_i$, $1 \leqslant i \leqslant N$. Let $\alpha = 5, \beta = 1, p = 3, q = 4$ and $r = 0.5$. We take various values N between 20 and 200. Initial positions $x_i(0)$, $1 \leqslant i \leqslant N$, are randomly distributed in the cubic domain $[0, 20]^3$ with all null initial velocities $v_i(0) = (0, 0, 0)$. The time T is fixed as $T = 120$ throughout the simulations. Simulation results for this is

given in Table 7.1. Figure 4.4 then shows dependence of MDS(T) on the total number N. In order to reduce the effect of the random initial positions to the result, for each value of N, we run 10 simulations each with different random initial positions in $[0, 20]^3 \subset \mathbb{R}^3$. The mean distance for each N is drawn by a cross $\times$. After that we take the mean value of these and then interpolate these values by a curve.

As seen, MDS(T) decreases monotonically as N increases. This means that the school becomes "more condensed" as N is larger. This agrees with the results stated in a number of works, such as [9, 36, 49, 51] in which the authors show that the mean distance to school mates decreases as a function of the population size. From Figure 4.4, we also see that the range of the simulation results for MDS decreases as N increases.

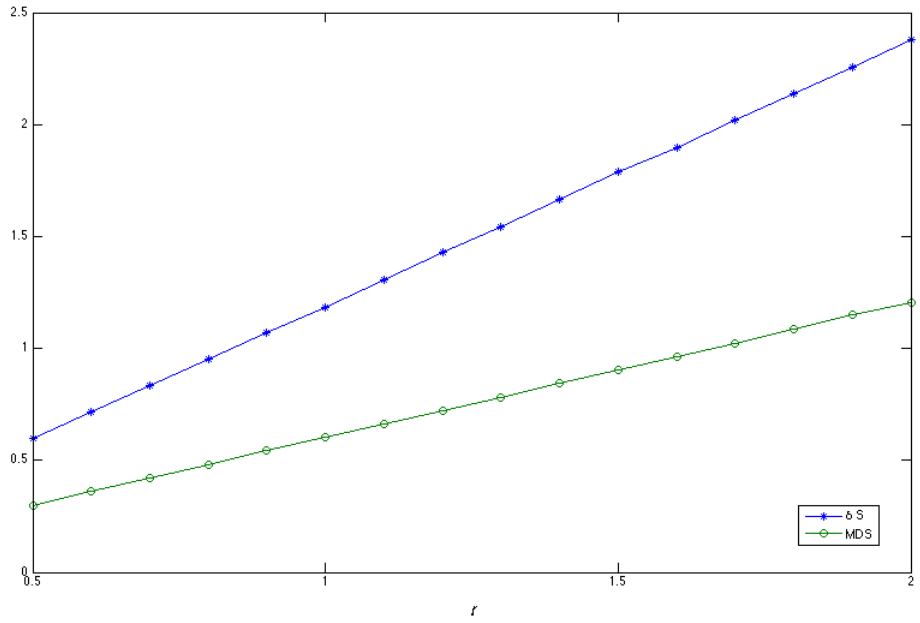

Figure 4.5: Dependence of mean distance and school diameter on critical distance

Diameter of school

The diameter of school is defined by

$$\delta S(t) = \sup_{1 \leqslant i \leqslant N} \|x_i(t) - \bar{x}(t)\|, \qquad 0 < t < \infty,$$

where $\bar{x}(t) = \frac{1}{N} \sum_{i=1}^{N} x_i(t)$ is the center of the group at time t.

The diameter of school is, by definition, the radius of the minimal ball centered at $\bar{x}(t)$ and containing all the individuals at time t.

Now we will report statistical results for the relationship between mean distance to school mate, diameter of school and the critical distance. The following numerical example shows that MDS(T) and $\delta S(T)$ are linearly dependent on r for sufficiently large time T. We consider a 50-fish system in the 3-dimensional space with $F_i = -5v_i$. Let $\alpha = 5$, $\beta = 1$, $p = 3$ with $q = p + 1$. Now, r is a tuning parameter which varies from 0.5 to 2. Initial positions $x_i(0)$, $1 \leqslant i \leqslant 50$, are randomly distributed in the cubic domain $[0, 20]^3$ with null initial velocities $v_i(0) = (0, 0, 0)$. The time T is fixed as $T = 150$. Figure 4.5 then illustrats the dependence of MDS(T) and δS(T) on the critical distance r. The plots of these values are approximately on linear lines $\delta S(T) = ar$ and MDS(T) $= br$, respectively. In this parameter setting we observe that $a = 1.18984$ and $b = 0.60158$. Simulation data for this is given in Tables 7.2 and 7.3.

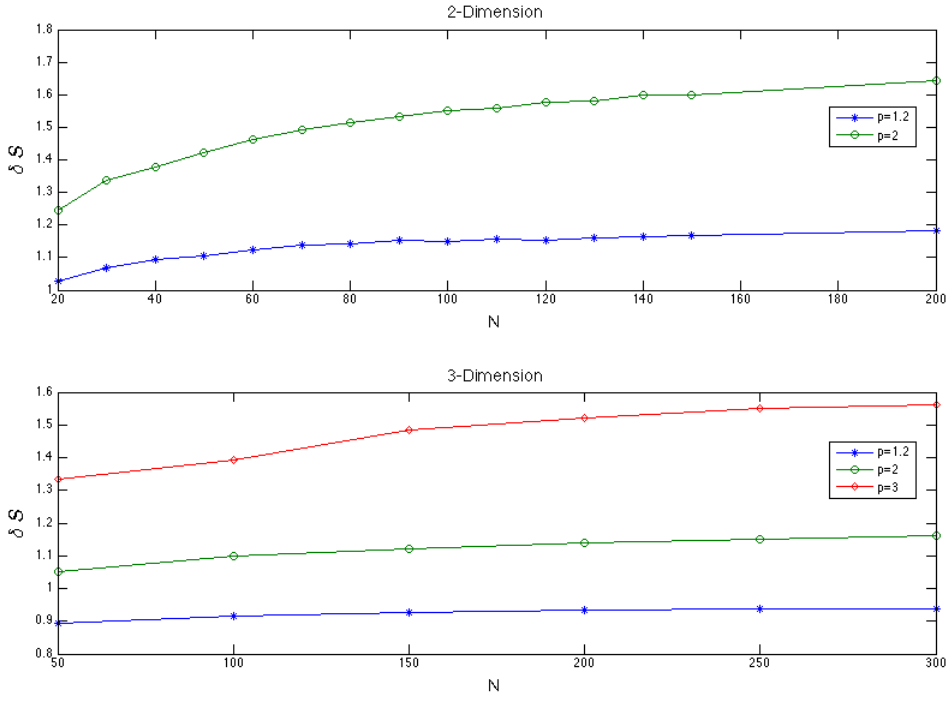

Figure 4.6: Dependence of school diameter on population size

How does $\delta S(T)$ respond when the total number N increases? To examine this question, we consider an N-fish system in the 2 or 3-dimensional space with $F_i = -5.0v_i$, and set $\alpha = 1$, $\beta = 0.5$, $p = 3$, $q = p+1$, $r = 1$ and $T = 20$. As stated before, in order to simplify the arguments, each value shown in the figure is calculated by taking the mean value of the corresponding values

for 10 simulations with different initial positions. Simulation data for this is given in Tables 7.4, 7.5 and 7.6. Figure 4.6 shows that the diameter of school typically increases with the fish number. This is generally true in animal flocks, cf. also [17].

By observing the figure we find that the slope of the school diameter as function of N is larger when p becomes larger.

Polarization

Polarization, denoted by Pol, is defined as the arithmetic average of the angular deviation of each fish from the average swim direction of the fish group

$$\text{Pol} = \sum_{i=1}^{N} \theta(v_i(t), \bar{v}(t)),$$

where $\bar{v}(t) = \frac{1}{N}\sum_{i=1}^{N} v_i(t)$ is the average of all fish's velocities in the group at time t; $\theta(x, y)$ is the angle (in degree) between vectors x, y. It is defined as

$$\theta(x,y) = \begin{cases} \arccos\dfrac{|<x,y>|}{\|x\|.\|y\|}, & \text{if } x, y \text{ are nonzero vectors} \\ 0, & \text{else.} \end{cases}$$

Here $< x, y >$ is the inner product of x, y and arccos is the inverse trigonometric function of cosine.

Variance of velocity

In order to measure matching of velocities, we will use the ordinary variance

$$\sigma\text{VS}(t) = \sqrt{\frac{1}{N}\sum_{i=1}^{N} \|v_i(t) - \bar{v}(t)\|^2}, \qquad 0 < t < \infty,$$

where $\bar{v}(t) = \frac{1}{N}\sum_{i=1}^{N} v_i(t)$ is the average of all velocities of fish at time t.

ε-Graph

We finally introduce the ε-graph notion. Let $\varepsilon > 0$ be a fixed length. The vertices of graph at time t are all the positions of particles, $x_i(t),\ 1 \leqslant i \leqslant N$. Two vertices $x_i(t)$ and $x_j(t)$ are connected by the edge of graph if and only if $\|x_i(t) - x_j(t)\| \leqslant \varepsilon$. This graph is called the ε-graph of group at time t and is denoted by $\text{GS}_\varepsilon(t)$. We also denote by $N_\varepsilon(t)$ the number of connected components of $\text{GS}_\varepsilon(t)$. When $N_\varepsilon(t) = 1$, we consider that the fish have created a single group with $\max\limits_{1\leqslant i\leqslant N} \text{DS}_i(t) \leqslant \varepsilon$. If $N_\varepsilon(t) \geqslant 2$, $N_\varepsilon(t)$ denotes the number of sub-groups.

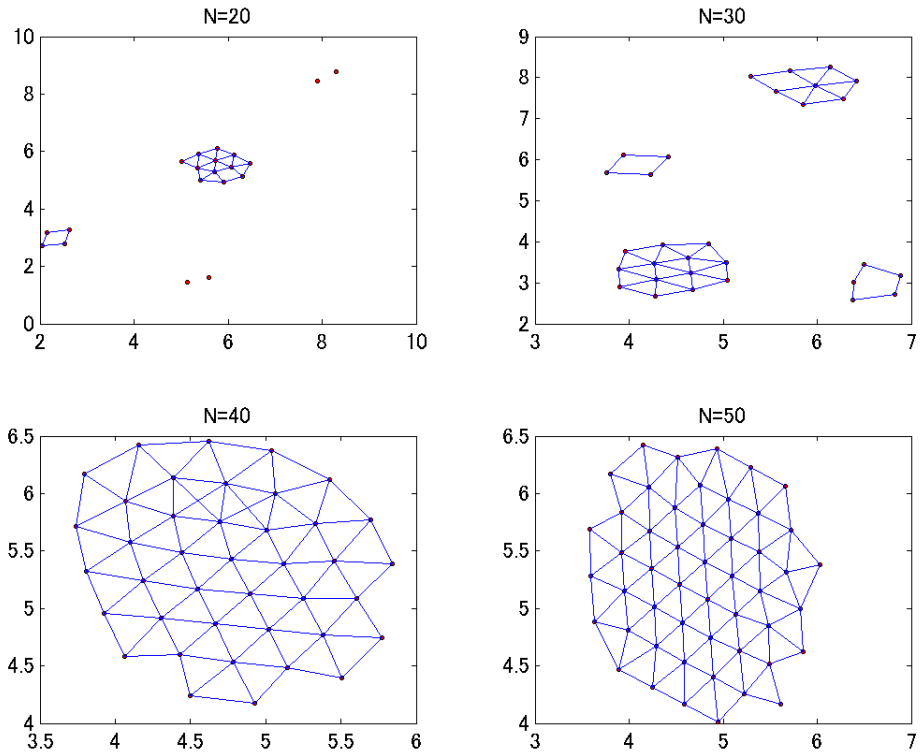

Figure 4.7: Effect of population size on number of connected components

Let us now examine effects of the population size N on $N_\varepsilon(t)$ for sufficiently large time t. To create a single group, N must be sufficiently large. To see this fact, consider an N-fish system in the 2-dimensional space with $F_i = -5.0v_i$. Let $\alpha = 1$, $\beta = 0.5$, $p = 4$, $q = p + 1$, $r = \varepsilon = 0.5$. Initial positions $x_i(0)$, $1 \leqslant i \leqslant N$, are randomly distributed in $[0, 10]^2$ with null initial velocities $v_i(0) = (0, 0)$. The population number N changes from 20 to 50. Figure 4.7 illustrates the graph $\mathrm{GS}_{0.5}(400)$ for each N. Up to $N = 39$, $N_{0.5}(400) \geqslant 2$ and so the fish are divided into a few sub-groups. But after a threshold number $N = 40$, they can create a single group.

4.4.2 Robustness of ε, θ-schooling against noise

As we know all biological dynamical systems evolve under stochastic forces. Fish school is not an exception. It is essential to understand and investigate the influence of noise in the dynamics. In some cases, the noise simply blurs the dynamics without quantitative effects. However, in some other cases especially in nonlinear dynamical systems, the noise drastically changes the corresponding deterministic dynamic behavior of the system. In this section, we consider the stochastic model (4.3.1). Under $\sigma_i > 0$, we want to study

how the terms $\sigma_i dw_i(t)$ affect the geometrical structure of school. Can the fish system still create a school?

Let us here give a mathematical definition of schooling with distance ε and tolerance speed difference θ.

Definition 4.4.2 (ε, θ-Schooling)**.** For a given length $\varepsilon > 0$ and a tolerance speed $\theta > 0$, we say that the fish system is in *ε, θ-schooling* if there exists a time $T > 0$ such that $N_\varepsilon(t) = 1$ and $\sigma \mathrm{VS}(t) < \theta$ for every $t \geqslant T$.

According to the above definition, a system forms a school only if velocities of all the fish tend to their average with the error less than tolerance θ. Therefore, the distance $\|x_i(t) - x_j(t)\|$ between any pair (i, j) will mostly remain unchanged for $t \geqslant T$. So, the school structure remains unchanged, too. The second condition ensures that all the fish keep the relation $\mathrm{DS}_i(t) \leqslant \varepsilon$ for $t \geqslant T$. As a consequence, $N_\varepsilon(t) = 1$ remains to hold for $t \geqslant T$.

Assume that a system is in ε, θ-schooling for $t \geqslant T$. According to Remark 4.4.1 (cf. also Figure 4.3), if $\|x_i(t) - x_j(t)\| > \varepsilon$, then i and j keep their distance far away and consequently

$$\left(\frac{r^p}{\|x_i(t) - x_j(t)\|^p} - \frac{r^q}{\|x_i(t) - x_j(t)\|^q} \right) (x_i(t) - x_j(t)) \tag{4.4.1}$$

is sufficiently small. In the meantime, if $\|x_i(t) - x_j(t)\| \approx \varepsilon$, then their distance is $\|x_i(t) - x_j(t)\| \approx r$ and consequently (4.4.1) is again sufficiently small. In addition, it is clear that

$$\left(\frac{r^p}{\|x_i(t) - x_j(t)\|^p} + \frac{r^q}{\|x_i(t) - x_j(t)\|^q} \right) (v_i(t) - v_j(t))$$

is sufficiently small because of $\|v_i(t) - v_j(t)\| \approx 0$. We thus verify that

$$\sum_{i=1}^N dv_i \approx \sum_{i=1}^N F_i(t, x_i, v_i) dt.$$

On the other hand, we have

$$\begin{aligned}
\sum_{i=1}^N dv_i = \sum_{i=1}^N \Big[& -\alpha \sum_{j=1,\, j\neq i}^N \left(\frac{r^p}{\|x_i - x_j\|^p} - \frac{r^q}{\|x_i - x_j\|^q} \right) (x_i - x_j) \\
& - \beta \sum_{j=1,\, j\neq i}^N \left(\frac{r^p}{\|x_i - x_j\|^p} + \frac{r^q}{\|x_i - x_j\|^q} \right) (v_i - v_j) + F_i(t, x_i, v_i) \Big] dt \\
= & -\alpha \sum_{i\neq j} \left\{ \left(\frac{r^p}{\|x_i - x_j\|^p} - \frac{r^q}{\|x_i - x_j\|^q} \right) [(x_i - x_j) + (x_j - x_i)] \right\} dt \\
& - \beta \left\{ \left(\frac{r^p}{\|x_i - x_j\|^p} + \frac{r^q}{\|x_i - x_j\|^q} \right) [(v_i - v_j) + (v_j - v_i)] \right\} dt
\end{aligned}$$

$$+\sum_{i=1}^{N} F_i(t, x_i, x_i)dt$$
$$=\sum_{i=1}^{N} F_i(t, x_i, x_i)dt.$$

That is, the sum of increments of all velocities equals to the sum of increments of $F_i(t, x_i, x_i)$.

In particular, if we take $F_i(t, x_i, x_i) = -cv_i$ $(i = 1, 2, \ldots, N)$ which is usually used to present the resistance in physical particle systems and initialize the system from no transport, namely the initial velocities of all fish in the group are zeros, then

$$\sum_{i=1}^{N} dv_i \approx -c\left(\sum_{i=1}^{N} v_i\right) dt.$$

Consequently, $\sum_{i=1}^{N} v_i(t)$ decays exponentially as $t \to \infty$ and the system converges to a steady state.

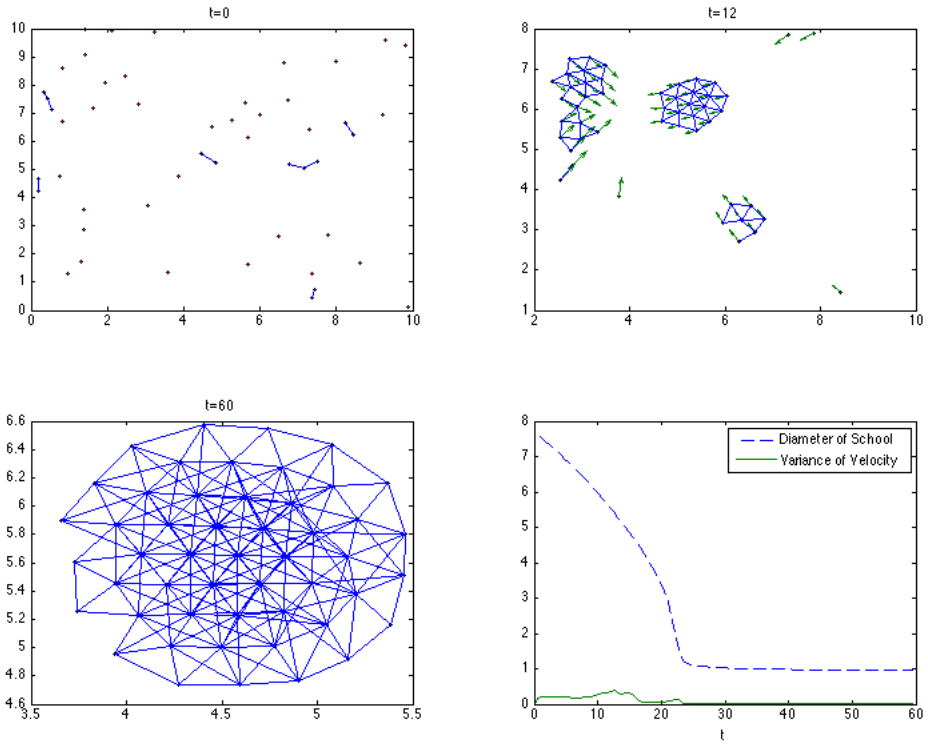

Figure 4.8: Example of ε, θ-schooling

Figure 4.8 shows an example of ε, θ-schooling generated by (4.3.1). 100 fish are situated at random positions in $[0, 10]^2 \subset \mathbb{R}^2$ with null velocities at

time $t = 0$. Then they interact with each other with $\alpha = 5$, $\beta = 1$, $p = 3$, $q = 4$, $r = 0.5$, $\sigma = 0$, $F_i = -5v_i$, $(1 \leqslant i \leqslant 100)$, we set $\varepsilon = 0.5 = r$.

In the first three subfigures, we show ε-graphs of the system at different instants t. Each of these figure shows the positions of fish by points, their velocities by vectors and ε-graph edges by lines. The last subfigure draws the variance of velocity and the diameter of school as functions of t.

Of course whether a system creates a school or not depends strongly on initial positions. It is also observed that 3-dimensional systems can create schools much easier than 2-dimensional ones.

Let us next study effects of the noise. First, let's consider the polarization of group respect to noise. In order to illustrate the influence of noise to polarization of fish group we take an initial position of 50-fish group randomly in $[0, 3]^3 \in \mathbb{R}^3$. We put noise with different magnitudes to that group. Initial velocities of fish are independent, uniformly distributed variables in $[-1, 1]^3$.

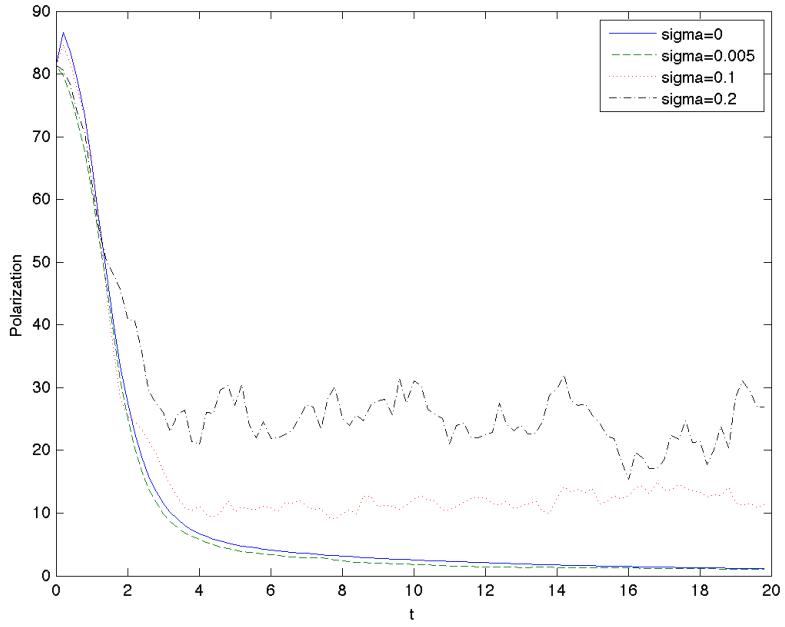

Figure 4.9: Polarization of group with respect to noise

From Figure 4.9 we find that with small value of σ, the group tend to optimal parallel orientation with 0 degree polarization. But for relatively large noise that does not happen.

Next, we see how noise affects schooling and school structure. We set $\sigma_i(t) = \sigma$, for $i = 1, 2, \ldots, N$. Simulations are implemented in the 3-dimensional space. We fix initial positions taking randomly in $[0, 5]^3 \subset \mathbb{R}^3$ with 50 fish, run 10 simulations with different realizations of the Wiener process for each value of σ. We observe the end point of each trajectories of $\sigma\text{VS}(T)$ and

$\delta \mathrm{S}(T)$ at $T = 50$. Other parameters are set as $p = 3$, $q = p + 1$, $\alpha = 5$, $\beta = 1$, $r = 0.5$, $F_i = -5.0v_i$, step size $\delta = 0.001$. Figure 4.10 shows that the fish can keep schooling against the noises when their magnitudes are small enough. To the contrary, when they are large, the noises prevent the fish from creating school. It might be allowed, however, to insist that the swarming behavior described by our model (4.3.1) possesses the robustness for schooling. Figure 4.11 shows the expectation of school diameter as a function of σ. From this figure, too, we can find a similar tendency.

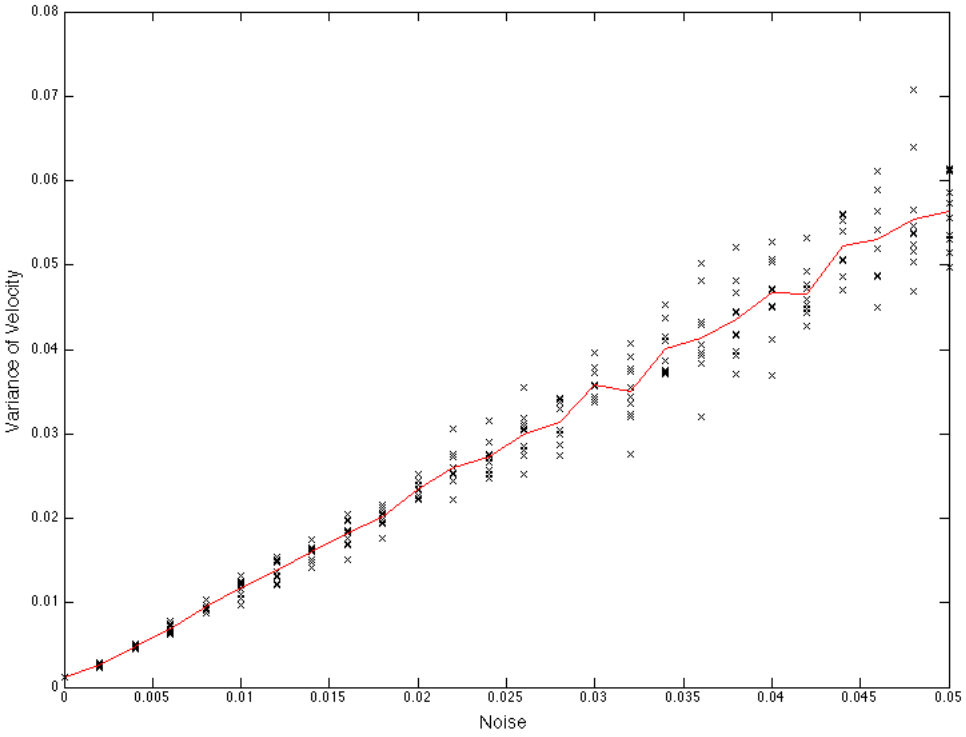

Figure 4.10: Influence of the noise on schooling

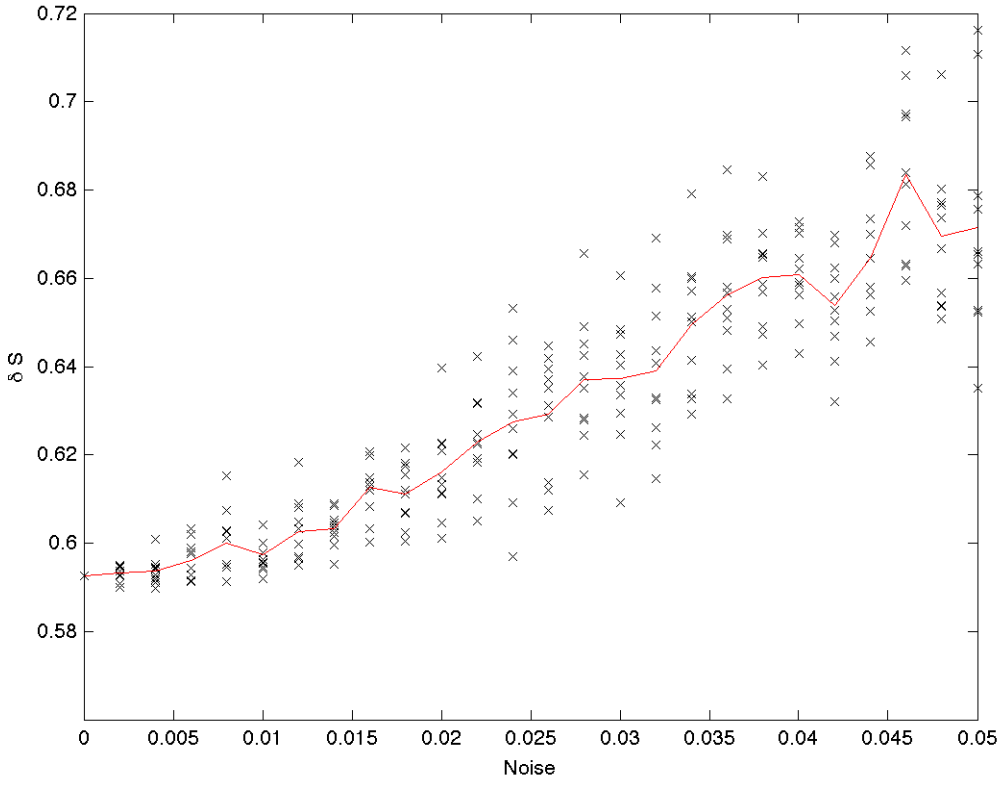

Figure 4.11: Influence of the noise on school diameter

Chapter 5

Cohesiveness and Foraging Advantages

5.1 Motivation

In the previous chapter, we considered the model for fish schooling in free-space. Parrish and Viscido in [52] argued that even when empirical data of real fish are similar to those in the model, their significance is unclear because in modeling, we usually make unrealistic assumptions. Ours of being free-space is one of such assumptions. The environment surrounding real school fish often includes other components such as, obstacles, food resources, predators, etc. In those situations, fish exhibit more complex behavior rather than cohesive parallel movement such as obstacle avoidance, food finding, escaping from predator. Sometimes fish make school for common purpose, for instance enhancing foraging success, higher success in finding mates or defencing against predators.

This chapter extends the model (4.3.1) handled in Section 4.3. Now we will consider the model in more realistic situations by adding components that always present in the environment of real fish, they are obstacles and food resources. We will give precise descriptions of such models which are derived from incorporating additional components to the basic fish schooling model. Then we present observation patterns that fish form when approaching to a static obstacle by means of numerical simulations in Section 5.2. These patterns give us information about the cohesiveness of school. Furthermore, by investigating which parameters in the model determine the school patterns, we acquire knowledge about the effect of these parameters to the structure of school. Finally, we consider how fish enjoy advantages of schooling to find out food resources in a challenging environment in Section 5.3. Main results in this chapter is contained in [44].

5.2 School cohesiveness with respect to behavioral patterns

Up to our knowledge, so far there are a few works considering swarming with presence of obstacles. We could mention here the works of C. W. Reynolds, Reza Olfati-Saber, D. E. Chang, and E. Rimon. Reynolds [53] only represents some descriptive simple rules for each individual without any precise mathematical model and then uses computer to simulate the behavior of birds while avoiding obstacles. Reza Olfati-Saber [54] uses the same point of view as Reynolds that the society of agents is viewed as a distributed system. He provides a dynamic graph theoretical frame work for flocking in presence of multiple obstacles. Recently, Chang et al. [13] have introduced techniques using gyroscopic forces and scalar potentials to create swarming behaviors for multiple agent systems in which agents perform collision avoidance between each others as well as obstacles. The use of gyroscopic forces is an alternative approach to obstacle avoidance using centralized constructions of potential functions by Rimon and Kodischek in [56].

In this section, we will provide another mathematical model which describes fish schooling in the environment with obstacles. Then we derive the cohesiveness of the school. In Subsection 5.2.1 we introduce our model equation for fish schooling with the presence of obstacles that we will call the fish schooling with obstacle model. Besides three fundamental behavioral rules which all individuals follow to interact with each other as in (4.3.1) now we add another rule that fish use to avoid obstacles on their way. Subsection 5.2.2 considers the model with a static obstacle. In this subsection, we present different patterns of school while avoiding the obstacle. Through that, we know about the cohesiveness of school. We are also able to predict stability and morphology of organization of the model by observing the school patterns. Subsection 5.2.3 surveys how some model parameters influence on the school cohesiveness.

5.2.1 Fish schooling with obstacle model

This model is derived from modifying the basic fish schooling model. But in order to make it convenient for the reader, we repeat detail descriptions. We consider an N-fish system making school in the environment with presence of static obstacles. Each fish is regarded as a moving particle in the Euclidean space $\mathbb{R}^d$ where $d = 2$ or 3. The direction toward which a fish proceeds is regarded as its forward direction. Because all individuals in the group act identically, we need only represent the dynamics of an arbitrary one, say the

i-th.

$$\begin{cases} dx_i(t) = & v_i dt + \sigma_i dw_i(t), \qquad i = 1, 2, \ldots, N, \\ dv_i(t) = & \Big[-\alpha \sum\limits_{j=1,\, j\neq i}^{N} \left(\dfrac{r^p}{\|x_i - x_j\|^p} - \dfrac{r^q}{\|x_i - x_j\|^q} \right) (x_i - x_j) \\ & \quad -\beta \sum\limits_{j=1,\, j\neq i}^{N} \left(\dfrac{r^p}{\|x_i - x_j\|^p} + \dfrac{r^q}{\|x_i - x_j\|^q} \right) (v_i - v_j) \\ & \quad -\gamma \left(\dfrac{R^P}{\|x_i - y_i\|^P} + \dfrac{R^Q}{\|x_i - y_i\|^Q} \right) (v_i - \mathrm{Rf}(x_i, v_i, \mathrm{Ob})) \Big] dt, \\ & \quad i = 1, 2, \ldots, N. \end{cases} \tag{5.2.1}$$

The unknown $x_i(t)$ is a stochastic process with values in $\mathbb{R}^d$ denoting a position of the i-th fish of system at time t; meanwhile, $v_i(t)$ is a stochastic process taking values in $\mathbb{R}^d$ denoting a velocity of the i-th fish at time t. They are continuous functions of t.

The first equation of (5.2.1) is a stochastic equation concerning x_i, where $\sigma_i dw_i$ denotes a noise resulting from the imperfectness of information-gathering and action of the i-th fish. In fact, $\{w_i(t),\, t \geqslant 0\}$ $(i = 1, 2, \ldots, N)$ are independent d-dimensional Brownian motions defined on a complete probability space with filtration $(\Omega, \mathcal{F}, \{\mathcal{F}_t\}_{t\geqslant 0}, \mathbb{P})$ satisfying the usual conditions. The second equation is a deterministic equation on v_i. Where $1 < p < q < \infty$, $1 < P < Q < \infty$ are fixed exponents, r, $R > 0$ are given fixed radius, α, β, γ are positive coefficients for interaction between fish, velocity matching and obstacle avoidance, respectively.

The rules of interactions between fish are explained in Section 4.3. Now we will explain in detail the rules that fish use to avoid obstacles.

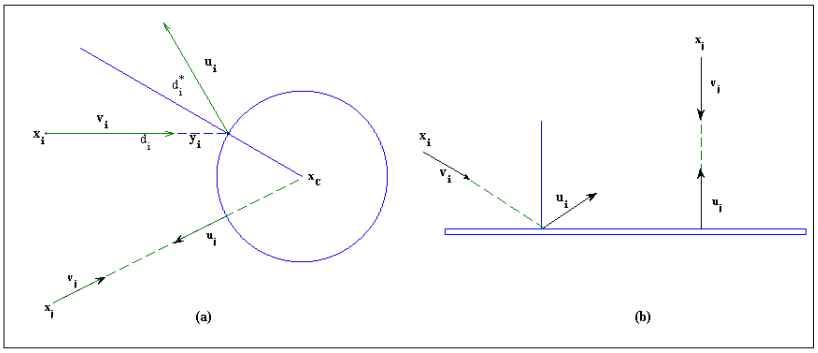

Figure 5.1: Obstacle avoidance rules in 2-dimensional case

We are interested in the influence of static obstacles on the school cohesiveness. We restrict our consideration to sphere obstacles and walls. For the former case, assume that the static obstacle is a sphere S with center at point

$x_C \in \mathbb{R}^d$ and radius $R_C > 0$, i.e.,

$$S = \{x \in \mathbb{R}^d : \|x - x_C\| \leqslant R_C\}.$$

Vector $\mathrm{Rf}(x_i, v_i, \mathrm{Ob})$ is the complete reflection of v_i from the obstacle. We note that if the i-th fish stays still, that is its velocity is zero, then we specify $\mathrm{Rf}(x_i, v_i, \mathrm{Ob}) = v_i$. Otherwise, it is defined as follows. Denote $d_i(t)$ the ray starting from $x_i(t)$ and having direction $v_i(t)$, that is

$$d_i(t) = \{x \in \mathbb{R}^d : x = x_i(t) + sv_i(t), s \geq 0\}.$$

If this ray cuts the sphere S at less than two points, then $\mathrm{Rf}(x_i, v_i, \mathrm{Ob}) = v_i(t)$, namely, the i-th fish is not affected by the sphere obstacle. In the other cases, we denote y_i the intersection point between d_i and S which is closer to x_i than the other. If $x_C \in d_i(t)$ then $\mathrm{Rf}(x_i, v_i, \mathrm{Ob}) = -v_i(t)$. Finally, if $x_C \notin d_i(t)$ then we denote $d_i^*(t)$ the symmetric line for $d_i(t)$ through the line $x_C y_i$. In this case, u_i is a direction vector of $d_i^*(t)$ which is outward of S and has length $\|u_i(t)\| = \|v_i(t)\|$. (This rule is illustrated in Figure 5.1(a)). For the sphere obstacle avoidance rule in 3-dimensional case, we first specify the plane that contain three points x_i, $x_i + v_i$ and x_C, then we find the reflection vector $\mathrm{Rf}(x_i, v_i, \mathrm{Ob})$ of v_i in this 2-dimensional plane using the rule presented above.

The later case- we consider wall obstacles. Similar to the previous case, we only consider the effect of obstacle at time t if the i-th fish "see" the obstacle on its way at that time. In other words, vector $\mathrm{Rf}(x_i, v_i, \mathrm{Ob})$ is specified completely the same as fully reflection of a light ray through a mirror (This rule is shown in Figure 1(b)). We note that for other basic shapes, for example triangular, square, rectangle, etc, we can apply wall collision avoidance rule by regarding their sides as walls.

The space in which fish move, there may be many obstacles. But at each time t, a fish is influenced by at most one obstacle which is closest to it among the ones it "can see" on its way at that time. This is different from the model introduced in [55] where more than one obstacles can have effect on one fish at a time. They are called "active obstacles" of the fish and the "activeness" is determined through the distances from the obstacles to the fish.

Similar to the rule when fish tries to avoid collision with its neighbor, to avoid obstacle, each particle will attempt to match velocity with its 'reflex' velocity $\mathrm{Rf}(x_i, v_i, \mathrm{Ob})$. That is, the i-th fish at position x_i and velocity v_i, has an orientation matching:

$$\gamma \left[\frac{R^P}{(\|x_i - y_i\|)^P} + \frac{R^Q}{(\|x_i - y_i\|)^Q} \right] (v_i - \mathrm{Rf}(x_i, v_i, \mathrm{Ob})).$$

5.2.2 School cohesiveness with respect to behavioral patterns of fish school while avoiding a static obstacle

In this subsection, we focus on studying the effect of obstacles to the school cohesiveness. For simplicity, we restrict our consideration to a system with

only one static sphere obstacle. By observing, we find four different patterns of school while avoiding a static sphere obstacle:

Pattern I (*Rebound*): The school changes their direction before approaching the obstacle, then all fish together move toward a common direction in one group.

Pattern II (*Pullback*): The school approaches to the obstacle then they separate into two directions to avoid the obstacle. The obstacle seems to lie deeply in the school and make the school structure be collapsed. But then, all the individuals of the initial school change their direction and come back to preserve their school structure.

Pattern III (*Pass and reunion*): When approaching to the obstacle, the school also separates into two subgroups to pass the obstacle, but all individuals tend to move along the border of the obstacle. After passing the obstacle, the two subgroups reunion into one. Then they recreate the school structure as before getting to the obstacle.

Pattern IV (*Separation*): The school has the same behavior as in Pattern III when avoiding the obstacle, that is school also separates into two subgroups to pass the obstacle but after that the two subgroups still move along two different directions and each creates a smaller new school.

Figure 5.2 illustrates these four patterns. In this figure, the sphere obstacle is drawn by the circle, position of each fish is represented by a point and its velocity by a vector.

From observing patterns of school while avoiding obstacle we can derive the cohesiveness of the school structure: As the index of the pattern type (defined above) increases, the cohesiveness of the school decreases. In Pattern I, the cohesiveness is the strongest, it is harder than the effect of the obstacle. So the school changes its direction before approaching to the obstacle. The school structure is not collapsed while school passes the obstacle. In Pattern II, the cohesiveness of the school is weaker than that in Pattern I. So that the school structure is partly destroyed by the effect of the obstacle. But then the cohesiveness in this case is still strong enough to make the individuals change their direction to come back to preserve their school without passing the obstacle. In Pattern III, the obstacle's effect causes the school to separate into two subgroups and then school passes obstacle as two subgroups. But after they have passed the obstacle, the effect of obstacle decreases, the cohesiveness of the school makes these two subgroups reunion and then recreate the school structure. In Pattern IV, the cohesiveness of the school is the weakest, so that after passing the obstacle, the two subgroups can not reunion. They still move along two different directions.

By observing the movement of school while avoiding obstacle in the simulation, we also see that for some case when the school reaches to some position at which the effects of school and obstacle to the fish group seem to be equal. So they cause the fish to stay in an stable positions (from a certain time) which is either in front of the obstacle, before the school reaches to the obstacle or when the obstacle lies deeply in the group (Figure 5.3).

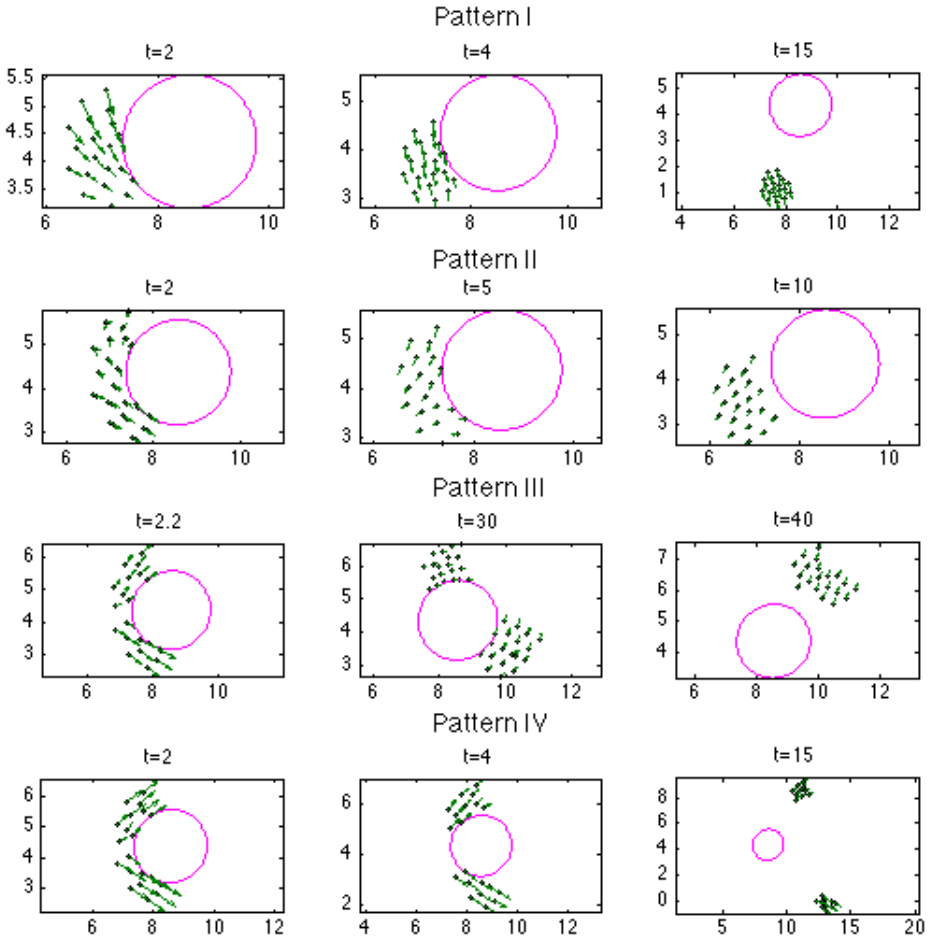

Figure 5.2: School patterns while avoiding obstacle

5.2.3 Effect of parameters on school cohesiveness

Because our model contains many parameters, it is very difficult to specify phase diagram for different patterns as in [17]. In the remaining part of this section, we will consider the effect of some parameters, one by one, to the cohesiveness of the school by observing the change in school pattern in obstacle presence space as these parameters change. The parameters under consideration includes power p, q, initial velocity of school, critical distance r, and magnitude of noise. These parameters differ from species to species. In order to get the best understanding of effects of only one parameter, at a time we change only the parameter being considered and keep all the others unchange. And in this section we firstly omit the presence of noise. Then, we consider how noise influences on school cohesiveness. We always start each

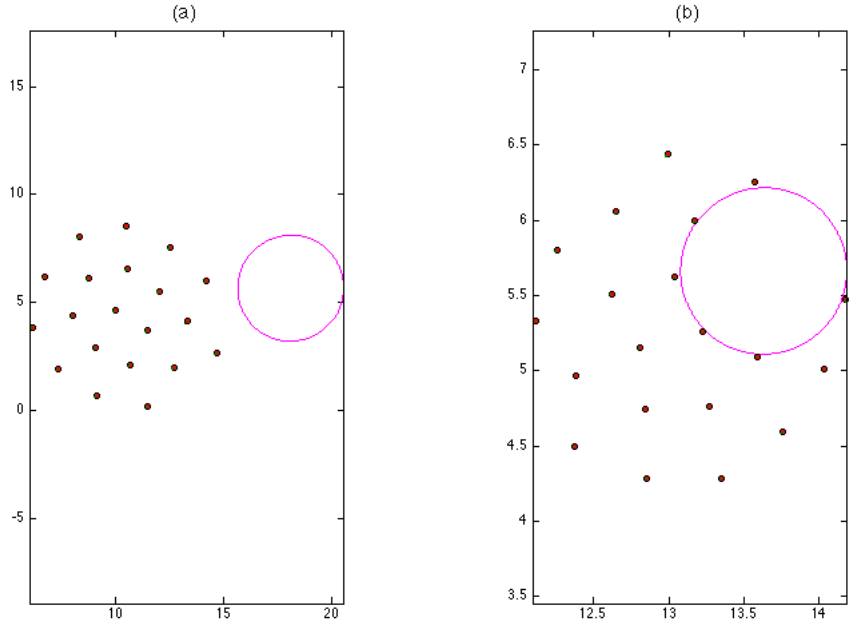

Figure 5.3: School reaches stable positions

simulation from an equilibrium position of the school so that we can see the effect of the obstacle to the school pattern. Note that by "schoolling" we mean ε, θ- schooling which is defined in Definition 4.4.2.

Effect of power p, q on the cohesiveness of school

First, we consider how powers p, q influence school patterns. Numerical simulations (in 2-dimensional case) show that the pattern of school changes orderly from I, to II, to III then IV as powers p, q increase (In this section we always take $q = p+1$). That is, when we fix all other parameters except for p (and q) and then change only p, q we find that the interval under consideration (1, 8] is divided into four subintervals in each of which the school follows one of four patterns defined above orderly.

For example we fix initial position of a 20-fish school whose center is 5 (length distance unit) far from the center of a static circle obstacle with radius 1.2. Initial velocities are taken the same for all fish in the school. The common velocity directs from the center of the school to the center of the obstacle with the length equals to half distance between these two centers. The other parameters are set as $\alpha = \beta = \gamma = 1$, $r = 0.5$. Then the division mentioned above is shown in Table 5.1 (the increment considered is 0.001):

From the simulations, we suggest that for $p > 8$, the school pattern is also Pattern IV.

Table 5.1: Powers p, q affect school pattern (a)

p	(1, 2.1]	[2.101, 3.371]	[3.372, 3.497]	[3.498, 8]
Pattern	I	II	III	IV

Of course, these subintervals will change according to other parameters, for example distance from the average initial positions of fish in school and the center of obstacle. But the order of subintervals for patterns I, II, III, IV remains the same as above. For example, when we change that distance to 3.5 (length distance unit), then we get the result shown in Table 5.2 (the increment considered is 0.01).

Table 5.2: Powers p, q affect school pattern (b)

p	(1, 2]	[2.1, 3.36]	[3.37, 3.7]	[3.71, 8]
Pattern	I	II	III	IV

It shows that when powers p, q increase, the cohesiveness of the school decreases. This result agrees with remark in [61] that powers p, q characterize for the interaction range between fish. More precisely, the larger p (q) is, the larger the interaction range, so the smaller the attractive force between fish in school.

Figure 5.2 illustrates four patterns received when we run simulations using parameters as set above except for initial position of the school to the center of obstacle is 3.5 and p takes value 2, 3, 3.62, and 4 respectively for patterns I, II, III, IV.

Effect of initial velocity on the cohesiveness of school

When considering the effect of initial velocity on school pattern, we find a result similar to the one found in the previous subsection. That is, school patterns I, II, III, IV change orderly as initial velocity of the school v_0 increases. Table 5.3 shows a numerical result illustrating that in 2-dimensional case. The parameters are set $N = 20$, $\alpha = \beta = \gamma = 1$, $p = 2$, $r = 0.5$, distance from average initial position of fish in school to the center of the obstacle is 3.5. The increment considered in these simulations is also 0.001.

Table 5.3: Initial velocity of school affects school pattern

Initial velocity	(0, 1.199]	[1.2, 2.589]	[2.59, 4.866]	[4.867, 20]
Pattern	I	II	III	IV

The result still holds true for 3-dimensional case.

Of course, when the initial velocity is too large, then collision may happen because large velocity makes fish not have enough time to adjust to avoid collision with other fish or with the obstacle.

Effect of critical distance on the cohesiveness of school

As mentioned in [42], when the critical distance increases, then the school diameter also increases. Because school diameter will also affect the school pattern when avoiding obstacle. So in this subsection, besides changing critical distance, we also change radius of obstacle. More precisely, after getting the equilibrium position of fish in a school for each simulation, we calculate the school diameter then take obstacle radius equals to 2/3 of school diameter.

Firstly we need initial positions for simulations. Taking a random position of 20-fish group in $[0, 10]^2$. We run the program for the model without obstacle with the same parameters except for r, which are taken values from 0.2 to 3 with increment 0.1, to the instant that groups make $r, 10^{-6}$-schooling. Then we make calculations for model including obstacle with $d = 2$, $\alpha = \beta = \gamma = 1$, $p = 3$. All fish in the $r, 10^{-6}$-schooling start with the same initial velocity v_0. Common velocity v_0 is parallel to and has the same direction as the vector which connects the center of school and center of the obstacle, and $\|v_0\| = 4$. The distance between centers of school and obstacle is 8. The result we get is shown in Table 5.4.

Table 5.4: Critical distance affects school pattern

r	0.2, 0.3	0.4, 0.5	0.6, 0.8–2.0	2.1–2.8
Pattern	IV	III	II	I

While making simulations, we also find that for some values of critical distance at which the school gets to stable positions: Stable case as in Figure 5.3 (a) happens when r is chosen too large ($r = 2.9, 3.0$) while the case stable as in Figure 5.3 (b) occurs somewhere in the domain of pattern II ($r = 0.7$).

Because the larger the critical distance is, the weaker the interaction between fish is, when critical distance increases, the school pattern change orderly from IV to III to II to I.

The following diagram shows the relationship between some model parameters, school cohesiveness and behavioral patterns.

- p, q increase$\Rightarrow$ cohesiveness decreases $\Rightarrow$ behavioral pattern index increases,
- v_0 increases $\Rightarrow$ cohesiveness decreases $\Rightarrow$ behavioral pattern index increases,
- r increases$\Rightarrow$ cohesiveness increases $\Rightarrow$ behavioral pattern index decreases.

Effect of noise on the results

We repeated the above simulations but now with presence of noise and found that when the noise is relatively small (comparing to other parameters) then the above results still remain true. But if the noise is larger than some critical one then those results are no longer true. Moreover, if the magnitude of noise is too large then the school structure is even broken due to collision between fish and between fish and obstacle. Of course, the critical values mentioned above depends relatively on other parameters.

Besides negative effects of noise, we also find its positive effect in the following sense. As mentioned above, there exist some parameter sets that fish school is trapped in stable states (in the case there is no noise). Under small noise, the situation is still the same. But when we enlarge magnitude of noise a little bit, then fish school can escape from stable states.

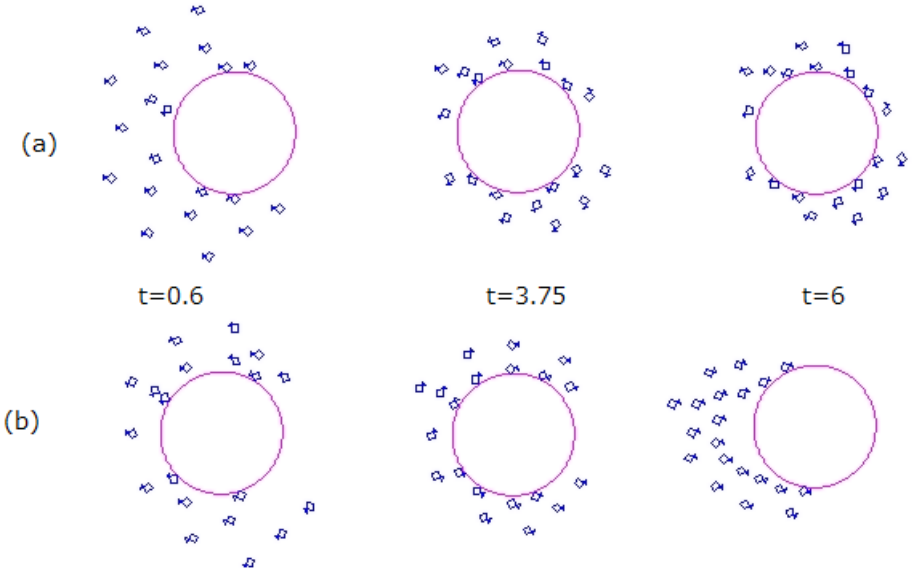

Figure 5.4: Positive effect of noise

We illustrate this result in Figure 5.4. Subfigures on the first row of this figure show the evolution of fish school until it traps in a stable state when $\sigma = 0$. The bottom row's subfigures represent positive effect of noise that helps fish school escaping from stable state.

However, if we choose σ quite large, then collision between fish and their neighbours or between fish and obstacles happens easily. With presence of positive noise, we can not predict the school pattern because different realizations of Wiener process lead to different patterns even though the magnitudes of noise are the same. Figure 5.4 (b) and Figure 5.5 illustrate school evolution with the same magnitudes of noises $\sigma = 0.005$ but different trajectories of Wiener process. These lead to different behavioral patterns.

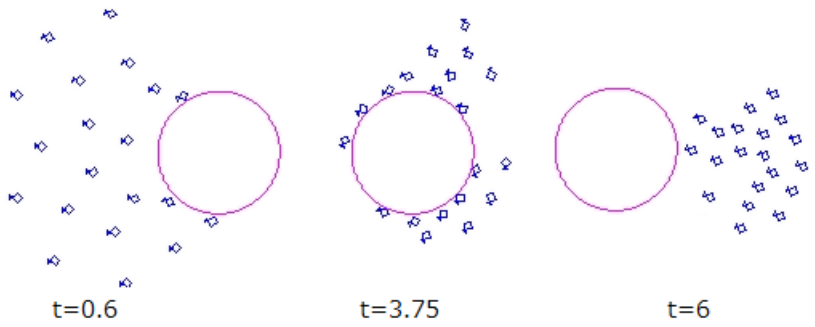

Figure 5.5: Unpredictable pattern under positive noise

5.3 Foraging advantages of fish schooling

Now, besides obstacles, we will consider also the presence of food resources in the environment. This section considers the another aspect of school, that is "Does school make any advantages for fish in finding food resources in their environment?".

5.3.1 Fish foraging model

$$\begin{cases} dx_i(t) = & v_i dt + \sigma_i dw_i(t), \qquad i = 1, 2, \ldots, N, \\ dv_i(t) = & \Big[-\alpha \sum\limits_{j=1, j\neq i}^{N} \left(\dfrac{r^p}{\|x_i - x_j\|^p} - \dfrac{r^q}{\|x_i - x_j\|^q} \right) (x_i - x_j) \\ & -\beta \sum\limits_{j=1, j\neq i}^{N} \left(\dfrac{r^p}{\|x_i - x_j\|^p} + \dfrac{r^q}{\|x_i - x_j\|^q} \right) (v_i - v_j) \\ & -\gamma \left(\dfrac{R^P}{\|x_i - y_i\|^P} + \dfrac{R^Q}{\|x_i - y_i\|^Q} \right) (v_i - u_i) \\ & + F_i(t, x_i, v_i) \Big] dt, \qquad i = 1, 2, \ldots, N. \end{cases} \tag{5.3.1}$$

The unknown functions and parameters are the same as in (5.2.1). The function $F_i(t,\, x_i,\, v_i)$ denotes an external force at time t which is a given function defined for $(x_i,\, v_i)$ with values in $\mathbb{R}^d$. It is assumed that $F_i(t,\, x_i,\, v_i)$ $(i = 1, 2, \ldots, N)$ are locally Lipschitz continuous.

To model food resource, we use a function f specified on the whole domain space Ω, and is resource which impacts on the movement of fish through its smell. Food smell will guide fish to food's locations along its concentration gradient. More precisely, we model the food resource's influence through function $F_i(t,\, x_i,\, v_i),\ (i = 1, 2, ..., N)$ in (5.3.1) as follows:

$$F_i(t,\, x_i,\, v_i) = k \nabla u(x_i),$$

where ∇ is the gradient notation, and k is the smell attractive coefficient. Consider $\mathcal{C}^1$ potential function $u : \mathbb{R}^d \to \mathbb{R}$,

$$\nabla u(z) = \left(\frac{\partial u}{\partial z_1}, \frac{\partial u}{\partial z_2}, \ldots, \frac{\partial u}{\partial z_d} \right), \quad z \in \mathbb{R}^d.$$

Function $u(z)$ denotes the smell from food resource at position z. It satisfies the following equation.

$$\begin{cases} -c\Delta u + au & = f(z), z \in \Omega \\ \dfrac{\partial u}{\partial \mathbf{n}} & = 0, \quad z \in \partial\Omega \end{cases} \tag{5.3.2}$$

This is an elliptic equation with Neumann boundary. Here notation Δ denotes the Laplace operator

$$\Delta u = \sum_{k=1}^{d} \frac{\partial^2 u}{\partial z_k^2}.$$

Ω is the space in which fish move and $\partial\Omega$ is the boundary of Ω. Coefficients c, a are positive. They can be constants or functions of position x and time t. In Neumann boundary equation, $\mathbf{n}$ denotes the (typically exterior) normal to the boundary $\partial\Omega$. The above boundary condition ensures that no smell can enter or leave the boundary of the domain, i.e., the domain is perfectly insulated.

5.3.2 Advantages of schooling in finding food resources

We now consider a system with presence of noise, obstacles and food resources. We will illustrate the roles of schooling in helping fish to find food resources by means of computer simulations. For simplicity, we will only demonstrate results in two-dimensional case.

In our simulations, we restrict the space for fish swimming in to be the rectangle domain $\mathrm{D} = [0, 7] \times [0, 4]$ whose boundary are wall obstacles. Inside this domain, we put three other obstacles $\mathrm{Ob}_1 = [2, 2.5] \times [1.75, 4]$, $\mathrm{Ob}_2 = [4.5, 5] \times [0, 2.5]$, Ob_3 is the below half of the circle centered at $[2.25, 1.75]$ with radius 0.25, i.e,

$$\mathrm{Ob}_3 = \{(x, y) \in \mathbb{R}^2 : x = 2.25 + 0.25\cos\theta,\ y = 1.75 + 0.25\sin\theta,\ \theta \in [-\pi, 0]\}.$$

We specify the area where the fish can move in is $\Omega = \mathrm{D} \setminus (\mathrm{Ob}_1 \cup \mathrm{Ob}_2 \cup \mathrm{Ob}_3)$. By the Neumann condition, smell also can not pass the boundary $\partial\Omega$ of this area.

There is one sphere food resource centered at $C = (5.5, 0.1)$ with radius 0.04. More precisely, we specify the food resource function as

$$f(x) = \begin{cases} 50, & \text{if } x \in \mathcal{B} = \{y \in \mathbb{R}^2 : \|x - C\| \leqslant 0.04\} \\ 0, & \text{else.} \end{cases} \tag{5.3.3}$$

In Figure 5.6, we draw the domain Ω. In our simulations, we let fish group take random positions in the small rectangle on the upper left corner of the domain. Fish group aims to get to food location which is represented by the small circle on the lower right corner.

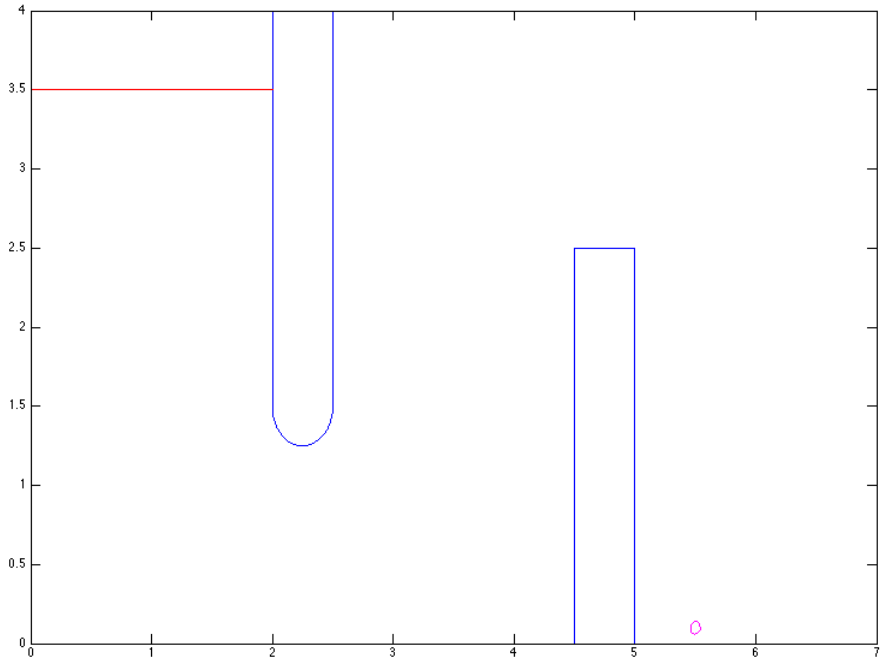

Figure 5.6: Simulation environment for fish foraging model

We can find the smell function from f specified in (5.3.3) by solving diffusion equation (5.3.2) with $c = 0.1$, $a = 0.2$. The smell function u for above setting is shown in Figure 5.7.

In order to survey positive effect of schooling on foraging tasks, we consider the role of school population on the process of finding food resource. In doing so, we make simulations using our model with all parameters are fixed except for parameter N, which is the number of fish in the school. We will change N from 1 to 20. For each value of n we take 10 independent runs. The simulations start at initial positions of N-fish randomly distributed in the rectangle domain $[0, 2] \times [3.5, 4]$ with all null velocities $v_i = (0, 0)$, $i = 1, 2, \ldots, N$. Other parameters are set $\alpha = \beta = \gamma = 1$, $p = P = 3$, $q = Q = 5$, $r = 0.1$, $R = 0.2$, $\sigma = 0.001$. We also included a parameter $v_{\max}$ to restrict the maximum speed of fish. If the magnitude of v_i exceeds $v_{\max}$, our program rescaled it to magnitude $v_{\max}$ while preserving its direction. This is reasonable because each species of fish has a tolerance of velocity that they can not

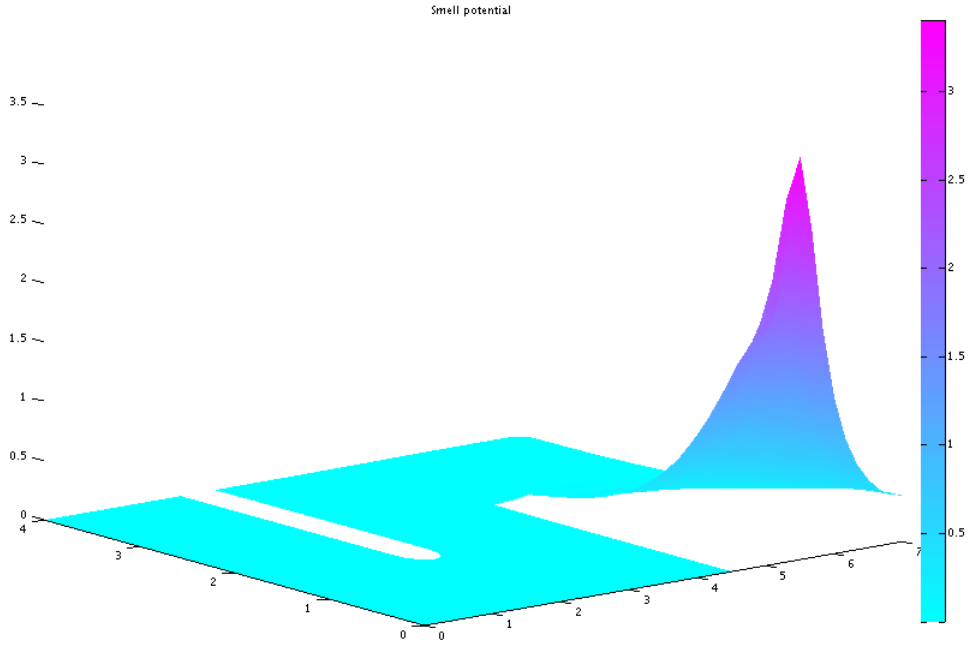

Figure 5.7: Food smell potential function

exceed. That is,

$$v_i(t) = \begin{cases} v_i(t) & \text{if} \quad \|v_i(t)\| \leqslant v_{\max}, \\ \frac{v_i(t)}{\|v_i(t)\|} v_{\max} & \text{otherwise.} \end{cases}$$

In our experiments we choose $v_{\max} = 0.8$.

Now let us show some numerical results we have obtained. We can see that a group of 20 fish can approach to food resource location after a period of time (see Figure 5.8), while a 5-fish group can not (Figure 5.9). The situation is even worse when there is only one fish. In this case, the fish is trapped, it can not pass even the first obstacle (Figure 5.10). In each of these three figures, four subfigures, from the left to right and then from the top to bottom, respectively present state of school at different instants $t = 30, 60, 90, 120$.

When fish in group all lies on the left side of Ob_1, the value of smell function is very small, so their movements are affected mostly by the fish-fish interaction force (including attractive and repulsive force) and fish-obstacle collision avoidance rule. Because of that, fish together make school very fast. Then all fish in the school will move together when interaction between them are chosen large enough.

In order to report our statistic results, we will classify the observed results into 3 states as follows:

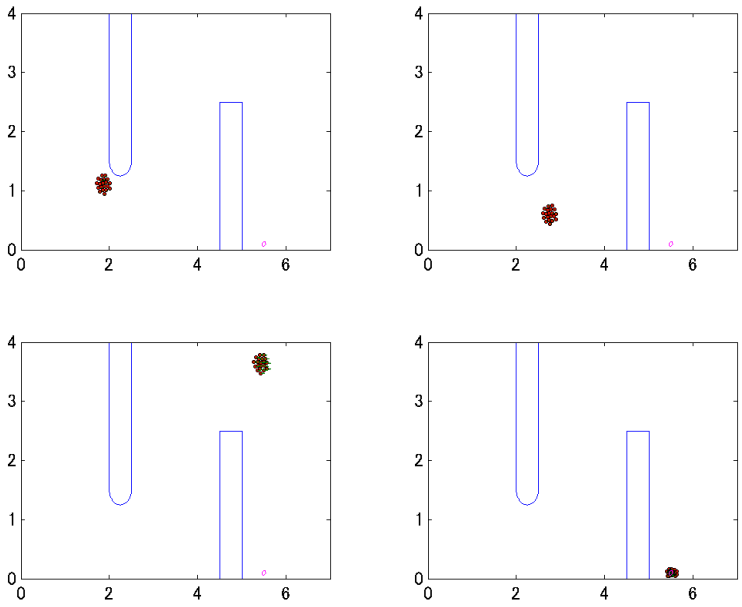

Figure 5.8: Big group can get to the target within allotted time

State I: The school reaches the goal at $T = 120$, that is at the 1200000-th step.

State II: The whole or a part of the school has pass the left wall of Ob_1 but has not reached the goal at $T = 120$.

State III: The whole school lies on the left of Ob_1 at $T = 120$.

These states are illustrated respectively in Figures 5.8, 5.9, 5.10. Because we choose parameter characterizing for the fish-fish interaction large enough, once school is created it will keep still. So we can say the school reaches to the goal when distance from the center of school ($\bar{x} = \frac{1}{n}\sum_{i=1}^{n} x_i$) to the center of food resource $C(5.5, 0.1)$ does not exceed 0.04.

In Figure 5.11, we give our numerical result with parameter setting as above and different value of smell attractive coefficient k.

If the school reaches to the goal within allotted time period (in our experiments, it is $T = 120$) that is it has State I then we call it "success" otherwise we say it "fail". Now we illustrate the percentage of successful case (among simulation trials) in Figure 5.11.

From the results we see that with all four values of k under consideration, a single fish fail to find food resource. As the number of fish is larger than 1 then the probability of foraging success is positive. Especially, when parameters are chosen appropriately then this probability seems to increases as the population of fish increase (until some large N). For example, we can see this in the case $k = 2$: the above remark holds true until $N = 18$. This can be explained as

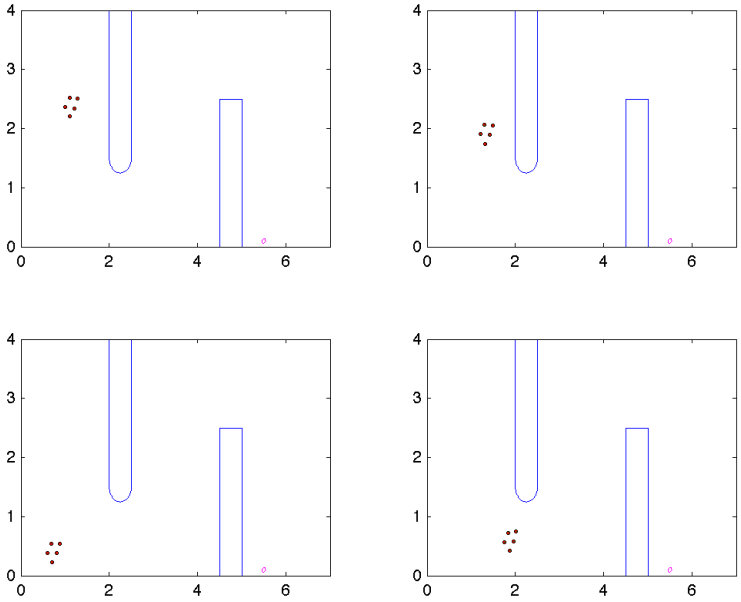

Figure 5.9: Small group can not get to the target within allotted time

follows. We let the fish take initial position in a small rectangle domain in the upper left side of the domain where the smell of food is very weak. So one fish senses the smell weakly. But if there are more fish at different positions, some fish can be at good positions to smell food better. They have tendency to move toward the food resource by moving along the smell's concentration gradient direction. Then their neighbor fish, thanks to attractive force, will follow them. This results in the success of the whole school in finding food resource. Another possible reason for this can be the total effect of food smell on a big group of fish is stronger than that on smaller group. From this we can conclude that the school provides advantage for its members getting to the food resource.

However, we can see in Figure 5.12 that from some large value of school population the graph of success percentage trends to decrease. For example in the case $k = 1$, the percentage of success case is 100% with $N = 16$, then it decreases to 80% and 50% for $N = 17$ and $N = 18$, respectively. While in the case $k = 0.5$, at $N = 17$, there are 8 successful case over 10 trials, but after that the probabilities for success are 0 for $n = 18, 19$. This is also reasonable because besides the food resource attraction, the movement of school fish is affected also by obstacles. When the number of fish increases, the cohesiveness of school is high. So, it will keep the school lying in on the left of the first obstacle or cause the school to spend a lot of time before reaching to the food resource. This suggests that for each parameter set which is chosen

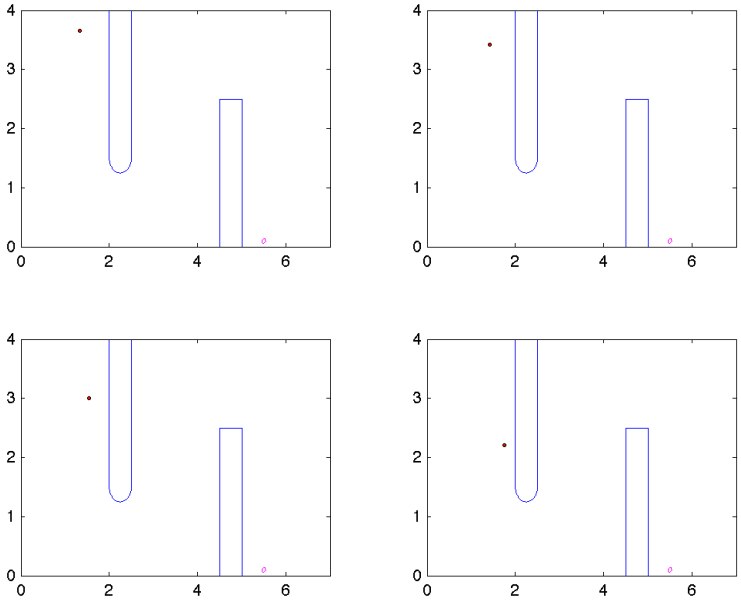

Figure 5.10: A single can not get to the target within allotted time

appropriately, there exist some optimal values of group population such that the school gets highest possibility in getting food. In our simulations, such optimal values are $N = 15$ for $k = 0.5$; $N = 16$ for $k = 1$; $N = 4, 5, \ldots, 18$ for $k = 2$.

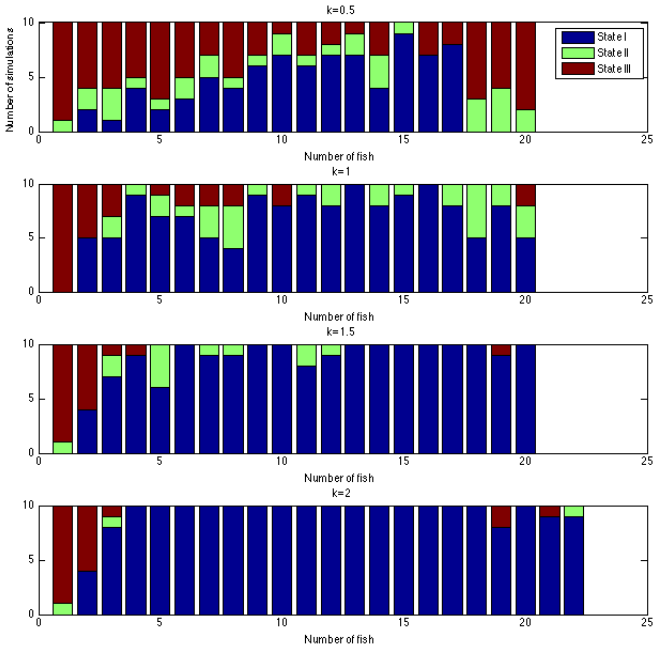

Figure 5.11: Foraging advantages of fish school (a)

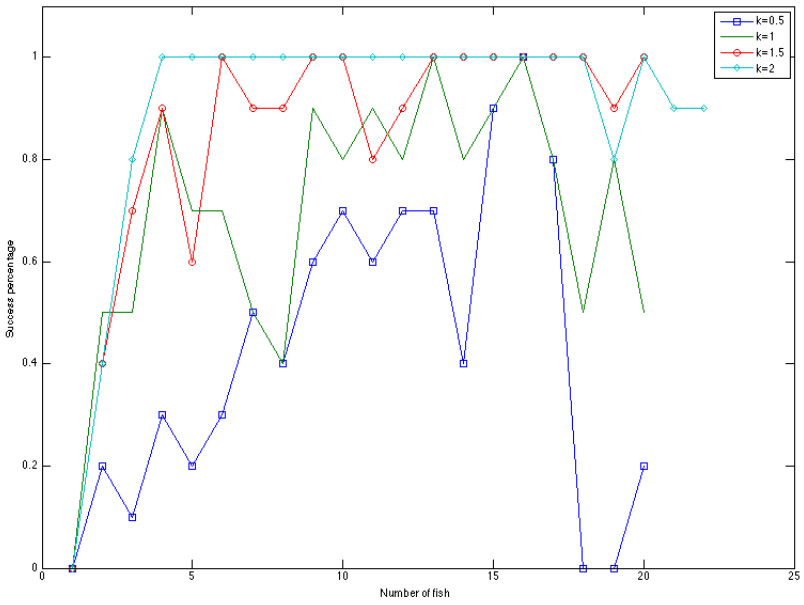

Figure 5.12: Foraging advantages of fish school (b)

Chapter 6

Conclusions and Future Researches

6.1 Conclusions

This dissertation handles stochastic models for two biological systems: growth of forest and schooling of fish. Stochastic differential equations are built up to describe these systems in order to create more realistic models than deterministic ones. Then we study these models by means of numerical techniques.

The main contributions of this dissertation are as follows:

For stochastic forest model

1. *Proved the existence and uniqueness of global positive solutions to the stochastic differential equations* (3.1.2). (See Theorem 3.3.1).
   This implies that we can describe the growth of forest by the evolution of this system's dynamics. It is the theoretical base that ensures for further numerical researches on this model.

2. *Showed the boundedness of the solutions to the forest model equations.* (See Subsection 3.3.1).

3. *Showed the sustainability of the forest when the mortality rate of old tree and noise is sufficiently small.* (See Subsection 3.3.2).

4. *Suggests the support of the stationary density function of random variable* $(u(t), v(t))$ *when it exists by numerical calculations* (See Subsection 3.3.2).

5. *Gave some sufficient conditions under which the forest declines.* (See Subsection 3.3.2, Theorem 3.3.5, Theorem 3.3.6).
   These results stated that if the mortality rate of old tree and noise factor exceeds some thresholds (which are functions of other parameters in the system), then the forest falls to decay.

For stochastic fish schooling models

1. *Studied flocking and non-flocking behaviors in a new stochastic Cucker-Smale system* (See Section 4.2).
2. *Gave some quantitative investigations of an ODE fish schooling model.* (See Section 4.4).
3. *Introduced a new mathematical definition for fish schooling.* (See Definition 4.4.2).
4. *Studied the influence of some model parameters to the geometrical structure of the school.* (See Subsection 4.4.1).
5. *Investigated the robustness of schooling against noises.* (See Subsection 4.4.2).
6. *Proposed a stochastic model describing fish movements in the environment with presence of obstacles and food resources.* (See Subsection 5.2.1, Subsection 5.3.1).
7. *Surveyed fish school cohesiveness through its behavioral patterns.* (See Subsection 5.2.2)
8. *Indicated how some model parameters influence school cohesiveness* (See Subsection 5.2.3).
9. *Checked the hypothesis that fish acquire foraging advantages by forming school.* (See Subsection 5.3.2).

6.2 Future researches

Let us suggest further study on the two present problems: growth of forest and fish schooling.

For forest model, it is important to study the asymptotic behavior of solutions of some "good" systems in which noise factor affects on several parameters. Conditions for the stationary density of solutions to such systems should be considered.

For fish schooling models, it may be attractive to construct a mathematical model describing fish schooling in the environment with presence of predator and prey fish. By this, we can acquire knowledge about the behaviors of these two kinds of fish in such situation. These information help us to understand how both predator and prey benefit from forming school, which is suggested in many literatures, both in experiment and computer simulations. We name here some of them [20, 21, 32, 34, 41, 48, 58, 69].

Besides ordinary differential equations, many biological systems are modelled by partial differential equations, for example Coat Model [46]. It is also a very interesting problem to investigate stochastic versions for these problems.

Chapter 7

Appendix

This chapter represents some numerical data of simulations. In order to reduce the effects of random factors on initial positions, initial velocities or Wiener trajectories, for each parameter set, we perform 10 simulations. Then, we take mean values over these trials.

In the tables below, we use notations:

S: simulation number,

N: population size,

μ: mean value over simulations,

p: power p,

r: critical distance.

Table 7.1: Simulation results illustrate dependence of mean distance on population size

S	N=20	30	40	50	60	70	80
1	0.35641	0.33278	0.31006	0.3001	0.28379	0.27538	0.26712
2	0.35776	0.33379	0.31417	0.3005	0.28482	0.27616	0.26829
3	0.35827	0.33432	0.31423	0.29642	0.28487	0.27635	0.26832
4	0.35967	0.33539	0.31619	0.29863	0.28498	0.27648	0.26841
5	0.36091	0.33545	0.31666	0.29883	0.28596	0.27664	0.26869
6	0.36098	0.33631	0.31667	0.30044	0.28625	0.27702	0.26898
7	0.36113	0.33636	0.31715	0.30117	0.28649	0.27722	0.26929
8	0.36216	0.33671	0.31731	0.30147	0.28654	0.27728	0.26936
9	0.36252	0.33691	0.31752	0.30161	0.28802	0.27749	0.26947
10	0.36266	0.33786	0.31907	0.30401	0.28875	0.27847	0.26983
μ	0.36025	0.33559	0.31590	0.30032	0.28605	0.27685	0.26878

S	N=90	100	110	120	130	140
1	0.26142	0.25364	0.2492	0.2428	0.2406	0.23402
2	0.26144	0.25364	0.24788	0.2447	0.23844	0.23405
3	0.26183	0.25422	0.24799	0.2449	0.23867	0.23472
4	0.26226	0.25473	0.24882	0.24307	0.23877	0.23507
5	0.26245	0.25506	0.24909	0.24317	0.23896	0.23525
6	0.26267	0.25508	0.24913	0.24392	0.23916	0.23528
7	0.26272	0.25576	0.24936	0.24439	0.23959	0.23532
8	0.26288	0.25591	0.24938	0.24466	0.24005	0.23554
9	0.26302	0.25593	0.24989	0.24472	0.24047	0.23584
10	0.26309	0.25637	0.25008	0.24481	0.24141	0.23617
μ	0.26238	0.25503	0.24908	0.24411	0.23961	0.23513

S	N=150	160	170	180	190	200
1	0.2305	0.2273	0.2242	0.22065	0.21761	0.2152
2	0.23056	0.22695	0.22384	0.22122	0.21828	0.21544
3	0.23059	0.22696	0.22426	0.22123	0.21838	0.21544
4	0.23062	0.22719	0.22431	0.22135	0.21842	0.21544
5	0.23084	0.22728	0.22432	0.22144	0.21847	0.21553
6	0.23085	0.22758	0.22433	0.22152	0.21876	0.21569
7	0.23097	0.22771	0.22442	0.22178	0.21876	0.21586
8	0.23127	0.22778	0.22454	0.22204	0.21884	0.21608
9	0.23135	0.22806	0.22465	0.22225	0.21915	0.21615
10	0.23197	0.22826	0.22466	0.21987	0.21917	0.21659
μ	0.23095	0.22751	0.22435	0.22134	0.21858	0.21574

Table 7.2: Simulation results illustrate dependence of mean distance on critical distance

S	$r = 0.5$	0.6	0.7	0.8	0.9	1.0
1	0.29709	0.35927	0.41975	0.47991	0.54301	0.60011
2	0.29625	0.36407	0.42083	0.48187	0.54291	0.60207
3	0.30125	0.35801	0.42034	0.48626	0.54617	0.59774
4	0.30124	0.35692	0.42632	0.48031	0.54296	0.60013
5	0.30097	0.3597	0.41945	0.47709	0.53381	0.60129
6	0.29698	0.35982	0.41727	0.4764	0.54604	0.60579
7	0.30042	0.36347	0.41645	0.48122	0.54252	0.60061
8	0.30113	0.36018	0.42029	0.48263	0.54703	0.60188
9	0.30079	0.3588	0.41898	0.48011	0.53824	0.60569
10	0.29952	0.35948	0.42672	0.4783	0.54025	0.60256
μ	0.29956	0.35997	0.42064	0.48041	0.54229	0.60179

S	$r = 1.1$	1.2	r=1.3	1.4	1.5
1	0.65904	0.72351	0.79227	0.8462	0.90144
2	0.65966	0.71604	0.7801	0.83851	0.91229
3	0.67156	0.72048	0.78244	0.8442	0.90068
4	0.66143	0.7221	0.78158	0.85165	0.89746
5	0.65452	0.71564	0.78158	0.84078	0.90179
6	0.66095	0.73118	0.77993	0.84382	0.90488
7	0.66218	0.71506	0.77641	0.83899	0.91383
8	0.66807	0.72307	0.77628	0.84023	0.89868
9	0.66541	0.72139	0.78157	0.84429	0.90053
10	0.66948	0.72178	0.7793	0.83981	0.90138
μ	0.66323	0.72103	0.78115	0.84285	0.9033

S	$r = 1.6$	1.7	1.8	1.9	2.0
1	0.95758	1.02451	1.07688	1.14588	1.19322
2	0.95885	1.0206	1.09782	1.14932	1.21876
3	0.95105	1.02321	1.09767	1.14147	1.20078
4	0.96072	1.02055	1.07022	1.15482	1.20478
5	0.96134	1.02189	1.08486	1.16042	1.20304
6	0.9636	1.02017	1.0892	1.15821	1.20141
7	0.96366	1.02132	1.08428	1.14466	1.2031
8	0.97156	1.02837	1.08406	1.13746	1.20362
9	0.95629	1.03251	1.08451	1.15514	1.20909
10	0.96091	1.02336	1.08383	1.14573	1.18721
μ	0.96056	1.02365	1.08533	1.14931	1.2025

Table 7.3: Simulation results illustrate dependence of school diameter on critical distance

S	$r = 0.5$	0.6	0.7	0.8	0.9	1.0
1	0.60726	0.72575	0.84129	0.96366	1.084	1.19581
2	0.60594	0.72218	0.83796	0.95602	1.08108	1.19396
3	0.60082	0.71941	0.83713	0.95594	1.07939	1.19188
4	0.59958	0.71784	0.83712	0.95084	1.07798	1.18939
5	0.59824	0.71651	0.83197	0.94896	1.07244	1.18879
6	0.59822	0.71609	0.83091	0.94786	1.07034	1.18597
7	0.59497	0.71609	0.82929	0.94779	1.06843	1.17857
8	0.59237	0.71049	0.82797	0.94773	1.06483	1.17522
9	0.59071	0.70987	0.8337	0.94388	1.06435	1.17422
10	0.58758	0.71915	0.8331	0.94258	1.06288	1.1798
μ	0.59757	0.71734	0.83404	0.95053	1.07257	1.18536

S	$r = 1.1$	1.2	1.3	1.4	1.5
1	1.32102	1.43478	1.55604	1.66726	1.79771
2	1.30946	1.43448	1.55264	1.66691	1.79579
3	1.30916	1.43177	1.55044	1.66573	1.79144
4	1.30788	1.43066	1.54973	1.66504	1.78793
5	1.29995	1.42944	1.54349	1.66476	1.78696
6	1.29756	1.42767	1.54129	1.65718	1.78547
7	1.29439	1.42475	1.53724	1.65323	1.78431
8	1.3095	1.42257	1.53599	1.6595	1.77857
9	1.3059	1.41167	1.52966	1.684	1.7954
10	1.31665	1.4366	1.52672	1.667	1.7786
μ	1.30715	1.42844	1.54232	1.66506	1.78822

S	$r = 1.6$	1.7	1.8	1.9	2.0
1	1.91723	2.02406	2.15627	2.23743	2.41724
2	1.91098	2.02271	2.15314	2.27818	2.38651
3	1.90168	2.01971	2.15169	2.27005	2.38538
4	1.90166	2.01775	2.15129	2.27099	2.38154
5	1.90108	2.01530	2.14335	2.26065	2.37635
6	1.89618	2.01527	2.14011	2.26034	2.36826
7	1.89169	2.01458	2.13555	2.25552	2.36758
8	1.89139	2.04387	2.13389	2.25124	2.36576
9	1.89009	2.03652	2.11821	2.25023	2.35511
10	1.88914	2.01461	2.1203	2.24818	2.3802
μ	1.89911	2.02244	2.14038	2.25828	2.37839

Table 7.4: Simulation results illustrate dependence of school diameter on population size in 2-dimensional case with $p = 1.2$

S	N=20	30	40	50	60
1	1.06972	1.08362	1.08708	1.09897	1.14457
2	1.05652	1.08116	1.08297	1.09840	1.14235
3	1.03907	1.07207	1.08134	1.09502	1.13746
4	1.03434	1.06598	1.07843	1.08386	1.12231
5	1.03699	1.06326	1.07745	1.12788	1.12121
6	1.0292	1.06106	1.11517	1.12529	1.12025
7	1.02414	1.05809	1.11474	1.11715	1.11829
8	1.03145	1.04227	1.11361	1.10918	1.10799
9	0.99628	1.03829	1.10461	1.10529	1.10357
10	0.97244	1.10653	1.07809	1.09747	1.10083
μ	1.02901	1.06723	1.09335	1.10585	1.12188
S	N=70	80	90	100	110
1	1.15432	1.15175	1.17393	1.16022	1.16493
2	1.14788	1.14663	1.16976	1.15511	1.16349
3	1.14781	1.14558	1.16769	1.15505	1.16332
4	1.14628	1.14437	1.15266	1.15226	1.16176
5	1.13987	1.13763	1.15064	1.15194	1.15846
6	1.13211	1.13501	1.14819	1.15021	1.15771
7	1.12466	1.13485	1.14803	1.14958	1.15469
8	1.11968	1.14091	1.14761	1.14763	1.14946
9	1.11952	1.12546	1.14001	1.14155	1.14522
10	1.1373	1.1474	1.13763	1.13921	1.15183
μ	1.13694	1.14096	1.15362	1.15028	1.15709
S	N=120	130	140	150	200
1	1.16222	1.16362	1.16743	1.16971	1.1805
2	1.15713	1.16343	1.16668	1.16833	1.17644
3	1.15707	1.16286	1.16663	1.16757	1.17657
4	1.15644	1.16146	1.16653	1.16669	1.17688
5	1.15353	1.15923	1.16579	1.16577	1.17803
6	1.15179	1.15759	1.16424	1.16543	1.17889
7	1.15105	1.15691	1.15818	1.16291	1.17899
8	1.14752	1.15687	1.15712	1.16259	1.18132
9	1.14697	1.1639	1.15688	1.16149	1.18369
10	1.14618	1.165	1.1656	1.1715	1.20931
μ	1.153	1.16109	1.16351	1.1662	1.18206

Table 7.5: Simulation results illustrate dependence of school diameter on population size in 2-dimensional case with $p = 2$

S	N=20	30	40	50	60
1	1.21247	1.3292	1.34834	1.432	1.41979
2	1.23284	1.3321	1.36466	1.4245	1.43709
3	1.26985	1.33478	1.36565	1.41613	1.46477
4	1.28027	1.33374	1.37639	1.41687	1.46768
5	1.2073	1.34617	1.37144	1.44209	1.44257
6	1.2961	1.27465	1.4021	1.4058	1.45993
7	1.20855	1.29737	1.36634	1.38578	1.46107
8	1.23738	1.30055	1.37001	1.41202	1.46394
9	1.24253	1.33194	1.37014	1.41604	1.46792
10	1.24471	1.33534	1.37711	1.41849	1.46831
μ	1.24550	1.33704	1.37958	1.42278	1.46309
S	N=70	80	90	100	110
1	1.47305	1.49686	1.51974	1.554	1.54846
2	1.47806	1.49887	1.52716	1.5524	1.55248
3	1.51018	1.50987	1.52935	1.55564	1.55376
4	1.54663	1.54312	1.53002	1.53293	1.56549
5	1.46059	1.5296	1.51845	1.54756	1.5581
6	1.47392	1.49882	1.52773	1.55237	1.5709
7	1.48117	1.50077	1.52791	1.55742	1.55519
8	1.48149	1.50683	1.53363	1.55874	1.55565
9	1.48422	1.51316	1.53967	1.55905	1.55998
10	1.49199	1.51944	1.53988	1.55913	1.5601
μ	1.49073	1.51382	1.53265	1.55292	1.55896
S	N=120	130	140	150	200
1	1.58137	1.57421	1.5918	1.59842	1.64489
2	1.58254	1.58843	1.59649	1.59937	1.65177
3	1.57936	1.58875	1.58321	1.59955	1.65248
4	1.57067	1.59421	1.58807	1.60322	1.64456
5	1.57344	1.55962	1.60326	1.61277	1.6343
6	1.57485	1.57665	1.63429	1.60021	1.63627
7	1.57596	1.58422	1.59774	1.59732	1.64359
8	1.58001	1.58611	1.6033	1.59281	1.64965
9	1.58091	1.58981	1.5969	1.59164	1.64484
10	1.58281	1.57188	1.59329	1.60207	1.64456
μ	1.57879	1.58139	1.59884	1.59974	1.64469

Table 7.6: Simulation results illustrate dependence of school diameter on population size in 3-dimensional case

S	N=50	100	150	200	250	300
1	0.86734	0.90354	0.9249	0.9387	0.9328	0.9313
2	0.88606	0.90726	0.92019	0.92725	0.9398	0.9369
3	0.88703	0.90765	0.92326	0.92899	0.9429	0.9376
4	0.88778	0.90789	0.92447	0.92971	0.93242	0.9416
5	0.89479	0.91024	0.92475	0.93116	0.93443	0.9419
6	0.89493	0.91047	0.92507	0.93264	0.93482	0.93957
7	0.89661	0.91957	0.92563	0.93269	0.93778	0.94069
8	0.89943	0.92521	0.92718	0.93657	0.93847	0.94164
9	0.89961	0.92717	0.92721	0.93919	0.93944	0.94237
10	0.90815	0.93038	0.93333	0.94765	0.93254	0.92181
μ	0.89217	0.91494	0.9256	0.93446	0.93654	0.93754

$p = 2$

S	N=50	100	150	200	250	300
1	1.02451	1.11282	1.11844	1.12682	1.14104	1.16026
2	1.03638	1.11883	1.1112	1.1433	1.1574	1.1596
3	1.04334	1.09053	1.1207	1.12228	1.13974	1.15085
4	1.04717	1.09120	1.11401	1.13104	1.14311	1.15873
5	1.05285	1.09321	1.11485	1.13555	1.14623	1.15896
6	1.05433	1.09484	1.12033	1.13973	1.14796	1.15957
7	1.05709	1.10396	1.12105	1.14046	1.14876	1.16008
8	1.06772	1.10984	1.12665	1.14222	1.14998	1.16456
9	1.06792	1.1016	1.12748	1.14239	1.15075	1.16496
10	1.06896	1.07971	1.12774	1.15065	1.15578	1.17724
μ	1.05203	1.09965	1.12104	1.13977	1.14892	1.16148

$p = 3$

S	$N = 50$	100	150	200	250	300
1	1.28711	1.37693	1.45226	1.51494	1.55542	1.5464
2	1.36216	1.383	1.4679	1.5353	1.5633	1.5794
3	1.28147	1.36553	1.45196	1.50365	1.52716	1.56169
4	1.29033	1.37129	1.46378	1.50424	1.53479	1.56234
5	1.32823	1.37761	1.47132	1.50905	1.54041	1.56274
6	1.33819	1.37824	1.48282	1.52223	1.54933	1.56952
7	1.35794	1.38788	1.49504	1.52662	1.56852	1.57824
8	1.39511	1.38981	1.50306	1.52876	1.57629	1.59012
9	1.41792	1.40221	1.55482	1.53381	1.56333	1.51157
10	1.28798	1.40844	1.48932	1.52488	1.52716	1.5464
μ	1.33464	1.39099	1.48323	1.52035	1.55057	1.56084

References

[1] M. Adioui, J. P. Treuil, and O. Arino, Alignment in a fish school: a mixed Lagrangian-Eulerian approach, *Ecol. Model.* **167** (2003), 19–32.

[2] S. M. Ahn and S. Y. Ha, Stochastic flocking dynamics of the Cucker-Smale model with multiplicative white noises, *J. Math. Phys.* **51** 103301 (2010).

[3] M. Ya. Antonovsky, Impact of the factors of the environment on the dynamics of population (mathematical model), *Proc. Soviet-American Symp. "Comprehensive Analysis of the Environment"*, Tbilisi 1974, Leningrad: Hydromet, (1975), 218–230.

[4] M. Ya. Antonovsky and M. D. Korzukhin, Mathematical modeling of economic and ecological-economic process, *Proc. Soviet-American Symp. "Integrated Global Monitoring of Environmental Pollution"*, Tbilisi 1981, Leningrad: Hydromet, (1983), 353–358.

[5] I. Aoki, A simulation study on the schooling mechanism in fish, *B. Jpn. Soc. Sci. Fish.* **48**(1982), 1081–1088.

[6] L. Arnold, *Stochastic Differential Equations: Theory and Applications*, Wiley, New York, 1972.

[7] K. J. Beers, *Numerical Methods for Chemical Engineering*, Cambridge, 2007.

[8] C. M. Breder, Studies on the structure of the fish school, *Bull. Smer. Mus. Nat. Hist.* **98** (1951), 1–28.

[9] C. M. Breder, Equation descriptive of fish schools and other animal aggregations, *Ecology* **35** (1954), 361–370.

[10] C. M. Breder, Studies on social grouping in fished, *Bull. Amer. Mus. Nat. Hist.* **117** (1959), 393–482.

[11] S. Camazine, J. L. Deneubourg, N. R. Franks, J. Sneyd, G. Theraulaz, and E. Bonabeau, *Self-Organization in Biological Systems*, Princeton University Press, 2001.

[12] J. M. Cullen, E. Shaw, and H. A. Baldwin, Methods for measuring the three-dimensional structure of fish schools, *Anim. Behav.* **13** (1965), 534–543.

[13] D. E. Chang, S. C. Shadden, J. E. Marsden, and Reza Olfati-Saber, Collision avoidance for multiple agent systems, *Proceedings of the 42nd IEEE Conference on Decision and Control* (2003).

[14] F. Cucker and S. Smale, On the mathematics of emergence, *Japan. J. Math.* **2** (2007), 197–227.

[15] F. Cucker and S. Smale, Emergence behavior in flocks, *IEEE Trans. Autom. Control* **52** (2007), 852–862.

[16] F. Cucker and E. Mordecki, Flocking in noisy environments, *J. Math. Pures Appl.* **89** (2008), 278–296.

[17] M. R. D' Orsogna, Y. L. Chuang, A. L. Bertozzi, and L. S. Chayes, Self-propelled particles with soft-core interactions: Patterns, stability, and collapse, *Phys. Rev. Lett.* **96** 104302 (2006).

[18] F. Ducatelle, G. A. Di Caro, C. Pinciroli, F. Mondada, and L. M. Gambardella, Communication assisted navigation in robotic swarms: self-organisation and cooperation, *Proceedings of the IEEE/RSJ International Conference on Intelligent Robots and Systems* (IROS), San Francisco, USA, September 25-30, 2001.

[19] A. Friedman, *Stochastic Differential Equations and their Applications*, Academic press, New York, 1976.

[20] S. M. Flaxman and Yuan Lou, Tracking prey or tracking the prey's resource? Machinisms of movement and optimal habitat selection by predators, *J. Theor. Biol.* **256** (2) (2009), 187–200.

[21] J. Garay, Cooperation in defence against a predator, *J. Theor. Biol.* **257** (1) (2009), 45–51.

[22] G. Garcia-Diaz, S. Salcedo-Sanz, J. Plaza-Laina, A. Portilla-Figueras, and J. Del Ser, A discrete particle swarm optimisation algorithm for mobile network deployment problems, *2012 IEEE 17th International Workshop on Computer aided modelling and design of communication links and networks* (CAMAD).

[23] C. W. Gardiner, *Handbook of Stochastic Methods for Physics, Chemistry and the Natural Sciences*, Springer, 1997.

[24] Yukio-Pegio Gunji, Yoshiyuki Kusunoki, Nobuhide Kitabayashi, Toshinao Mochizuki, Masaki Ishikawa, and Takanori Watanabe, Dual interaction producing both territorial and schooling behavior in fish, *Biosystems* **50** (1) (1999), 27–47.

[25] S.-Y. Ha and J. Liu, A simple proof of the Cucker-Smale flocking dynamics and mean-field limit, *Commun. Math. Sci.* **7** (2) (2009), 297–325.

[26] S.-Y. Ha, K. Lee, and D. Levy, Emergence of time-asymptotic flocking in a stochastic Cucker-Smale system, *Commun. Math. Sci.* **7** (2) (2009), 453–469.

[27] D. Helbing, J. Keltsch, and P. Molnar, Modelling the evolution of human trail systems, *Nature* **388** (1997), 47–50.

[28] D. J. Higham, An algorithmic introduction to numerical simulation of stochastic differential equations, *SIAM Rev.* **43** (3) (2001), 525–546.

[29] S. Hubbard, P. Babak, S. T. Sigurdsson, and K. G. Magnusson, A model of the formation of fish schools and migrations of fish, *Ecol. Model.* **174** (4) (2004), 359–374.

[30] A. Huth and C. Wissel, The simulation of the movement of fish school, *J. Theor. Biol.* **156** (1992), 365–385.

[31] N. Ikeda and S. Wantanabe, *Stochastic Differential Equations and Diffusion Processes*, North-Holland, Amsterdam, 1981.

[32] C. C. Ioannou and J. Krause, Searching for prey: the effects of group size and number, *Anim. Behav.* **75** (2008), 1383–1388.

[33] Y. Inada, Steering mechanism of fish schools, *Complexity International*, **8** (2001), 1–9.

[34] J. M. Jeschke and R. Tollrian, Prey swarming: which predators become confused and why?, *Anim. Behav.* **74** (3) (2007), 387–393.

[35] I. Karatzas and S. E. Karatzas, *Brownian Motion and Stochastic Calculus*, Springer-Verlag, Berlin, 1991.

[36] M. Keenleyside, Some aspects of the schooling behaviors of fish, *Behaviour* **8** (1995), 183–248.

[37] P. E. Kloeden and E. Platen, *Numerical Solution of Stochastic Differential Equations*, Springer, 2005.

[38] P. E. Kloeden, E. Platen, and H. Schurz, *Numerical Solution of SDE Through Computer Experiments*, Springer, 2003.

[39] P. E. Kloeden and E. Platen, A survey of numerical methods for stochastic differential equations, *Stoch. Hydrol. Hydraul.* **3** (1989), 155–178.

[40] P. E. Kloeden and E. Platen, Higher-order implicit strong numerical scheme for stochastic differential equations, *J. Stat. Phys.* **66** (1-2) (1992), 283–314.

[41] S.-H. Lee, H. K. Pak, and T.-S. Chon, Dynamics of prey-flock escaping behavior in response to predator's attack, *J. Theor. Biol.* **240** (2006), 250–259.

[42] N. T. H. Linh, T. V. Ton, and A. Yagi, Quantitative investigations for ODE model describing fish schooling, *Sci. Math. Jpn.* (accepted for publication).

[43] N. T. H. Linh, T. V. Ton, and A. Yagi, Stochastic forest model, *Proceedings of Conference on Functional Analysis and Applications*, Kobe University, Feb. 2013 (accepted for publication).

[44] N. T. H. Linh, T. V. Ton, and A. Yagi, Schooling of fish in noisy environment with obstacles and food resources, (in preparation).

[45] R. Livermore, A multi-agent system approach to a simulation study comparing the performance of aircraft boarding using pre-assigned seating and free-for-all strategies, Open University, Technical report No 2008/25.

[46] J. D. Murray, *Mathematical Biology, II, Spatial Models and Biomedical Applications* (3rd ed.,) Springer, 2003.

[47] A. I. S. Nascimento and C. J. A. Bastos-Filho, Designing cellular network using particle swarm optimisation and genetic algorithms, *International Journal of computer information systems and industrial management application*, **4** (2012), 496–505.

[48] S. I. Nishimura, A predator's selection of an individual prey from a group, *Biosystems* **65** (2002), 25–35.

[49] J. R. Nursall, Some behavioral interactions of spottail shiner (Notropis hudsonius), yellow perch (Perca flavescens) and northern pike (Esox lucius), *J. Fish. Res. Board Can.* **30** (1973), 1161–1178.

[50] T. Oboshi, S. Kato, A. Mutoh, and H. Itoh, Collective or scattering: evolving schooling behaviors to escape from predator, *Artif. Life*, MIT Press, Cambridge, MA, **VIII** (2002), 386–389.

[51] B. L. Partridge, T. Pitcher, J. M. Cullen, and J. Wilson, The three-dimensional structure of fish schools, *Behav. Ecol. Sociobiol.* **6** (1980), 277–288.

[52] J. K. Parrish and S. V. Viscido, *Traffic Rules of Fish Schools; a Review of Agent-based Approaches*, Cambridge Univ. Press, Cambridge, 2005.

[53] C. W. Reynolds, Flocks, herds, and schools: a distributed behavioral model, *Comput. Graphics* **21** (1987), 25–34.

[54] Reza Olfati-Saber, Flocking with obstacle avoidance, Technical Report CIT-CDS 03-006.

[55] Reza Olfati-Saber, Flocking for multi-agent dynamic systems: Algorithms and Theory, *IEEE Trans. Autom. Control* **51** (3) (2006), 401–420.

[56] E. Rimon and D. E. Koditschek, Exact robot navigation using artificial potential functions, *IEEE Trans. Robot. Autom.* **8** (5) (1992), 501–518.

[57] S. Stöcker, Models for tuna school formation, *Math. Biosci.* **156** (1999), 167–190.

[58] M. Szulkin, P. Dawidowicz, and S. I. Dodson, Behavioural uniformity as a response to cues of predation risk, *Anim. Behav.* **71** (2006), 1013–1019.

[59] T. V. Ton, N. T. H. Linh, and A. Yagi, Flocking and non-flocking behavior in a stochastic Cucker-Smale system, *Anal. Appl.* **12** (1) (2014), 63–73.

[60] T. V. Ton, N. T. H. Linh, and A. Yagi, Asymptotic behavior of solutions to stochastic forest model, (in preparation).

[61] T. Uchitane, T. V. Ton, and A. Yagi, An ordinary differential equation model for fish schooling, *Sci. Math. Jpn.* **75** (2012), 339–350, **e-2012**, 415–426.

[62] T. Uchitane and A. Yagi, Optimization scheme based on differential equation model for animal swarming, *Open Journal of Optimization* **2** (2013), 45–51.

[63] R. Vabϕ and G. Skaret, Emerging school structure and collective dynamics in spawning herring: A simulation study, *Ecol. Model.* **214** (2008), 125–140.

[64] T. Vicsek, A. Czirók, E. Ben-Jacob, I. Cohen, and O. Shochet, Novel type of phase transition in a system of self-driven particles, *Phys. Rev. Lett.* **75** (1995), 1226–1229.

[65] S. V. Viscido, J. K. Parrish, and D. Grünbaum, Individual behavior and emergent properties of fish schooling: a comparison of observation and theory, *Mar. Ecol. Prog. Ser.* **273** (2004), 239–249.

[66] S. V. Viscido, J. K. Parrish, and D. Grünbaum, The effect of population size and number of influential neighbours on the emergent properties of fish schools, *Ecol. Model.* **183** (2-3) (2005), 347–363.

[67] S. V. Viscido, J. K. Parrish, and D. Grünbaum, Factors influencing the structure and maintenance of fish schools, *Ecol. Model.* **206** (1-2) (2007), 153–165.

[68] K. Warburton and J. Lazarus, Tendency-distance models of social cohesion in animal groups, *J. Theor. Biol.* **150** (1991), 473–488.

[69] M. Zheng, Y. Kashimori, O. Hoshino, K. Fujita, and T. Kambara, Behavior pattern (innate action) of individuals in fish schools generating efficient collective evasion from predation, *J. Theor. Biol.* **235** (2005), 153–167.

Publications

1. Ta Hong Quang, Ta Viet Ton and Nguyen Thi Hoai Linh, Dynamics of a non-autonomous three-dimensional population system, *Electron. J. Differ. Equations* **157** (2009), 1–12.

2. Nguyen Thi Hoai Linh and Ta Viet Ton, Dynamics of stochastic ratio-dependent predator-prey model, *Anal. Appl.* **9** (3) (2011), 329–344.

3. Ta Viet Ton, Nguyen Thi Hoai Linh and Atsushi Yagi, Flocking and non-flocking behavior in a stochastic Cucker-Smale system, *Anal. Appl.* **12** (1) (2014), 63–73.

4. Nguyen Thi Hoai Linh, Ta Viet Ton and Atsushi Yagi, Quantitative investigations for ODE model describing fish schooling, *Sci. Math. Jpn.* (accepted for publication).

5. Nguyen Thi Hoai Linh, Ta Viet Ton and Atsushi Yagi, Stochastic forest model, *Proceedings of Conference on Functional Analysis and Applications*, Kobe University, Feb. 2013 (accepted for publication).

6. Nguyen Thi Hoai Linh, Ta Viet Ton and Atsushi Yagi, Schooling of fish in noisy environment with obstacles and food resources, (in preparation).

7. Ta Viet Ton, Nguyen Thi Hoai Linh and Atsushi Yagi, Asymptotic behavior of solutions to stochastic forest model, (in preparation).

Acknowledgments

Foremost, I would like to express my gratitude to Professor Atsushi Yagi for his supervision, support, encouragement and guidance throughout my doctoral course, for his immense knowledge, motivation and patience.

Besides, I would like to express my appreciation to the other members of this dissertation committee: Professor Yasumasa Fujisaki, Professor Hiroshi Morita, Associate Professor Yoshitaka Yamamoto for their careful reading and valuable comments and suggestions to improve the quality of this dissertation.

Special thanks are given to Assistant Professor Toshiharu Hatanaka, Ms. Yukari Arai, Ms. Yumi Yoshida, senior Takeshi Uchitane for their valuable help during the years of my study.

My sincere thanks go to Mrs. Nobue Yagi for her warm sentiment for me and my family.

I would like to thank my family: my parents, my sisters, my brother, especially, my mother who has passed a very long way to help me taking care of my little baby.

I would never have been able to finish my course as well as my dissertation without the support and encouragement in all aspects from my loving husband and my two children.